

Sean Sullivan, Chairman  
Bruce Hamilton, Vice Chairman  
Jessie H. Roberson  
Daniel J. Santos  
Joyce L. Connery

**DEFENSE NUCLEAR FACILITIES  
SAFETY BOARD**

Washington, DC 20004-2901



October 12, 2017

Mr. James Owendoff  
Acting Assistant Secretary for  
Environmental Management  
U.S. Department of Energy  
1000 Independence Avenue, SW  
Washington, DC 20585-1000

Dear Mr. Owendoff:

The enclosed Defense Nuclear Facilities Safety Board Technical Report is provided for your information and use. It provides an analysis of the Department of Energy's proposed control strategies to address safety issues associated with flammable gas and criticality hazards in the Pretreatment Facility at the Waste Treatment and Immobilization Plant.

Sincerely,

A handwritten signature in black ink, appearing to read "Sean Sullivan", written over a white background.

Sean Sullivan  
Chairman

Enclosure

c: Mr. Joe Olencz

**FLAMMABLE GAS AND CRITICALITY HAZARDS  
AT THE WASTE TREATMENT AND  
IMMOBILIZATION PLANT**

---

**Defense Nuclear Facilities Safety Board  
Technical Report**



**June 2017**

# FLAMMABLE GAS AND CRITICALITY HAZARDS AT THE WASTE TREATMENT AND IMMOBILIZATION PLANT



This Technical Report was prepared for the Defense Nuclear Facilities Safety Board by:

Brittany Boser  
Roman Kazban, Ph.D.  
Perry Meyer, Ph.D.

Arielle Miller, P.E.  
Scott Seprish, P.E.  
Sonia Thangavelu, Ph.D.

With the assistance of:

Matthew Forsbacka, Ph.D.  
Jerry McKamy, Ph.D.

Alexander Velazquez-Lozada, P.E.

## **ACKNOWLEDGEMENTS**

The authors of this Technical Report would like to thank Daniel Bullen, Timothy Dwyer, and Robert Oberreuter for their in-depth technical reviews. The authors also would like to thank the following individuals for their contributions to this report: Matthew Duncan, Thecla Fabian, Padraic Fox, David Gutowski, Patrick Migliorini, Adam Poloski, Austin Powers, and Megan Randby.

## EXECUTIVE SUMMARY

The Department of Energy (DOE) is designing and constructing the Waste Treatment and Immobilization Plant (WTP) to treat 56 million gallons of radioactive waste stored in 177 underground tanks at the Hanford site near Richland, Washington. The Defense Nuclear Facilities Safety Board (Board) has formally identified safety issues with the design of the Pretreatment Facility at WTP. Many of these issues are related to the unique challenges associated with the Hanford tank waste and the Pretreatment Facility design. In 2009, the Board reported that stagnant waste in piping could lead to the buildup of hydrogen and potentially create an explosion hazard. Since 2010, the Board also has raised issues with the performance of the pulse jet mixing systems. Inadequate mixing could lead to: accumulation of hydrogen in vessels, a potential explosion hazard; and accumulation of fissile material at the bottom of the process vessels, a potential criticality hazard. DOE limited engineering, procurement, and construction work at the Pretreatment Facility in 2012 due to unresolved safety issues and misalignment between the design and the nuclear safety basis.

On January 24, 2017, the Acting Assistant Secretary for Environmental Management transmitted a letter to the Board describing progress made to address safety issues with the Pretreatment Facility. The letter described resolution strategies for longstanding technical issues, which addressed the following Board safety issues:

- Generation and accumulation of hydrogen in process vessels;
- Heat transfer analysis;
- Inadvertent criticality in process vessels; and
- Hydrogen in piping and ancillary vessels (HPAV).

DOE considers the work done on these issues sufficient to direct resumption of design in areas of the Pretreatment Facility affected by these safety issues. The Board reviewed DOE's proposed strategies. This Technical Report provides an analysis of DOE's proposed control strategies to address issues associated with flammable gas and criticality hazards in the Pretreatment Facility at the Waste Treatment and Immobilization Plant.

**Hydrogen in Process Vessels Strategy.** DOE's control strategy for hydrogen in vessels includes preventive and mitigative controls based on waste and vessel types. For high-solids vessels, the safety strategy relies on periodic operation of an air sparge system, rather than pulse jet mixers, to prevent gas buildup in the waste. For low-solids vessels, DOE determined it is not necessary to include a control to prevent gas buildup in the waste. For both vessel types, the strategy incorporates air purge systems to reduce the hydrogen concentrations in the vessel headspaces as hydrogen is released. The strategy for both vessel types also relies on specific administrative controls to limit hydrogen generation.

DOE's proposed strategy for control of hydrogen in process vessels also addresses the Board's heat transfer issue. DOE previously relied on the results of heat transfer calculations to determine a mixing frequency. The revised control strategy no longer relies on heat transfer calculations. Instead, it uses the hydrogen generation rates specified in the waste acceptance criteria, in some cases adjusted for changes in process conditions, to establish mixing frequency. The Board identified the following deficiencies with the control strategy for hydrogen in vessels:

- The air sparge system may not be an effective preventive control given previous test data showing the presence of a significant unmixed heel.
- DOE has not yet addressed the long-term reliability of the sparge system to ensure its operability when called upon to perform its safety function.
- The analysis supporting the control strategy for the low-solids Newtonian vessels following loss of agitation contains unverified assumptions.
- DOE has not yet specified how waste parameters important to the control strategy will be verified during operations.

**Criticality in Process Vessels Strategy.** DOE has not decided whether to direct its contractor to update the WTP design basis to include treatment of waste containing heavy plutonium particulate in the Pretreatment Facility. Making this decision early would allow DOE to integrate the heavy plutonium particulate control strategy into the design.

If DOE chooses to treat waste containing heavy plutonium particulate in the Pretreatment Facility, the proposed criticality safety strategy does not provide an adequate basis for safely processing heavy plutonium particulate in the Pretreatment Facility. The Board identified the following deficiencies with the control strategy for criticality in vessels:

- The nuclear modeling calculations used to define mass limits do not comply with American National Standards Institute/American Nuclear Society (ANSI/ANS) 8 series standards and may not be conservative.
- Key assumptions regarding implementation of mass control and soluble neutron poisons lack sufficient technical rigor.
- Vessel heel cleanout operations are not identified as a safety-related control in the test plan for full-scale testing of the new standard high-solids vessel design to demonstrate that vessel heel cleanout operations are effective.
- Assumptions regarding the location, quantity, and properties of heavy plutonium particulate in the Hanford Tank Farms contain uncertainties. DOE has proposed the Tank Waste Characterization and Staging Facility to ensure that the waste feed meets the WTP waste acceptance criteria. However, DOE has not defined that facility's functions and requirements or updated the waste acceptance criteria to protect tank waste assumptions related to heavy plutonium particulate.

If DOE cannot comply with ANSI/ANS 8 series standards for the proposed strategy, DOE has the option to apply ANSI/ANS Standard 8.10, *Criteria for Nuclear Criticality Safety Controls in Operation with Shielding and Confinement*. ANSI/ANS-8.10 allows greater flexibility for mass control and waste characterization requirements.

**HPAV Strategy.** DOE proposes using quantitative risk analysis to design safety controls for a portion of the HPAV control strategy. HPAV events are initiators for spray leaks and vessel spills. DOE has not completed the safety analysis for spray leaks or vessel spills, but has proposed control strategies for HPAV-initiated spray leaks with safety-related consequences. For piping used in some of the pipe routes in WTP, the HPAV control strategy relies on a passive pipe barrier to mitigate an HPAV event and prevent a spray leak or spill. DOE plans to use quantitative risk analysis to design this safety-related piping. The Board identified the following deficiencies with the control strategy for HPAV:

- DOE is using quantitative risk analysis to determine the adequacy of a safety control. However, DOE is not applying DOE Standard 1628, *Development of Probabilistic Risk Assessments for Nuclear Safety Applications*, to the quantitative risk analysis models.
- Because quantitative risk analysis calculations are used to demonstrate that a safety control is adequate to perform its credited safety function, DOE's proposed strategy is inconsistent with Subpart B of Title 10, Code of Federal Regulations (CFR) Part 830, *Nuclear Safety Management*.
- DOE has not defined how quantitative risk analysis input parameters will be maintained and protected to ensure the calculations remain valid over the life of the facility.

Instead of using quantitative risk analysis calculations to design passive safety controls, DOE has the option to credit HPAV preventive controls on pipe routes with safety-related spray consequences. DOE could complete a revised spray leak calculation to inform its decision process regarding the HPAV control strategy.

**Standard High-Solids Vessel Design.** Because many of the Board's longstanding safety issues stemmed from inadequate performance of the mixing systems, DOE's proposed path forward includes replacement of Pretreatment Facility process vessels that contain high solids concentrations with a new standard high-solids vessel design. DOE has begun full-scale testing of the standard high-solids vessel to verify the design and performance of the pulse jet mixing systems. However, the new safety control strategies do not rely on the pulse jet mixing systems as preventive controls to address hydrogen or criticality hazards. Therefore, the planned full-scale tests are not designed to verify the effectiveness of the safety-related controls in the strategies. For example, the test program does not address the safety-related aspects of the sparge system or the vessel heel cleanout operations.

DOE must identify and implement effective safety strategies for flammable gas and criticality hazards to assure safe operation of the Pretreatment Facility. This Technical Report provides an analysis of DOE's proposed control strategies to address issues associated with flammable gas and criticality hazards in the Pretreatment Facility.

## ACRONYMS

ANS	American Nuclear Society
ANSI	American National Standards Institute
AoA	area of applicability
BNI	Bechtel National, Incorporated
CAD	computer-aided design
CFR	Code of Federal Regulations
CSE-ES	criticality safety evaluation engineering study
DCP	double contingency principle
DOE	Department of Energy
DSA	documented safety analysis
EM	Environmental Management
FRP	waste feed receipt process
HGR	hydrogen generation rate
HLP	high-level waste lag storage and feed blending process
HLW	high-level waste
HPAV	hydrogen in piping and ancillary vessels
HPP	heavy plutonium particulate
HSLs	half-scale lag storage
LANL	Los Alamos National Laboratory
LFL	lower flammability limit
MSM	minimum subcritical margin
ORP	Office of River Protection
PDSA	preliminary documented safety analysis
PFP	Plutonium Finishing Plant
PJM	pulse jet mixer
PNNL	Pacific Northwest National Laboratory
PRA	probabilistic risk analysis
PSD	particle size distribution
PT	Pretreatment Facility



PVP	pretreatment vessel vent process
PVV	process vessel vent exhaust
QRA	quantitative risk analysis
RANS	Reynolds-Averaged Navier-Stokes
SAC	specific administrative control
SHSV	standard high-solids vessel
SPB	sodium pentaborate
SRD	safety requirements document
SRNL	Savannah River National Laboratory
SSC	structures, systems, and components
S/U	sensitivity and uncertainty (analysis)
TSR	technical safety requirements
TWCSF	Tank Waste Characterization and Staging Facility
UFP	ultrafiltration process
UHGR	unit hydrogen generation rate
USL	upper subcritical limit
USQ	unreviewed safety question
VSL	Vitreous State Laboratory
WAC	waste acceptance criteria
WTP	Waste Treatment and Immobilization Plant
ZOI	zone of influence

## TABLE OF CONTENTS

<b>1. INTRODUCTION</b> .....	1-1
<b>2. BACKGROUND</b> .....	2-1
<b>2.1 Design Challenges</b> .....	2-1
<b>2.2 Board Safety Issues</b> .....	2-2
<b>2.3 Recent Work</b> .....	2-3
<b>3. HYDROGEN GENERATION AND ACCUMULATION IN PROCESS VESSELS</b> .....	3-1
<b>3.1 Issue Summary</b> .....	3-1
<b>3.2 Sparger Effectiveness</b> .....	3-4
<b>3.3 Sparger Reliability</b> .....	3-6
<b>3.4 Low-Solids Vessels</b> .....	3-7
<b>3.5 Verification of Limiting Process Conditions</b> .....	3-13
<b>4. CRITICALITY IN PROCESS VESSELS</b> .....	4-1
<b>4.1 Issue Summary</b> .....	4-1
<b>4.2 Upper Subcritical Limit</b> .....	4-4
<b>4.3 Mass Control</b> .....	4-6
<b>4.4 Soluble Neutron Poison</b> .....	4-9
<b>4.5 Tank Waste Assumptions</b> .....	4-11
<b>5. HYDROGEN IN PIPING AND ANCILLARY VESSELS</b> .....	5-1
<b>5.1 Issue Summary</b> .....	5-1
<b>5.2. DOE Standard 1628 Applicability</b> .....	5-3
<b>5.3. Relationship of QRA to the Safety Basis</b> .....	5-4
<b>5.4. Maintenance and Protection of QRA Input Parameters</b> .....	5-5
<b>6. CONCLUSIONS</b> .....	6-1
<b>REFERENCES</b> .....	R-1
<b>Appendix A - Gas Retention and Release in Low Solids Vessels</b> .....	A-1
<b>Appendix B - Dependence of Hydrogen Generation Rate and Time-to-Lower Flammability Limit on Settled Fraction in Low-Solids Vessels</b> .....	B-1
<b>Appendix C - Hydrogen Generation in Standard High-Solids Vessel Following Loss of Agitation</b> .....	C-1

## 1. INTRODUCTION

On January 24, 2017, the Acting Assistant Secretary for Environmental Management transmitted a letter to the Defense Nuclear Facilities Safety Board (Board) describing progress made to address safety issues with the Pretreatment (PT) Facility at the Waste Treatment and Immobilization Plant (WTP) [1]. In the enclosures to the letter, the Department of Energy (DOE) describes resolution strategies for longstanding technical issues, which address the following Board safety issues:

- Generation and accumulation of hydrogen in process vessels;
- Heat transfer analysis for process vessels;
- Criticality in process vessels; and
- Hydrogen in piping and ancillary vessels (HPAV).

DOE considers the work done on these issues sufficient to resume design in areas of the PT Facility affected by these safety issues. The Board reviewed DOE's proposed nuclear safety strategies and identified deficiencies with them. This Technical Report provides an analysis of DOE's proposed control strategies to address safety issues associated with flammable gas and criticality hazards in the PT Facility.

## 2. BACKGROUND

### 2.1 Design Challenges

DOE is designing and building WTP to treat 56 million gallons of radioactive waste stored in 177 underground tanks at the Hanford site near Richland, Washington. WTP includes four primary nuclear facilities: the Analytical Laboratory, Low-Activity Waste (LAW), High-Level Waste (HLW), and PT Facilities. The PT Facility is designed to receive the Hanford tank waste and separate it into two streams for immobilization at the LAW and HLW Facilities.

Hanford tank waste presents unique design challenges and hazards. The waste generates hydrogen and other flammable gases through radiolysis and thermolysis. Hanford waste slurries also possess rheological properties that further complicate processing, e.g., some waste types exhibit a shear strength. Because of these rheological properties, high-solids Newtonian and non-Newtonian wastes can retain generated hydrogen. In addition, the solids contained in the waste can settle out if not adequately agitated.

The design of the PT Facility uses a black cell concept. Each black cell is a room in the PT Facility that is designed to be inaccessible during its 40-year design life. The black cells contain the vessels and piping necessary to process the waste. Components located in a black cell are intended to be maintenance-free for the life of the PT Facility. This limitation requires that the mixing systems have no moving parts. Therefore, the PT Facility design uses pulse jet mixers (PJM) rather than conventional mechanical agitators with rotating impellers [2].

The following hazards arise from the challenges associated with the characteristics of Hanford waste and the limitations of the PT Facility design, as noted in the Board's 27<sup>th</sup> Annual Report to Congress [3]:

- Solids could accumulate in process vessels as a result of inadequate PJM mixing, leading to the retention of hydrogen in the unmixed waste volume. If a sufficient quantity of hydrogen accumulates in the waste and releases rapidly, the concentration of flammable gas in the vessel headspace could exceed the lower flammability limit (LFL) and potentially ignite and explode. The explosion could rupture the vessel and initiate a spill or spray release.
- Fissile materials could accumulate in the bottom of the process vessels as a result of inadequate PJM mixing. Particles of fissile material could separate from neutron absorbers intrinsic to the waste and subsequently accumulate to pose a criticality hazard.
- Flammable gases could collect in process piping and ancillary vessels (i.e., non-process vessels) when waste stagnates (e.g., stoppage of flow in pipes). Hydrogen accumulation in concentrations greater than the LFL has the potential to ignite and explode within a pipe or component. The explosion could rupture the pipe or component and initiate a vessel spill or pipe spray release.

## 2.2 Board Safety Issues

The Board first identified an issue with hydrogen accumulation and potential explosions in process piping and ancillary vessels in its June 2009 Quarterly Report to Congress [4]. In February 2010, the DOE Office of River Protection (ORP) approved a revised design approach for the HPAV hazard, which incorporated quantitative risk analysis (QRA). The Board first communicated concerns with the revised approach, including the use of QRA, in its April 15, 2010, Quarterly Report to Congress [5]. The Board has communicated additional concerns with the revised strategy in subsequent reports to Congress.

In a January 6, 2010, letter to DOE, the Board identified safety issues related to the inadequate performance of PJM systems at WTP [6]. The letter identified safety issues related to potential nuclear criticality accidents and hydrogen accumulation in process vessels. In the letter, the Board stated that dense particles rich in plutonium could settle preferentially on the bottom of process vessels. The settled particles could accumulate to pose a criticality hazard. Additionally, samples drawn from inadequately mixed vessels would not be representative and therefore could not be relied upon to ensure such an event does not occur. The Board also stated that inadequate mixing could result in the accumulation of flammable gas. If enough gas is retained in the waste, it could release episodically creating a flammable condition in the vessel headspace and explode if ignited.

On December 17, 2010, the Board transmitted Recommendation 2010-2, *Pulse Jet Mixing at the Waste Treatment and Immobilization Plant*, calling on the Secretary of Energy to address the inadequate performance of the mixing systems [7]. The Board concluded that inadequate mixing could lead to the accumulation of solids in process vessels, potentially resulting in nuclear criticality accidents. The Board also concluded that inadequate mixing could lead to the accumulation of hydrogen and potentially result in explosions. At the time, DOE was relying on small-scale testing and computer simulations to demonstrate mixing performance. Therefore, in Recommendation 2010-2, the Board included a sub-recommendation for DOE to develop a large-scale mixing test plan.

In an August 3, 2011, letter to DOE, the Board identified safety issues related to the heat transfer calculations used by the WTP project in establishing post-accident hydrogen mixing requirements [8]. These requirements establish the mixing frequency necessary to release accumulated hydrogen and prevent explosions in PT Facility process vessels.

In 2012, DOE restricted engineering, procurement, and construction work at the PT and HLW Facilities due to unresolved safety issues and misalignment between the design and the nuclear safety basis. On September 24, 2013, DOE released the *Hanford Tank Waste Retrieval, Treatment, and Disposition Framework*, which describes an alternative approach for addressing the risks and challenges associated with completing the Hanford tank waste clean-up [9]. The Framework included the Tank Waste Characterization and Staging capability to stage, sample, mix, and characterize waste feed to WTP to ensure the feed meets the WTP waste acceptance criteria (WAC) [10]. The Framework also discussed a technical issue resolution plan that included full-scale vessel testing. In a December 2013 briefing to the Board, DOE communicated a new technical approach to resolve safety issues with PJM mixing, which

included replacement of PT Facility process vessels that will contain high solids concentrations with a standard high-solids vessel (SHSV) design.

Based on these developments, the Board determined that DOE's revised technical approach differed significantly from the technical basis upon which Recommendation 2010-2 was originally constructed, such that individual sub-recommendations were no longer relevant. In a January 28, 2014, letter to the Secretary of Energy, the Board closed Recommendation 2010-2, but also stated that the underlying safety issues with PJM mixing, which included hydrogen and criticality in vessels, remained unresolved [11].

### **2.3 Recent Work**

In 2016, DOE focused on resolving the safety issues associated with hydrogen in process vessels, criticality in process vessels, and HPAV. Bechtel National, Incorporated (BNI), personnel developed a series of engineering studies and calculations to identify nuclear safety control strategies for these issues. The Board reviewed the proposed strategies in October 2016 and held follow-on discussions with DOE and BNI personnel. On December 8, 2016, the Board communicated the conclusions from its review in a closeout meeting with personnel from DOE ORP, the DOE Office of Environmental Management (EM), and BNI.

On November 21, 2016, the ORP manager sent a memorandum to the Assistant Secretary for Environmental Management (EM-1) stating that ORP had resolved the criticality safety issue [12]. The ORP manager transmitted a resolution memorandum on hydrogen generation and accumulation, including the heat transfer calculations, to EM-1 on December 2, 2016 [13]. Lastly, on December 19, 2016, the ORP manager submitted a memorandum to EM-1 stating that the HPAV issue was resolved [14]. All three memoranda communicated that ORP had determined that the WTP project was ready to resume engineering work to complete PT Facility design in areas affected by these safety issues. Also in December 2016, DOE began full-scale testing of the SHSV design [12] [13].

On January 24, 2017, the acting EM-1 transmitted a letter to the Board stating that the WTP project had made significant progress in addressing issues associated with: the generation and accumulation of hydrogen and inadvertent criticality in PT Facility process vessels; HPAV; and heat transfer analysis [1]. The letter concluded that DOE and BNI had performed a comprehensive set of work activities that provided DOE with sufficient confidence to direct the resumption of PT Facility design activities affected by these safety issues.

The Board has reviewed DOE's proposed nuclear safety strategies and developed this Technical Report.

### **3. HYDROGEN GENERATION AND ACCUMULATION IN PROCESS VESSELS**

On January 24, 2017, the acting EM-1 transmitted a letter to the Board stating that the WTP project had made significant progress in addressing the Board's safety issues associated with the generation and accumulation of hydrogen in PT process vessels, as well as heat transfer analysis [1]. In the letter, DOE proposes a new control strategy for hydrogen explosion events in PT process vessels equipped with PJMs. The control strategy is described in more detail in BNI's engineering study [15].

The Board reviewed the control strategy and identified deficiencies. Specifically, the air sparge system may not be an effective preventive control given previous test data showing the presence of a significant unmixed heel. Additionally, DOE has not yet addressed the long-term reliability of the sparge system to ensure its operability when called upon to perform its safety function. The analysis supporting the control strategy for low-solids vessels contains unverified assumptions. Finally, DOE has not yet specified how waste parameters important to the control strategy will be verified during operations.

#### **3.1 Issue Summary**

Hanford tank waste generates hydrogen and other flammable gases through radiolysis and thermolysis. The release mechanism of hydrogen in process vessels from the waste to the vessel headspace depends on the waste rheology. Hydrogen releases continuously from well-mixed waste (i.e., non-episodic release). Non-Newtonian waste, as well as settled Newtonian waste containing solids, retain generated hydrogen until the waste is agitated or a spontaneous gas release occurs (i.e., episodic release). If a sufficient quantity of hydrogen accumulates in the waste and releases quickly, such that the vessel headspace concentration exceeds the LFL, the potential for a deflagration or detonation exists. Hydrogen explosions in the process vessel headspaces can result in dose consequences challenging the evaluation guideline and requiring safety class controls.

To address hydrogen explosion hazards in PT Facility process vessels, the WTP project previously used a preventive control strategy for off-normal and post-accident conditions. The original control strategy relied on periodic PJM operation to agitate the waste and prevent hydrogen accumulation. It also credited a forced air purge system to maintain the hydrogen concentration in the vessel headspace below the LFL.

The revised hydrogen control strategy relies on preventive and mitigative controls to provide an adequate level of risk reduction to ensure adequate protection of the public [15]. The selected engineered and administrative controls are based on waste and vessel types (see Table 3.1). The hydrogen control strategy distinguishes vessels in the PT Facility as either "high-solids" or "low/no-solids" based on their solids loading and anticipated rheology. The low/no-solids vessels include vessels already installed in the PT Facility. These vessels are designed to contain liquids or have lower concentrations of solids. The high-solids vessels are those using the SHSV design and include "high-solids Newtonian vessels" and "non-Newtonian vessels." The high-solids Newtonian vessels have significant solids loadings where the solids can settle

under the effects of gravity and can be difficult to re-suspend. The non-Newtonian vessels are anticipated to contain slurries, which exhibit a yield stress and do not easily settle.

**Table 3.1.** Safety controls for hydrogen explosions in PJM process vessels.

<b>Strategy</b>	<b>Control</b>	<b>Episodic Release in High-solids Newtonian and Non-Newtonian Vessels</b>	<b>Episodic Release in Low-solids Newtonian Vessels</b>	<b>Non-Episodic Release in High- and Low-solids Newtonian Vessels</b>
<b>Preventive</b>	SHSV to minimize material at risk	√		High-solids vessels
	Spargers and air supply systems to agitate the waste to prevent hydrogen accumulation	√		
	Active ventilation of vessel headspace by forced air purge and PVV/PVP systems	√	√	√
	Control sparging frequency	√		
	Batch processing plan (waste/vessel headspace volume control)	√	√	√
	Control hydrogen generation rate	√	√	√
	PJM restart sequence	√	√	√
<b>Mitigative</b>	SHSV for confinement	√		High-solids vessels
	PVV/PVP systems for confinement and filtration	√	√	√
	Applicable facility structure (e.g., black cells) and C5V confinement ventilation system for confinement and filtration	√	√	√
<b>Defense-in-Depth</b>	PJM operations	√	√	√



The preventive component of the revised strategy is intended to maintain the hydrogen concentration in the vessel headspace below LFL for off-normal and post-accident conditions. It does not credit PJMs as a control. For high-solids vessels, the strategy relies on periodic operation of an air sparge system to provide sufficient agitation to release hydrogen from the waste. For low-solids vessels, it does not include a control to prevent gas buildup in the waste. For all vessel types, the preventive strategy also relies on the process vessel vent exhaust and pretreatment vessel vent process (PVV/PVP) systems to maintain hydrogen concentration in the vessel headspace below LFL. The control strategy incorporates an assumption that, once the hydrogen releases from the waste, it completely and instantaneously mixes with the air already present in the headspace.

The mitigative component of the revised strategy is intended to confine hazardous materials and reduce the consequences of an explosion. It imposes challenging safety requirements on the SHSV and PVV/PVP systems to maintain confinement following a deflagration or detonation event. The mitigative portion of the control strategy does not prevent damage from explosion events to safety structures, systems, and components (SSC) located either within or in proximity to these safety systems. Also, the control strategy does not identify means to “monitor facility conditions during and after an event, and provide for response to accidents to achieve a safe condition,” as required by DOE Order 420.1B, *Facility Safety*.

The WTP Safety Requirements Document (SRD) addresses the functional requirements for hydrogen control systems [16]. The SRD states that safety controls are required for process vessels with a time to reach LFL (i.e., time-to-LFL) less than or equal to 1,000 hours. To support the previous hydrogen control strategy, BNI personnel calculated the hydrogen generation rates (HGR) and times-to-LFL for PT Facility process vessels. They planned to use these calculations to establish the mixing frequency to release hydrogen from the waste. These calculations involved performing heat transfer analyses to obtain time-dependent waste temperatures during off-normal conditions for 1,000 hours, assuming loss of agitation [17]. BNI personnel used these temperatures as input to the HGR correlation [18]. In an August 3, 2011, letter to DOE, the Board identified issues with the modeling assumptions, input parameters, and methodology used in the heat transfer calculations [8]. To address the Board’s safety issues, the revised control strategy no longer relies on heat transfer calculations to establish agitation frequency. Instead, it uses the HGR specified in the WAC [10]. However, BNI analysts used heat transfer calculations to analyze gas retention and release in low-solids vessels [15].

The SHSV mixing system is designed to handle both Newtonian and non-Newtonian slurries. The SHSVs are 16 feet in diameter and have a normal operating capacity of about 22,000 gallons of waste with a headspace volume of about 16,000 gallons [15]. The SHSV design incorporates an array of six downward firing PJMs. The design includes 13 air sparge tubes (i.e., spargers) as a supplemental mixing system. The spargers are effective at mixing the upper region of the waste, whereas the PJMs generate a high mixing intensity in the lower region of the vessel. The hydrogen control strategy specifies neither the air flowrates through the spargers nor the operating frequency to prevent hydrogen accumulation.

The Board identified several deficiencies in the hydrogen control strategy. The deficiencies are summarized below and discussed in detail in the following sections.

*Sparger effectiveness*—The air sparge system may not be an effective preventive control given previous test data showing the presence of a significant unmixed heel. Estimates of the size of the unmixed sparge heel rely on previously obtained data for a different vessel design.

*Sparger reliability*—DOE has yet to address the long-term reliability of the sparge system to ensure its operability when called upon to perform its safety function.

*Low-solids vessels*—The strategy for control of hydrogen in low-solids Newtonian vessels relies on a specific administrative control (SAC) on vessel level. The analysis supporting the SAC contains unverified assumptions such as the settling rate of solids, solids layer thickness, and gas generation rate during settling.

*Verification of limiting process conditions*—The hydrogen control strategy, while relying on waste properties, does not specify how these properties will be verified during plant operations. The control strategy does not identify which process parameters require monitoring or how the process parameters will be monitored.

### **3.2 Sparger Effectiveness**

The SHSV will have a significant unmixed heel during sparge-only operation [15]. Flammable gas could build up in the unmixed heel and episodically release into the vessel headspace, posing an explosion hazard. To account for the presence of an unmixed sparge heel, DOE included SACs for process vessels implementing the SHSV design. These SACs would ensure the total volume of hydrogen generated and retained in the heel during off-normal conditions would not exceed the LFL if the gas were released into the vessel headspace. The volume of the unmixed sparge heel is a key input for defining these SACs. The Board is concerned that DOE's unmixed heel volume estimates may not be conservative.

Pacific Northwest National Laboratory (PNNL) previously performed testing of the half-scale lag storage (HLS) vessel design that showed a significant unmixed sparge heel [20]. As part of these tests, PNNL also developed a methodology to estimate the sparge heel volume [20]. The method involves using a correlation for sparge mixing effectiveness together with a three-dimensional computer-aided design (CAD) model of the vessel. This correlation is based on single sparge tube testing in a cone-bottom vessel [19]. The correlation gives the zone of influence (ZOI) as a function of depth for a single sparge tube operating at various flow rates. The ZOI is the region of mobilized fluid around a single sparge tube during operation. Within the ZOI, the waste is mobilized, while outside of the ZOI, the waste is stagnant. The volume outside of these mixed regions can be interpreted as the unmixed heel volume.

Figure 3.1 shows the result of the ZOI/CAD model for the HLS [20]. The egg-crate-shaped sparge heel (shown in yellow in Figure 3.1) results from the parabolic shape of the mobilized region predicted for each sparge tube. The HLS test vessel design had similarities to the current SHSV design. Therefore, DOE used a similar ZOI/CAD methodology to estimate the sparge heel volume in the SHSV.

Table 3.2 shows results from the HSLs tests and the HSLs ZOI/CAD model. These results show the ZOI/CAD method under-predicts the measured heel volume by a factor of two for the HSLs tests. The HSLs tests showed a sparge heel volume of 1,808 gallons, or 25.8 percent of the vessel volume. The ZOI/CAD model applied to the HSLs vessel resulted in a sparge heel volume of 898 gallons, or 12.8 percent of the non-PJM volume.

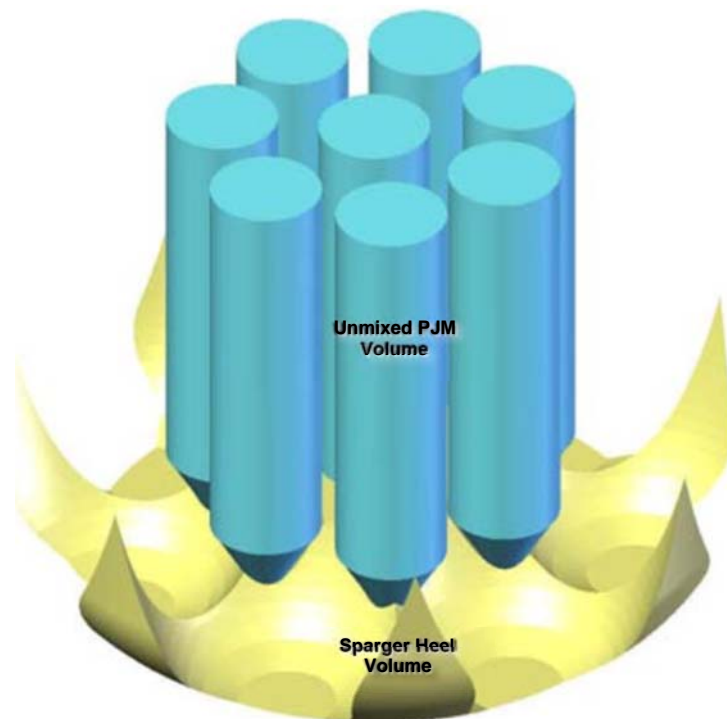


**Figure 3.1.** *Unmixed regions in the sparge heel and PJMs from the ZOI/CAD model for the HSLs mixing system (adapted from Appendix B of [20]).*

Table 3.2 also shows the results of DOE’s ZOI/CAD analysis for the SHSV. BNI calculated an unmixed sparge heel volume of 2,174 gallons (12.2 percent of the non-PJM volume). These calculations assume normal batch volumes. Given the similarities in the vessel designs and the predicted sparge heel volumes, BNI concluded that assuming an SHSV sparge heel volume of 25.8 percent of the non-PJM volume is conservative [15].

The Board is concerned that the basis for assuming 25.8 percent is not conservative. HSLs test results showed the measured unmixed volume was as high as 42 percent of total volume [20]. This suggests the measured heel volume could be larger than the modeled heel volume by a factor of about 2.4.

The Board identified additional assumptions that suggest the unmixed heel volume of 25.8 percent may not be conservative. The waste volume shown in Table 3.2 for the SHSV is the normal batch volume. For the maximum operating volume, BNI’s analysis indicated the sparge heel would be about 17 percent larger [15]. This is due to the reduction in sparger air flowrate resulting from increased hydrostatic pressure due to the increased waste level. Also, BNI’s analysis assumed all sparge tubes were operable. The assumption may not be

conservative, because the project has yet to demonstrate that all sparge tubes will be fully operable during off-normal or post-accident conditions (see discussion in Section 3.3).

The Board also notes that the relationship between the actual sparge heel volume and the volume computed using the ZOI/CAD method may not be the same for the HSLs and SHSV designs. Differences in vessel geometry, PJM layout, the number of sparge tubes, individual sparger air flowrates, and test vessel scales could potentially influence the relationship. Further, the SHSV must also operate in the high-solids Newtonian regime. The previous HSLs testing did not include sparge heel measurements with high-solids Newtonian simulants. Hence, these tests do not provide an adequate technical basis for determining the sparge heel in the SHSV for high-solids Newtonian conditions.

Measuring the sparge heel in the SHSV during the full-scale test program could eliminate the significant uncertainties discussed above and establish a conservative value for the sparge heel volume. Methods similar to those used previously in the HSLs program, such as the chloride tracer technique, could provide sufficient information to accurately determine the volume of the sparge heel.

**Table 3.2.** *Heel volume data from previous HSLs testing and the current SHSV analysis.*

<b>Volume</b>	<b>HSLs Sparge Mixing Tests</b>	<b>HSLs ZOI/CAD Model<sup>a</sup></b>	<b>SHSV ZOI/CAD Model<sup>c</sup></b>
Total volume (gallons)	8,395	8,395	22,059
PJM volume (gallons)	1,382	1,382	4,193
Non-PJM volume (gallons)	7,013	7,013	17,866
Heel volume (gallons)	1,808	898	2,174
Unmixed volume (heel + PJMs) (gallons)	3,190	2,280	6,367
Unmixed volume percent	38.0 <sup>b</sup>	27.2	28.9
Heel volume percent (excluding PJMs)	25.8	12.8	12.2

a) Values reported in Appendix B of [20].  
b) The average of measurements reported in [20] is 37 percent; Appendix M of [15] reports 38 percent.  
c) Values reported in Appendix M of [15] for normal batch operation.

### 3.3 Sparger Reliability

The spargers are the only credited safety system for the release of accumulated hydrogen gas generated in the waste in the SHSV. DOE Order 420.1B requires that safety SSCs “must be designed, commensurate with the importance of the safety functions performed, to perform their safety functions when called upon...” DOE has yet to demonstrate the long-term reliability of the sparge systems to ensure their operability when called upon to perform their safety function.

The Board considers sparger plugging to be a significant vulnerability. There are known instances of sparger plugging during testing with Hanford waste simulants. During aerosol testing conducted by Parsons Constructors and Fabricators, Incorporated, spargers experienced plugging in small-scale and medium-scale testing [21]. BNI attributed an increase in aerosol

production to air jetting through the restricted sparge tubes due to plugging. In its March 25, 2015, letter to DOE, the Board expressed concern with the sparger plugging during the aerosol testing [22].

Spargers also plugged during testing with melter feed simulants at the Vitreous State Laboratory (VSL) [23]. The VSL report notes that “[d]uring the testing with the high bound melter feed, two of the air spargers became clogged and had to be cleared with the 1,300 psi pressure washer.” The high bound melter feed simulant was a clay simulant with a yield stress of 27 Pa ( $3.9 \times 10^{-3}$  psi), which is similar to the rheology anticipated in the non-Newtonian vessels using the SHSV design.

After the Parsons aerosol testing observed sparger plugging, DOE requested that Savannah River National Laboratory (SRNL) provide consultation on the WTP bubbler, and air and steam sparger issues [24]. SRNL staff concluded in their report that the exact cause of sparger plugging is unknown, and may depend on the combined chemical composition of slurries as well as specific operating conditions. SRNL further noted that “BNI should provide a basis for the air sparger purge rate being sufficient to prevent plugging of the air spargers and a plan for establishing the frequency of cleaning operations and capabilities.”

From a mechanistic perspective, one possible explanation for sparger plugging is that bubble formation at the sparger nozzle results in an unsteady interface between the waste and the air. This could result in backwash or splatter, which could continuously coat the inside of the sparger nozzle with fresh slurry. As the air flows past this coated surface, any resulting evaporation of water from the slurry would increase the local solids concentration. For non-Newtonian slurries, the yield stress is a strong function of water content. Hence, it is reasonable that a high yield stress coating could continue to grow, ultimately plugging the sparge tube nozzle. The BNI report proposed a similar mechanism for sparger plugging [21]. This mechanism would suggest plugging may be inherent to sparger operation.

During the Board’s review of the hydrogen control strategy, BNI personnel expressed confidence that a robust means to prevent sparger plugging would be determined in the future using some combination of humidified sparge air and/or water or chemical flushes. A demonstration of the proposed solution for plugging prevention and/or mitigation methods for the spargers is warranted given the importance of the spargers as a credited safety system. The current hydrogen control strategy assumes all the spargers are operational on demand during off-normal and post-accident conditions. If some of the spargers are not operational, there could be a significantly larger unmixed sparge heel with the potential to cause flammable headspace conditions. Further, the support systems for sparger effectiveness, including unplugging methods, could become important safety features.

### **3.4 Low-Solids Vessels**

The control strategy for low-solids Newtonian vessels relies on a specific administrative control (SAC) on vessel level to prevent flammable conditions in the headspace. The analysis supporting the SAC contains unverified assumptions regarding gas generation and retention in the settling solids layer during off-normal and post-accident conditions. The Board performed an

independent analysis and concluded that the strategy of limiting waste volume in the low-solids vessels is viable. However, it is unclear if the assumptions employed in the BNI analysis are sufficiently conservative. A more technically defensible determination of a safe vessel fill level could ensure a flammable headspace is not credible. This could be accomplished by collecting data from measurements of gas retention and release behavior of settling slurries under a range of low-solids conditions, together with more representative modeling of hydrogen generation in settling solids layers.

The hydrogen control strategy identifies different sets of controls for high-solids and low-solids vessels. For example, the low-solids vessels do not rely on spargers to agitate the waste to prevent hydrogen accumulation during off-normal and post-accident conditions. The Board found that the technical basis for distinguishing low-solids vessels from high-solids vessels was unclear. The Board performed calculations showing that, during loss of mixing in the low-solids vessels, the concentration of solids increases in the settling solids layer to concentrations comparable to the high-solids vessels. The increased solids concentration could result in hydrogen retention. Figure 3.2 shows the calculated solids loading in the settling layer for the FRP-VSL-00002A/B/C/D vessels as a function of the settling layer height.

DOE considers the waste feed receipt vessels, FRP-VSL-00002A/B/C/D, to be low-solids Newtonian vessels. These vessels use the original vessel design and have a design basis solids loading of 3.8 weight percent [25]. The FRP-VSL-00002A/B/C/D vessels are very large, with a diameter of 47 feet and nominal fill height of approximately 30 feet [15]. DOE considers the ultrafiltration feed preparation vessels, UFP-VSL-00001A/B, to be high-solids Newtonian vessels. These vessels use the SHSV design and have an anticipated solids loading of 6.2 weight percent [27]. At these solids concentrations, the Hanford waste has exhibited zone settling behavior where the solids form a settling solids layer that compresses downward from the top of the vessel with time. Experiments have shown significant settling prior to the 1,000-hour time-to-LFL limit [26]. As settling continues, the average solids loading within the settling layer increases along the blue line shown in Figure 3.2.

Figure 3.2 also shows two additional high-solids Newtonian vessels: the ultrafiltration feed vessels UFP-VSL-00002A/B and the HLW feed receipt vessels HLP-VSL-00022A/B/C. These vessels have solids loadings of 10, and 13.3 weight percent, respectively [27]. The vessels that use the SHSV design are filled to nominally 16 feet. Note that when the solids in the FRP-VSL-00002A/B/C/D vessels have settled to 16 feet, the settling solids layer has an average solids loading of 7.0 weight percent, a value within the range of the SHSV vessels. As settling continues, the solids loading within the settling solids layer continues to rise. After loss of mixing in the FRP-VSL-00002A/B/C/D vessels, the solids loading in the settling solids layer is sufficiently high to retain hydrogen, similar to the SHSV vessels.

The SHSV design incorporates sparge mixing to prevent unsafe hydrogen accumulations, whereas the FRP-VSL-00002A/B/C/D vessels do not have this capability. The hydrogen control strategy for low-solids vessels identified a SAC that ensures the FRP-VSL-00002A/B/C/D vessel waste level remains below an identified threshold [15]. The reduced waste level creates additional headspace that allows for the time-to-LFL to increase. DOE and BNI are also considering physical modifications to these vessels to lower the vessel overflows to ensure the

waste level does not exceed the threshold value. Because limiting waste volume is the primary control for preventing a flammable headspace, the technical rigor underpinning this SAC on vessel level is vital.

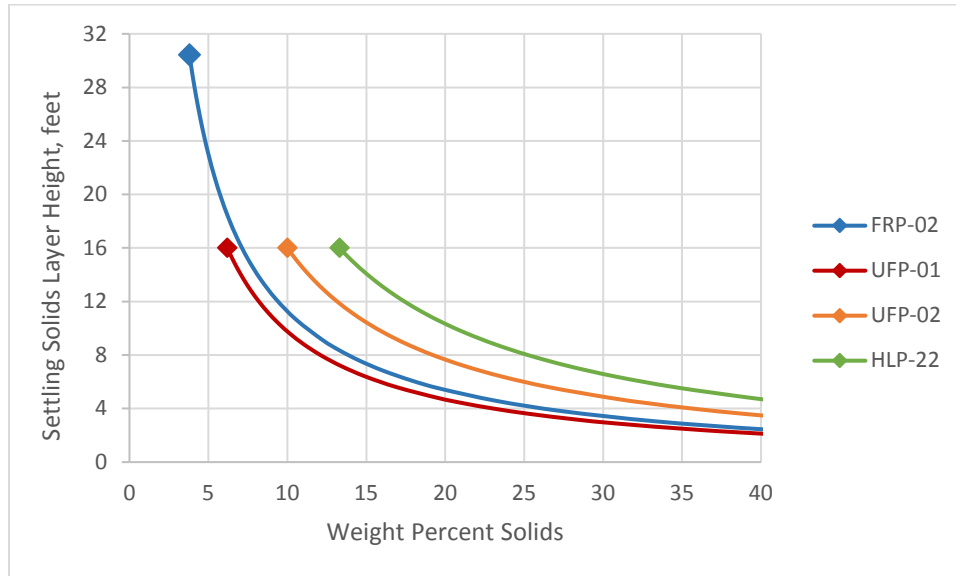


**Figure 3.2.** Calculated solids loading in the settling solids layer in the FRP-02 vessels as a function of solids layer height. Shown also for comparison are three of the high-solids vessels using the SHSV design.

BNI documented the technical basis for the SAC on vessel level in Appendix K of the engineering study [15]. The BNI analysis models gas generation and build-up in a settling solids layer, and calculates the time to accumulate sufficient hydrogen in the solids layer to reach the LFL in the headspace for the instantaneous release of hydrogen. The analysis contains several modeling assumptions that may be non-conservative. In particular, the Board notes three areas where the analysis may be non-conservative:

- The BNI analysis assumes the solids settle to a thin layer, which may not represent the conservative case for total hydrogen generated.
- The BNI analysis assumes the solids layer settles exponentially, and that most of the settling occurs in the first 300–400 hours. A slower settling rate would provide more time for hydrogen to be generated and retained as the solids layer settles.
- The BNI analysis assumed the unit hydrogen generation rate (UHGR) varied linearly between the value reported in the WAC [10] for the fully mixed vessel and a higher value derived from a heat transfer analysis for a stationary solids layer [17]. This may not be conservative based on the spatially and temporally changing solids distribution and the evolving heat transfer boundary conditions.

The Board independently analyzed gas retention and release from the settling solids layer in low-solids vessels to address potential non-conservatism (Appendix A). Some differences between the Board analysis and BNI’s analysis are shown in Table 3.3 and described in detail below.

**Table 3.3.** *Key phenomena and assumptions for the BNI analysis and the Board analysis.*

<b>Physical Characteristic</b>	<b>BNI Analysis</b>	<b>Board Analysis</b>
Fully settled solids layer thickness	Thin layer	Parametrically varied
Solids layer settling behavior	Exponential	Linear
UHGR spatial variation in solids layer	Linear	Linear, Calculated
Spontaneous gas release potential	Assumed to occur	Analyzed

The Board analysis uses a parametric approach for evaluating spontaneous gas releases in low-solids vessels during off-normal and post-accident conditions. It also provides a means of deriving conservative estimates of the waste volume below which the headspace will not exceed the LFL within 1,000 hours in low-solids vessels. The approach follows the method presented in a PNNL report (PNNL-24255), where the settling solids layer thickness is parameterized in terms of the fraction of solids settled [29]. This allows results to be obtained without making any assumptions about the thickness of the settling solids layer. The Board also used the stability criteria for spontaneous gas releases described in the PNNL report to evaluate the potential for gas releases in the settling solids layer in the FRP-VSL-00002A/B/C/D vessels.

To address the issue of the settling rate, the Board evaluated Hanford waste settling data. The data show that actual settling is reasonably approximated by an exponential function [26]. Because the time constant for the exponential function is not known for all waste, we used a linear function, which conservatively bounds the exponential function with respect to the amount of gas generated (see Figure A-3 of Appendix A). The Board conservatively assumed that the settling time to achieve a given fraction settled is 1,000 hours.

To determine how the settled fraction affects the amount of hydrogen generated in the solids layer in the FRP-VSL-00002A/B/C/D vessels, the Board calculated the UHGR using temperature distributions obtained for various fractions of solids settled (see Appendix B). The results of the calculation confirmed that, while the UHGR is higher for a more compacted solids layer, the total amount of generated hydrogen is smaller. Therefore, assuming an instantaneously settled thin solids layer is not conservative because it results in lower estimates of the total generated hydrogen volume during a mixing outage.

Figure 3.3 shows the results for our calculated UHGR at 1,000 hours as a function of the settled fraction. The Board obtained these results by curve-fitting the calculated UHGR values. The Board’s model assumes the UHGR is only a function of the settled fraction (i.e., it is not a function of time). This assumption is conservative because it uses the final UHGR at 1,000 hours for each intermediate settling fraction throughout the settling process. This assumption is discussed further below. Figure 3.3 also shows the linear UHGR assumption employed in Appendix K of the engineering study [15]. The Board analysis incorporated both the calculated UHGR and the linear UHGR assumption.



The Board calculated the retained gas fraction in the settled solids layer after 1,000 hours. The total gas retained is the combination of hydrogen and other gases. The Board compared the retained gas fraction with the stability criteria for two different spontaneous release mechanisms: bubble cascade and buoyant displacement gas release. Bubble cascade gas release occurs in weak sludges and depends on the local yield stress. The buoyant displacement gas release requires a stratified layer and occurs when the bulk density of the lower solids layer reaches that of the liquid above it. The Board's analysis indicated that for most conditions, one or both of the stability criteria for gas release were exceeded. The main factor affecting stability is the amount of generated non-hydrogen gas. Samples from Hanford waste tanks demonstrate the fraction of non-hydrogen gas varies considerably (Appendix H of [15]). A large non-hydrogen gas fraction results in a significant amount of total retained gas. This retained gas exceeds the stability limits for spontaneous gas releases during settling in the FRP-VSL-00002A/B/C/D vessels.

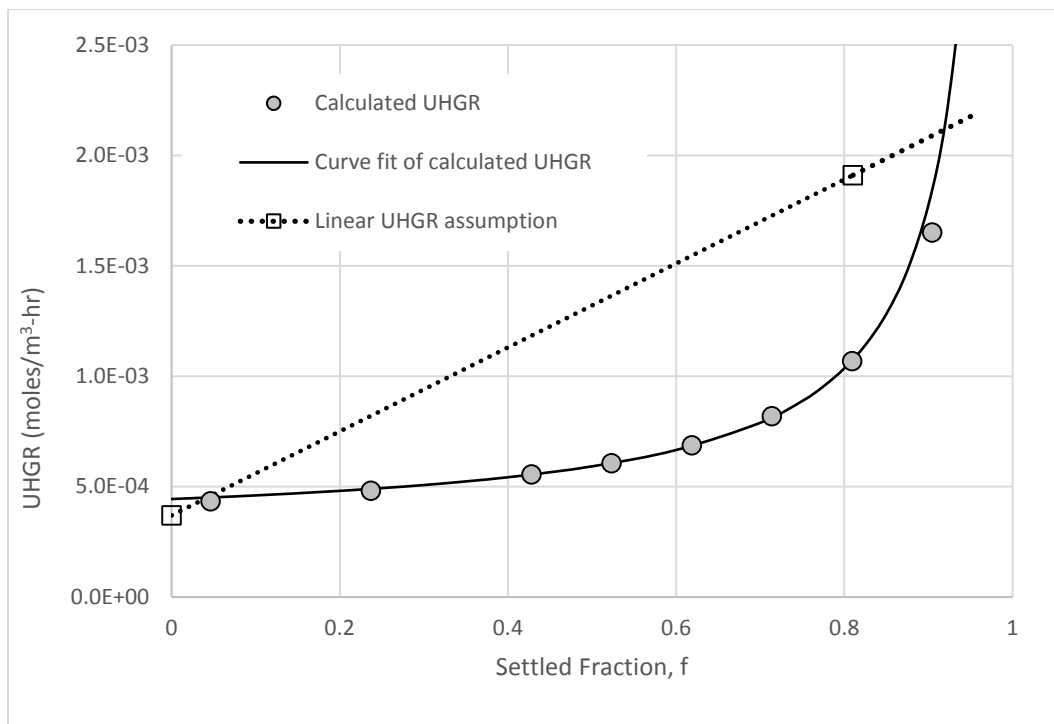


**Figure 3.3.** UHGR at 1,000 hours versus settling fraction from the Board's calculations (Appendix B) and the linear assumption used in Appendix K of [15].

The Board's analysis calculates the hydrogen gas concentration in the vessel headspace following an instantaneous release of gas retained in the settling solids layer. Figure 3.4 shows the headspace hydrogen concentration as a function of solids settling fraction. The figure includes two cases: the calculated UHGR and the linear UHGR assumption. Also, for comparison, Figure 3.4 shows the LFL for hydrogen. Figure 3.4 indicates that the LFL is exceeded for all fractions settled for both UHGR distributions. The settling fraction,  $f$ , corresponding to the maximum hydrogen headspace concentration depends on the UHGR distribution. For the linear assumption, the maximum occurs at  $f = 0.6$ . For the calculated UHGR, the maximum occurs at  $f = 0$  (no settling).

The Board also computed the time to reach LFL as a function of the settled fraction for different waste volumes. Table 3.4 presents the maximum values from our results for the two UHGR distributions. In addition, the table shows BNI's results. For the current maximum operating volume, the Board's analysis found the time-to-LFL was 375 hours for the linear UHGR. This is compared with 930 hours for similar conditions predicted by BNI's analysis. The main contributor to this difference is BNI's assumption of exponential settling behavior. Table 3.4 also shows the time-to-LFL for various operating volumes, including values analyzed by BNI. Reducing the operating volume not only decreases the amount of hydrogen generated, but also increases the headspace volume. Hence, the time-to-LFL increases considerably.

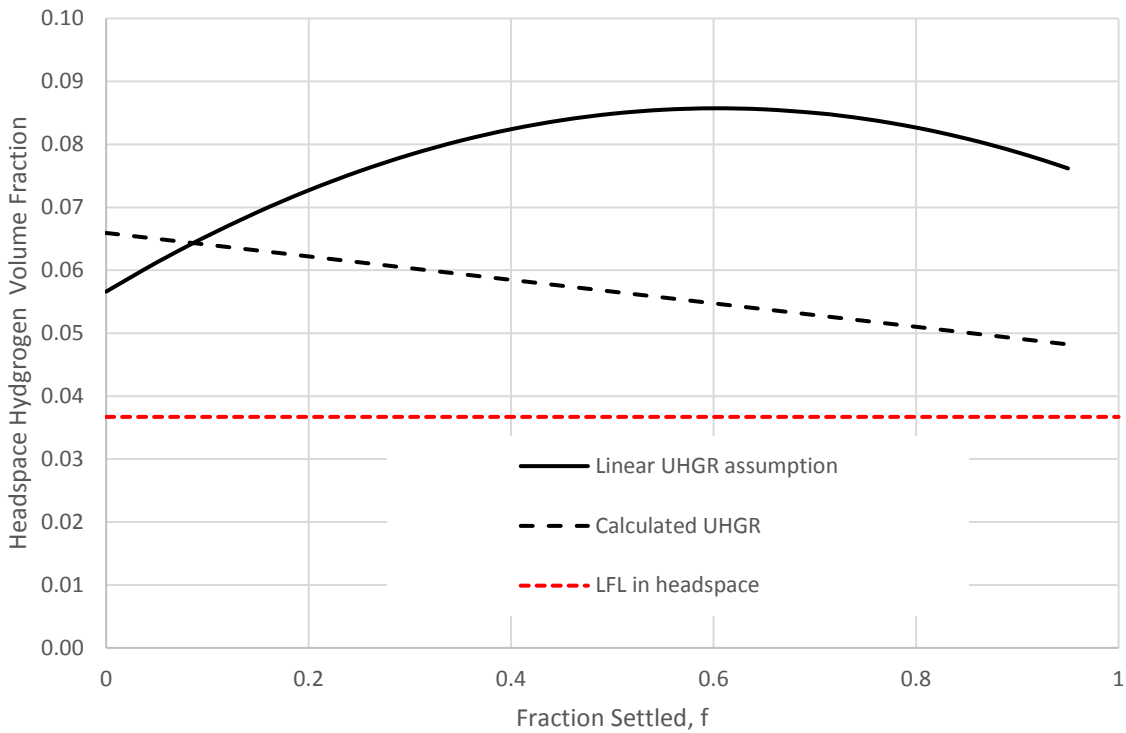


**Figure 3.4.** Predicted headspace hydrogen concentration after a spontaneous release at 1,000 hours for both cases of gas generation variations.

**Table 3.4.** *Computed time to reach the LFL in FRP-VSL-00002A/B/C/D vessels.*

Operating Volume, gallons	Operating Volume Reduction		Time to reach LFL in headspace, hours		
	gallons	percent	Linear UHGR	Calculated UHGR	Linear UHGR-BNI
391,000	0	0	375	508	930
380,000	11,000	3	435	588	1,260
298,000	93,000	24	1,014	1,372	–
254,000	133,000	34	1,432	1,940	7,030

The Board’s analysis predicts shorter times-to-LFL than the results obtained by BNI. The most significant factors affecting the results are the assumed UHGR distribution and the assumed settling rates. The linear UHGR profile yields more conservative results than the calculated UHGR. Both employ the conservative assumption that the 1,000 hour UHGR applies at all times during settling. However, it is not clear that either of these bound the actual UHGR because the heat transfer calculations assume stationary solids layers with uniform properties. A more accurate result would require a full transient heat transfer analysis of the settling solids layer, incorporating a more realistic distribution of solids within the settling layer.

The Board concludes that the strategy of limiting waste volume in the low-solids vessels is viable. DOE could ensure a flammable headspace is not credible by considerably reducing the operating volume in the FRP-VSL-00002A/B/C/D vessels. However, it is unclear if the assumptions employed in the BNI analysis are sufficiently conservative to establish safe vessel fill levels. BNI’s modeling of hydrogen generation and retention entails assumptions with limited supporting data. A more rigorous determination of a safe vessel fill level could ensure a flammable headspace is not credible. This could be accomplished by collecting data from measurements of gas retention and release behavior of settling slurries under a range of low-solids conditions, together with more representative modeling of hydrogen generation in settling solids layers.

### **3.5 Verification of Limiting Process Conditions**

Previously, BNI personnel relied on calculated UHGRs and time-to-LFL for PT Facility process vessels for establishing agitation frequency. These calculations involved performing heat transfer analyses to obtain time-dependent waste temperatures during off-normal conditions for 1,000 hours, assuming loss of agitation [17]. The Board identified issues with the modeling assumption, input parameters, and methodology used in the heat transfer calculations [8]. To address the Board’s safety issues, BNI’s revised control strategy no longer relies on the heat transfer calculations to establish agitation frequency. Instead, it uses the UHGRs for the waste feed specified in the WAC [10]. However, BNI analysts adjust these values for some vessels based on changes in process conditions (e.g., concentration, maximum operating temperature).

The UHGR depends on several factors, including radionuclide content, temperature, the solids-to-liquid ratio, concentration of organics, and concentration of key chemical constituents (e.g., nitrites, hydroxide, and aluminate) [18]. BNI also assumes that, during off-normal and

post-accident conditions, the waste in PT process vessels remains at or below the maximum operating temperature [15].

The Board performed a computational study to assess whether the UHGRs in PT process vessels during off-normal and post-accident conditions exceed those reported in the WAC (see Appendix C). The Board calculated the UHGR and the amount of hydrogen accumulated using the spatial and temporal distribution of the solid layer temperature during the first 1,000 hours following loss of agitation. The results of this study show that the temperature at the center of the solids layer increases during the first 1,000 hours following a loss of agitation. Hence, BNI's assumption that the temperature remains below the maximum operating temperature is not conservative. This temperature increase leads to an increase in the volumetric average UHGR. The Board concluded that using the bulk time-independent temperature and UHGR reported in the WAC may not be conservative for determining the sparging schedule.

The Board also found that the proposed hydrogen control strategy, while relying on assumptions for waste properties, does not specify how these properties will be verified and controlled during plant operations. The control strategy does not identify which process parameters require monitoring or how these process parameters will be monitored. Identification of limiting process conditions would support the implementation of the hydrogen control strategy. A limiting process condition in this context is any waste property (e.g., solids loading, rheological properties, temperature, gas generation rate) that must be maintained below the values assumed in the safety analysis.

## 4. CRITICALITY IN PROCESS VESSELS

DOE's January 24, 2017, letter to the Board describes a proposed control strategy to address the Board's safety issue with criticality in PJM vessels at the PT Facility [1]. DOE's strategy includes a series of engineering studies and calculations which address treatment of both co-precipitated plutonium and heavy plutonium particulate (HPP) wastes in the PT Facility. DOE's proposed controls for treatment of waste containing HPP are largely contained in BNI's criticality safety evaluation engineering study (CSE-ES) [30]. The strategy in the CSE-ES is dependent on many assumptions about the characteristics of Hanford tank waste. Therefore, to augment the strategy in the CSE-ES, DOE has proposed the Tank Waste Characterization and Staging Facility (TWCSF) to protect the assumptions and provide waste feed from the Hanford Tank Farms that complies with the WTP WAC [12] [31].

The Board reviewed the proposed strategy for treatment of HPP in the PT Facility and identified deficiencies. Our independent analysis shows that the criticality safety strategy in the CSE-ES is not fully developed. In particular, the Board finds that key assumptions regarding validation of the nuclear models used to define mass limits and implementation of the double contingency principle (DCP) lack sufficient technical rigor. The DCP is a mitigation and control strategy that requires two unlikely, independent, and concurrent changes in process conditions to occur for criticality to become possible [32].

Further, the Board questions the validity of many of the assumptions regarding the location, quantity, and properties of HPP in the tank farms. DOE has proposed TWCSF to characterize the waste and assure it complies with the WAC. However, DOE has not defined the functions and requirements for TWCSF or defined which waste streams will be fed through TWCSF. We determined that the proposed strategy does not provide an adequate basis for safely processing waste containing HPP in the PT Facility.

The Hanford System Plan states that all tank waste will be processed through WTP, which includes the tanks containing HPP [33]. However, DOE has not decided whether to direct an update to the WTP design basis to include treatment of HPP in the PT Facility [1]. DOE considers the work done on the criticality safety issue sufficient to resume design in affected areas of the PT Facility. Making the decision to update the design basis early would allow DOE to integrate the HPP control strategy into the design.

If BNI cannot establish compliance with American National Standards Institute/American Nuclear Society (ANSI/ANS) 8 series standards for the proposed strategy, BNI has the option of proposing the application of ANSI/ANS-8.10, *Criteria for Nuclear Criticality Safety Controls in Operation with Shielding and Confinement*, for shielded facilities. ANSI/ANS-8.10 allows for greater flexibility for mass control and waste characterization requirements while providing protection to workers in the unlikely event (as described in ANSI/ANS-8.10 when invoking single contingency operations) of a criticality accident [34].

### 4.1 Issue Summary

Inadequate PJM mixing could lead to the accumulation of fissile material at the bottom of

the process vessels at the PT Facility. DOE and BNI developed a proposed control strategy to address criticality in PJM vessels. DOE and BNI categorize the fissile material into two types of waste: co-precipitated plutonium and HPP. Co-precipitated plutonium is plutonium that precipitated with neutron absorbers when the waste was neutralized prior to storage in the tank farms. HPP consists of plutonium oxides, plutonium metal fines, and plutonium-bismuth compounds. During treatment of wastes containing HPP, the HPP could separate from neutron absorbers intrinsic to the waste and subsequently accumulate to pose a criticality hazard. DOE's proposed control strategy for treatment of HPP is largely described in BNI's CSE-ES. The strategy in the CSE-ES is dependent on many assumptions about the Hanford tank waste based on information in RPP-RPT-50941, *Review of Plutonium Oxide Receipts into Hanford Tank Farms* [35]. DOE and BNI apply the fundamental assumption that HPP waste is limited to 16 Hanford Tank Farms tanks. The plutonium in the remaining tanks is assumed to be co-precipitated plutonium [30] [36].

In the CSE-ES, BNI provides a tiered strategy using a combination of mass control and added neutron absorbers based on assumed bounding values of HPP. The strategy applies to 13 of the 16 Hanford Tank Farms tanks that contain HPP, as summarized in Table 4.1. RPP-RPT-50941 provides the mass estimates of HPP contained in the tanks that serve as the basis for mass control. The mass control strategy in the CSE-ES relies on several assumptions. The first assumption is that the information in RPP-RPT-50941 is accurate and suitable for use in criticality safety evaluations. The second assumption is that the entire inventory of HPP listed in RPP-RPT-50941 for a given tank gets transferred to WTP on the first batch transfer from the tank farms. The third assumption is that HPP continues to accumulate in WTP process vessels over multiple batches until the WTP operator cleans out the process vessel heels. The strategy in the CSE-ES does not include a requirement to sample for HPP upon transfer to the PT Facility or throughout the process to verify these assumptions during operations. As part of its broader strategy, DOE has proposed TWCSF to characterize the waste and assure the feed complies with the WTP WAC [1] [12] [31]. However, DOE's strategy does not require sampling for HPP upon transfers between PT Facility process vessels [1].

The CSE-ES applies two mass limits: 1) 450 g of  $^{239}\text{Pu}$ ; and 2) 2.7 kg of  $^{239}\text{Pu}$ ; in the following tiers with additional controls, as applicable:

- Tier 1. For the 450 g mass limit, the CSE-ES invokes the single parameter limit defined in ANSI/ANS-8.1, *Nuclear Criticality Safety in Operations with Fissionable Material Outside Reactors*, so no other control is necessary to prevent an inadvertent criticality [32].
- Tier 2. Once the cumulative mass exceeds the single parameter limit, the CSE-ES defines a higher mass limit of 2.7 kg based on the upper subcritical limit (USL; see Section 4.2), fluid mechanics arguments, and assumed conservatism in nuclear modeling. This USL must be derived from calculations that comply with ANSI/ANS-8.24, *Validation of Neutron Transport Methods for Nuclear Criticality Safety Calculations* [37]. As a second independent control, the CSE-ES requires the addition of a soluble neutron absorber. The CSE-ES proposes using sodium pentaborate (SPB) as the preferred soluble neutron absorber. The absorber control

must meet requirements in ANSI/ANS-8.14, *Use of Soluble Neutron Absorbers in Nuclear Facilities Outside Reactors* [38]. Calculations involving SPB must also comply with ANSI/ANS-8.24.

- **Tier 3.** Once the cumulative mass approaches 2.7 kg, the CSE-ES requires heel cleanout (i.e., de-inventory) operations in process vessels to flush out residual HPP and effectively reset the inventory to zero. The mass control limit of 2.7 kg and the addition of soluble neutron absorbers remain in effect.

**Table 4.1. Proposed HPP Control Strategy.**

Sum of Tank HPP Content	Tank	RPP-RPT-50941 Reported Plutonium Inventory (g)		Proposed HPP Safety Control Approach			
		PuO <sub>2</sub>	Pu Metal Fines	Mass Control	Soluble Neutron Absorber	Heel Cleanout <sup>a</sup>	
≤ 450 g (single subcritical limit)	S-111	30	0	Tier 1: Applied	Not Applied	Not Applied	
	SX-114	30	0				
	C-104	40	0				
	BX-101	150	0				
>450 g, < 2.7 kg	S-107	260	0		Tier 2: Applied		Tier 3: Applied
	B-101	320	0				
	A-105	400	0				
	TX-101	400	0				
	C-102	770	0				
≤2.7 kg	S-108	1,000	0		Cannot be Processed under the DCP and Heel Cleanout as Derived for the PT Facility		
	TX-244	845	155				
	AN-101	1,600	0				
	TX-105	2,320	54				
> 2.7 kg (in a single tank)	TX-118	2,710	9	Cannot be Processed under the DCP and Heel Cleanout as Derived for the PT Facility			
	SY-102	10,685	1,965				
	TX-109	4,050	90				

<sup>a</sup> The CSE-ES refers to this operation as “de-inventory.”

For Tier 2 and 3 mass limits, BNI plans to implement the DCP. Implementation of the DCP is a “should” statement in ANSI/ANS-8.1. However, the DCP is a requirement in DOE Order 420.1B, Ch. III, 3.b.(4), which states, “The double contingency principle defined in ANSI/ANS 8.1 is a requirement that must be implemented for all processes, operations and facility designs within the scope of this chapter unless the deviation is documented, justified, and approved by DOE” [39].

Per RPP-RPT-50941, three Hanford Tank Farms tanks exceed the 2.7 kg limit of HPP in each tank. The CSE-ES states it cannot implement the DCP in these cases (see Table 4.1). The CSE-ES notes that processing these three remaining tanks will require further evaluation of other options such as direct feed to the HLW Facility or application of ANSI/ANS-8.10. ANSI/ANS-

8.10 gives guidance for allowing for singly contingent operations where adequate distance and shielding are provided to protect personnel.

The Board identified the following deficiencies with DOE's proposed strategy.

*Upper Subcritical Limit*—The USL calculation, which is used to establish the 2.7 kg HPP limit, does not meet the requirements of ANSI/ANS-8.24. BNI did not properly validate the calculated USL, therefore, the resulting HPP mass limits may not be conservative.

*Mass Control*—BNI plans to administratively control mass limits based on information derived from historical process knowledge rather than sampling and performing mass balances during waste recovery and transfers as required by ANSI/ANS-8.1 to establish a defensible mass control. Mass values derived from historical process knowledge do not constitute mass control for the purposes of criticality safety. The mass control strategy also does not address inadvertent accumulations of fissionable material and therefore does not comply with the DOE Order 420.1B requirement to detect and characterize such accumulations. Additionally, the 2.7 kg mass limit depends on the presence of co-precipitated neutron poisons. These poisons are treated as an assumed characteristic of the waste but are not a credited control in compliance with ANSI/ANS-8.14.

*Soluble Neutron Poison*—The use of additional soluble neutron poisons has not been fully evaluated for chemical compatibility under waste processing conditions. The CSE-ES does not provide sufficient information to demonstrate the soluble neutron absorber control will meet ANSI/ANS-8.14 requirements.

*Tank Waste Assumptions*—The Board also identified concerns with the assumptions regarding the location, quantity, and properties of HPP in the tank farms. These assumptions may affect the strategy presented in the CSE-ES and the testing of the SHSV design. DOE's broader strategy proposes TWCSF to protect these assumptions and provide WAC-compliant waste feed from the Hanford Tank Farms to WTP. However, DOE has not yet defined the functions and requirements for TWCSF.

## 4.2 Upper Subcritical Limit

The USL is the maximum effective multiplication factor ( $k_{\text{eff}}$ ) at which the system may be considered subcritical. Any value of  $k_{\text{eff}}$  equal to or greater than the USL must be considered critical. The USL considers several types of uncertainty in analyzing benchmark criticality experiments and is defined as:

$$USL = 1 + bias - \sigma_{bias} - \sigma_{AoA} - \sigma_{MSM}$$

<i>USL</i>	Upper subcritical limit is the $k_{\text{eff}}$ associated with subcriticality of the system being analyzed.
<i>bias</i>	The bias is calculated as the difference between calculated $k_{\text{eff}}$ and the critical experiment modeled. Because a positive bias may be non-conservative, the bias is set to zero if the calculated $k_{\text{eff}}$ is greater than one [40].



$\sigma_{bias}$	The statistical uncertainty in the bias [40].
$\sigma_{AoA}$	The uncertainty due to the extrapolation of the area of applicability (AoA) from the benchmark experiments [37].
$\sigma_{MSM}$	The minimum subcritical margin (MSM) or margin of subcriticality is an allowance beyond the calculational margin to ensure subcriticality [40] [37]. The calculational margin is defined as the allowance for bias, $\sigma_{bias}$ , and $\sigma_{AoA}$ [37].

BNI selected 0.962 as the USL for HPP [30]. The Board concludes that this USL is not adequately justified. Based on information in the CSE-ES and supporting documentation, the Board's specific observations include:

- BNI selected a value of 0.992 for  $1 + bias - \sigma_{bias}$  [41]. The Board determined that the benchmark experiments selected may not be applicable to the WTP system for HPP. This would invalidate the bias and bias uncertainty applied to the USL calculation. The benchmark experiments use plutonium in various forms (e.g., metal, oxide, or solution) in the presence of absorbers that are not interstitial with the fissile material, as would be the case in WTP vessels. Instead the benchmark experiments used heterogeneous absorbers. In some benchmark experiments, interstitial absorbers are included but only as impurities, in small amounts that have a negligible impact on  $k_{eff}$ . Therefore, the reactivities of the benchmark experiments selected are not as dependent upon, or sensitive to, the credited absorbers as the WTP system. For benchmark experiments to be applicable and useful in determining the USL, they must display the same reactivity sensitivities as the WTP system.
- BNI selected a value of zero for  $\sigma_{AoA}$ . The Board observed that the justifications from the *Preliminary Co-precipitated Plutonium Criticality Safety Evaluation Report* and *Validation of MCNP5* [Monte Carlo N-Particle Version 5] *for Hanford Waste Criticality Safety Calculations* (validation report) do not address the differences in the systems (i.e., co-precipitated plutonium versus HPP) [36] [41]. The justifications also do not address the possible reactivity sensitivity differences between the interstitial absorbers in the waste and the heterogeneous absorbers in the benchmark experiments.
- BNI selected a value of 0.03 for  $\sigma_{MSM}$ . The *Plutonium Absorber Limits from MCNP Calculations* [42] report provides justification for the  $\sigma_{MSM}$  to account for a co-precipitated plutonium system. BNI's  $\sigma_{MSM}$  may not account for uncertainties in the characterization of the WTP waste that contains HPP and underlying uncertainties in the nuclear data since BNI did not provide justification for the  $\sigma_{MSM}$  for the HPP system.

The Board identified *Licensing Issues Associated with PuO<sub>2</sub> and Mixed Oxide Powder Processes* [43], a paper published by the U.S. Nuclear Regulatory Commission, which outlines

sensitivity and uncertainty (S/U) analyses performed on mixed oxide (plutonium-uranium) experiments to determine sensitivity of parameters. To date, BNI has not incorporated any S/U methods into the validation.

If BNI chooses perform S/U analyses for the benchmark experiments selected for the validation report [41], the S/U analyses should focus on differences between the benchmark experiments and the range of potential compositions of the fissile materials and absorbers during waste processing. The results of the analyses could ensure the established USL accounts for the uncertainty in the nuclear data. The S/U analyses would also allow for better selection of benchmarks and better determination of the margin of subcriticality. Depending on the applicability of the benchmarks and uncertainties in the nuclear data, as analyzed with S/U methods, the USL could result in a value between 0.8 and 0.9 [44].

If BNI chooses not to perform the S/U analyses and apply the USL from those analyses, then BNI should consider a USL of 0.8. Systems with a calculated  $k_{\text{eff}}$  of 0.8 or less can be confidently considered subcritical, and “the validation can be general and can tolerate significant uncertainty in the cross sections and modeling assumptions” [44].

BNI could determine a USL higher than 0.9 by conducting new critical experiments that are representative of fissile materials and absorbers anticipated under waste processing conditions [44]. In this case, the criticality analyst must understand the underlying neutronic sensitivities across the energy regimes driving the reactivity of the actual process and work with the experiment designers to match those sensitivities as closely as possible in the new benchmark experiments.

### **4.3 Mass Control**

BNI plans to administratively control mass limits based on information in RPP-RPT-50941 derived from historical process knowledge rather than sampling and performing mass balances during operations. The CSE-ES states, “A conservative assumption of the total HPP mass received by PT Facility will be made so that batch sampling for HPP is not needed. The waste transferred from a Hanford waste tank containing HPP will be assumed to contain the total HPP mass reported by RPP-RPT-50941 for that tank and received into one PT Facility vessel.”

ANSI/ANS-8.1 states, “Nuclear criticality safety is achieved by controlling one or more parameters of the system within subcritical limits and by allowances for process contingencies.” ANSI/ANS-8.19, *Administrative Practices for Nuclear Criticality Safety*, states, “Fissile material shall be identified and tracked by effective methods appropriate to the activity or process” [45]. Mass values derived from historical process knowledge do not constitute mass control for the purposes of criticality safety, even when coupled with mass balance during operations.

In addition, the Board identified that the information in RPP-RPT-50941 may not be adequate for criticality safety applications. RPP-RPT-50941 provides several factors that increase its mass estimates to account for missing or incomplete data; yet, the report does not provide a technical rationale for the factors. RPP-RPT-50941 highlights multiple instances where data were missing and the report’s authors constructed HPP estimates using historical

information or process knowledge. The following example from RPP-RPT-50941 illustrates this:

Detailed records on the quantity and form of plutonium that was shipped to REDOX and PUREX from the 234-5 Building over the operating lifetimes of the facilities were not located. What was located were the Chemical Process Statistics Books I & II (handwritten), which provided nuclear material information on the plant operations including transfer and receipt of plutonium between 234-5, and PUREX, and between 234-5 and REDOX from 1957 through 1972, (HW63089, Chemical Processing Statistics Book I; HW-63090, Chemical Processing Statistics Book II). A notation indicated that the data came from various Accountability Material Balance and Net Production Reports. The data did not specify the composition, physical state, [or] properties, only that it was plutonium.

DOE Order 420.1B is required for the WTP project in accordance with the *Safety Requirements Document* [16]. DOE Order 420.1B Ch. III, 3.b(6) states, “Facilities that conduct operations using fissionable material in a form that could inadvertently accumulate in significant quantities must include a program and procedures for detecting and characterizing accumulations.” DOE’s strategy proposes TWCSF to characterize the waste feed to WTP. If TWCSF includes sampling requirements for HPP, it could support development of compliant mass controls that meet the DOE Order 420.1B Ch. III, 3.b(6). However, TWCSF would not address sampling when conducting transfers between PT Facility process vessels or when performing heel cleanout operations in PT Facility process vessels to ensure fissile mass is removed.

Therefore, DOE’s complete strategy, including TWCSF, does not address mass control or the risk of inadvertent accumulation in the PT Facility per DOE Order 420.1B Ch. III, 3.b(6). Section 4.5 of this report contains additional observations related to the TWCSF design and heel cleanout operations that could impact mass control. DOE could include a mass balance and sampling approach to confirm that the fissile material inventory in a PJM vessel does not exceed the HPP criticality mass control limits consistent with the requirements of DOE Order 420.1B Ch. III, 3.b(6). The strategy should involve a representative sampling approach that avoids grab samples from a PJM vessel. Examples are available from industry [49].

The Board also observed that heel cleanout is not clearly identified as a safety-related control in the full-scale test plan for the SHSV [46]. Tier 3 of the mass control strategy relies on the ability to remove solids from process vessels to prevent accumulation of more than the 2.7 kg limit. An effective heel cleanout system is a necessary credited safety system for removal of HPP mass accumulations for prevention of inadvertent criticality. DOE could identify heel cleanout as a safety-related control in the test plan for full-scale testing of the SHSV design. The tests should demonstrate that the heel cleanout operations are effective, such that only a *de minimis* quantity of HPP remains in the vessel.

BNI plans to perform informational heel cleanout testing to support future DOE decisions related to HPP treatment. BNI states that there is presently no quantitative heel cleanout criterion for processing HPP within the current WTP design basis. In lieu of this criterion, BNI proposes to perform a full-scale heel cleanout test to evaluate the performance of the SHSV for

removal of HPP. The heel cleanout tests start with an initial inventory of an HPP simulant in a carrier fluid. The mixing systems are operated and the vessel is pumped down. Subsequent pump-down operations are performed by adding additional carrier fluid and repeating the mixing and pump-down steps. The test is considered successful if the results show that the SHSV vessel is capable of decreasing the solids concentration of the HPP simulant on each pump-down [47]. These heel cleanout tests are not designed to address the DOE Order 420.1B requirement to detect and characterize inadvertent accumulations of fissionable material.

The Board also observed that crediting the presence of absorbers in the mass limit is non-conservative. The mass limit derived from the USL depends on the presence of co-precipitated neutron poisons. ANSI/ANS-8.1 Section 4.2.1 states, “All controlled parameters and their limits shall be specified. The influence of variations in these parameters on the  $k_{\text{eff}}$  of the system shall be understood.” BNI modeled the HPP system as a homogeneous mixture of plutonium dioxide ( $\text{PuO}_2$ ) with 5 volume percent co-precipitated plutonium solids and water at an optimal moderation ratio. Some of the elements in the co-precipitated plutonium solids act as neutron absorbers (e.g., iron and other metals). In addition, the ratio of iron to plutonium in the co-precipitated plutonium solids varies by waste stream [48].

To determine the safe mass of HPP, BNI’s calculation varied the concentration of co-precipitated plutonium solids between 5 and 30 volume percent. An increase in neutron absorbers allows for a higher amount of HPP to be accommodated in the model before that calculated  $k_{\text{eff}}$  of the model exceeds the USL. Therefore, the mass limit of HPP increases with increasing volume percent of co-precipitated plutonium solids, as illustrated in Table 4.2 [48].

The CSE-ES did not indicate any plans to control the composition of any specific neutron absorbers. Therefore, the strategy is not in compliance with the ANSI/ANS-8.1 Section 4.2.1 controlled parameter requirement. Because the 2.7 kg mass limit for HPP already relies on the presence of insoluble neutron absorbers, further addition of soluble neutron absorbers for mass control is not independent and cannot be credited as one of the two parameters required to meet the DCP. A change in a single parameter, the effectiveness of the neutron absorbers, can drive the system critical. As stated above, the USL should be calculated in accordance with ANSI/ANS-8.24, with applicable benchmark experiments, and technically justifiable  $\sigma_{MSM}$  and  $\sigma_{AOA}$ . With that USL, BNI could calculate mass limits independent or dependent of neutron absorbers. If mass limits are calculated independent of neutron absorbers, then neutron absorbers meet DCP definition for a secondary control in accordance with ANSI/ANS-8.1. If mass limits are calculated with a dependency on neutron absorbers, those assumptions should be documented and protected. This includes sampling to verify the quantities of neutron absorbers. This condition precludes crediting the effectiveness of neutron absorbers as the second contingency to satisfy DCP requirements per ANSI/ANS-8.1. Compliance with ANSI/ANS-8.14 is required for credited absorbers whether or not they are part of a DCP strategy.

**Table 4.2.** *Estimated safe HPP mass with various concentrations of co-precipitated plutonium solids [48].*

<b>Volume % co-precipitated plutonium solids</b>	<b>Estimated safe HPP mass (kg)</b>
5	2.70
10	3.18
15	3.72
20	4.12
25	4.59
30	5.08

#### **4.4 Soluble Neutron Poison**

The CSE-ES identifies SPB as a feasible soluble neutron absorber (e.g., neutron poison) to add to process vessels. The CSE-ES acknowledges that additional analyses are necessary to ensure SPB remains dissolved in solution and that the resulting SPB concentration is maintained throughout the treatment process. This is a necessary step to demonstrate that the safety strategy complies with ANSI/ANS-8.14 to ensure the neutron absorber is effective. The Board acknowledges SPB is a suitable neutron poison to control nuclear criticality. However, we found that the analysis in the CSE-ES contains technical gaps regarding SPB characteristics, namely its neutronic and chemical properties. Further detail on these topics is provided below.

*Neutronics*—CSE-ES states that SPB can be an effective absorber at concentrations as low as 200 ppm, but it neither provides justification for this value nor does it account for the range of conditions under which HPP could accumulate. A sediment layer/pile could reduce the relative effectiveness of the <sup>10</sup>B isotope as a neutron absorber. The sediment layer/pile can result in a close packed condition that reduces the interstitial water in the spaces between the accumulated HPP. This reduces moderation of the system. This condition also contradicts an assumption in the CSE-ES, which states: “SPB is a soluble poison that reduces the ability of water to add reactivity to the system by absorbing neutrons before they have a chance to moderate to thermal/lower energies and subsequently [be] captured by fissile nuclides and cause fission.”

*SPB Solubility*—ANSI/ANS-8.1 requires an evaluation demonstrating the continued presence of the absorbers within the intended distributions and concentrations of the process conditions. Additionally, ANSI/ANS-8.14, Section 4.3.4, requires, “Evaluations shall consider the effect on nuclear criticality safety of potential nonuniform distribution of the neutron absorber.” Section 4.3.5 requires, “Evaluations shall consider the impact on the neutron absorber and subsequent effect on system reactivity of changes to process conditions that lead to adverse environmental and operating conditions.” The Board determined that the CSE-ES does not provide a complete evaluation of SPB in accordance with these requirements.

The Board also found the boron solubility used in the CSE-ES is inconsistent with solubility data available in literature [50]. The CSE-ES assumes that SPB, once introduced to WTP facilities, will exhibit the same solubility behavior as boron already present in the waste (Figure 4.1, black line). The CSE-ES also acknowledges that boron solubility needs to be

confirmed for the waste conditions in WTP. Figure 4.1 shows the CSE-ES boron solubility data and curve fit (represented by red dots and a black line) and the Yongquan et al. SPB solubility data [50] (represented by blue squares).

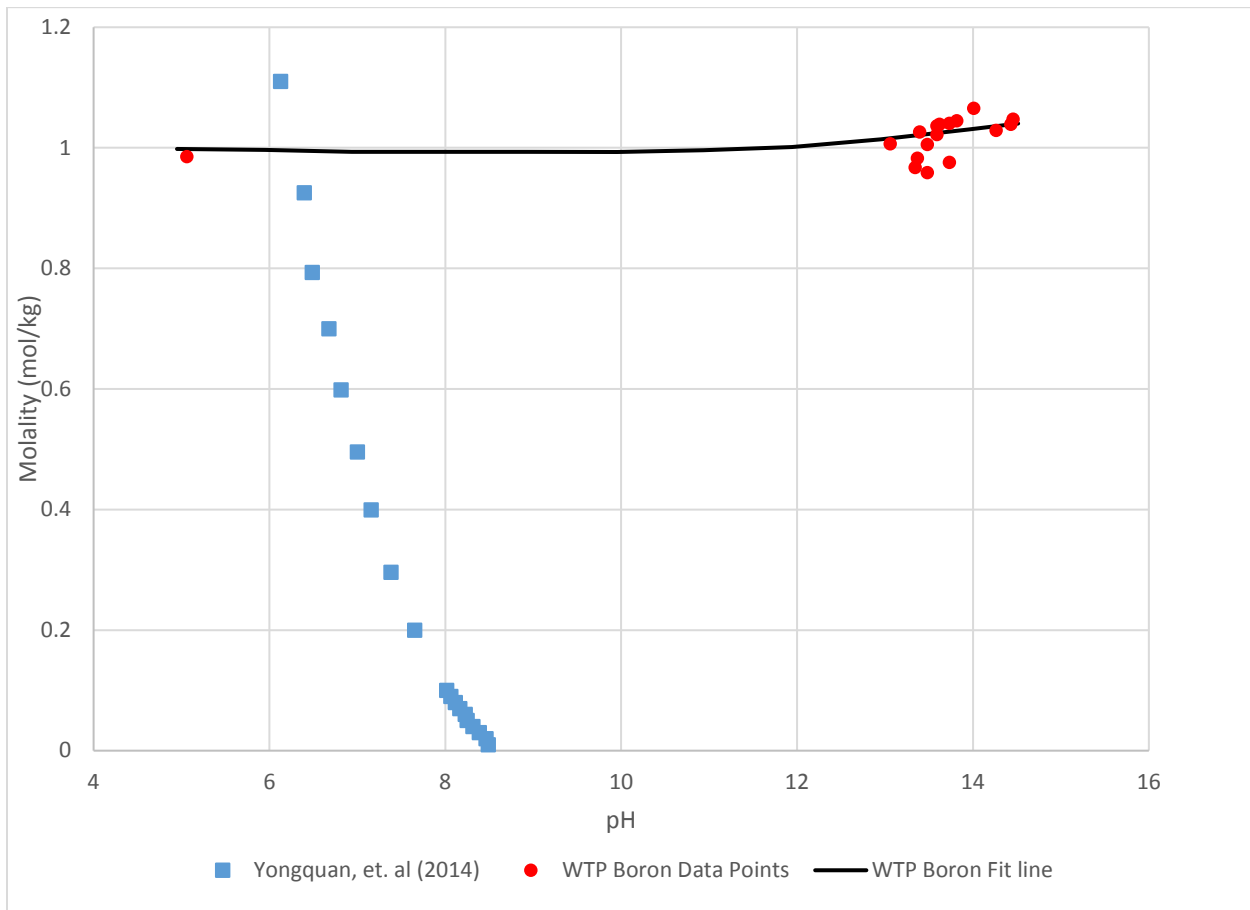


**Figure 4.1.** The solubility of sodium pentaborate at 298 K reported by Yongquan et al. [50] (blue squares) and by the WTP CSE-ES [30] (solid black line and red circles).

The boron solubility from the CSE-ES is relatively constant over a broad pH range. However, SPB solubility reported by Yongquan et al. shows a strong SPB concentration dependence on pH. Also, the CSE-ES does not specify the chemical composition of boron used to derive the data. Therefore, the assumption made by the CSE-ES that boron and SPB have the same solubility may be incorrect. [Note: The original solubility curve for boron in the CSE-ES is represented in units of molarity (mol/L), whereas the solubility data reported by Yongquan et al. is in units of molality. To provide an accurate comparison of the solubility curves for both boron and SPB (Figure 4.1), the Board converted the molarity of boron to molality using the theoretical density of 1 g/cm<sup>3</sup> for water.]

Variations in the solubility of SPB with pH have a direct impact on the effectiveness of boron as a neutron absorber for criticality control. For example, SPB could precipitate out of solution during process operations, such that SPB is not interstitially mixed with HPP particles at the concentration used in the criticality safety models.

If DOE decides to treat HPP in the PT Facility, DOE could address the concerns with neutron poison solubility by taking actions such as:

- Performing additional criticality safety calculations to understand the effect of variations in HPP (e.g.,  $^{239}\text{Pu}$ ), neutron absorber (e.g.,  $^{10}\text{B}$ ), and moderator (e.g., hydrogen) concentrations on the  $k_{\text{eff}}$  of the system for all credible ranges of these parameters.
- Conducting studies of the selected neutron absorber (e.g., SPB) chemistry over a range of pH conditions in Hanford tank supernatant and developing a control strategy that ensures the selected neutron absorber remains dissolved throughout the PT Facility processes. For example, this strategy could include credited controls to maintain pH within an acceptable range.

#### 4.5 Tank Waste Assumptions

DOE's criticality safety strategy for co-precipitated plutonium and HPP relies on many assumptions about the characteristics of Hanford tank waste. One fundamental assumption is that HPP waste is limited to 16 Hanford Tank Farms tanks. Based on information in RPP-RPT-50941, DOE and BNI use the assumption that waste in tanks outside of the 16 HPP tanks contains co-precipitated plutonium. Also, the strategy described in the CSE-ES relies on assumptions related to the quantity and physical characteristics of HPP. The January 24, 2017, letter from the acting EM-1 to the Board states that waste feed from Hanford Tank Farms to WTP must comply with the WAC as specified in Interface Control Document-19 (ICD-19) [12] [10]. DOE has proposed TWCSF to characterize waste from the tank farms and assure it complies with the WAC. However, DOE has not yet defined the functions and requirements for TWCSF or the waste types to be processed through the facility.

DOE's assumptions regarding the location, quantity, and physical characteristics (i.e., size, density, and shape) of plutonium-rich particles contain uncertainties. These uncertainties remain to be addressed as DOE further develops the criticality safety strategy, tests the SHSV design, and designs TWCSF. The final PT Facility design must be able to safely process the waste that enters the facility. Therefore, DOE should protect the selected assumptions in the WAC, which could include designing TWCSF to protect those assumptions. The following sections describe specific uncertainties with the tank waste assumptions.

*Location and Quantity of Plutonium-rich Particles*—The Preliminary Criticality Safety Evaluation Report addresses treatment of plutonium co-precipitated with absorbers through the PT facility [36]. BNI assumes plutonium co-precipitated with absorbers will not segregate from its absorber in tank waste, such that the waste will remain subcritical under all process conditions at WTP. BNI credits co-precipitation as a safety control to ensure the ratio of plutonium with absorber ions (specifically iron) is maintained given the high abundance of iron in the waste. This assumption is based on a chemistry report developed by PNNL (PNNL-23468) to assess potential interactions of plutonium with neutron absorbers and chemical constituents present in the waste [51].

In the PNNL-23468 report, the authors acknowledge that plutonium association with iron is likely given the similarity in the chemical properties of both metal ions. The authors also acknowledge that plutonium can associate with heavy ions that are not transition metals. The report states, “Plutonium association with bismuth as  $\text{Bi}(\text{OH})_3$ ,  $\text{Bi}_2\text{O}_3$ ,  $\text{BiPO}_4$ , and in mixed bismuth/metal compounds in alkaline tank wastes is likely” [51]. This statement implies that both co-precipitated plutonium and dense plutonium particles (e.g., plutonium-bismuth) may have formed in Hanford tank wastes.

Many of the assumptions used in the CSE-ES rely on information in RPP-RPT-50941 [35]. The purpose of RPP-RPT-50941 is to conservatively estimate the inventory of plutonium solids (i.e.,  $\text{PuO}_2$ ) that entered the tank farms with the Plutonium Finishing Plant (PFP) aqueous waste. The estimates are based on historical information, available records, and process knowledge. RPP-RPT-50941 acknowledges that other plutonium-rich particles, for instance, plutonium and bismuth rich particles (Pu–Bi particles), were found in addition to  $\text{PuO}_2$ . However, the report does not expand on the characterization or location of Pu–Bi particles in the tank farms. Further, the CSE-ES states, “A review of RPP-RPT-50941 and WHC-SD-CP-RPT-014, Rev 0, *Plutonium and Tritium Produced in the Hanford Site Production Reactors*, performed for this CSE-ES, concludes that the plutonium bismuth association particulates are already adequately accounted for in RPP-RPT-50941.”

The Board identified several reports that show Pu–Bi particles were discovered in tanks that received waste from PFP (i.e., SY-102 and TX-118) [52] [53] [54] [55]. The CSE-ES categorizes tanks SY-102 and TX-118 as HPP tanks. Report PNNL-23468 states, “Tank characterization data evaluations for TX-118 and from BBI [Best Basis Inventory] in TWINS [Tank Waste Information Network System] data indicate that bismuth is more highly associated with the PFP waste layer than with the salt cake of other origin. Therefore, it is likely that the plutonium-bismuth and plutonium-bismuth-phosphorus originated from the PFP process chemicals or from the PFP feed sources” [51].

PNNL-23468 also concludes Pu–Bi and Pu–Bi–P particles were not present in tank AZ-101 (i.e., a co-precipitated tank). This supports the conclusion that Pu–Bi particles are coming from PFP waste and were not co-precipitated. However, a characterization report [55] states, “No automated SEM [scanning electron microscopy] analysis was conducted on the AZ-101 sample due to equipment failure, therefore, no SEM-EDS [SEM-energy dispersive spectroscopy] speciation could be performed, and no particle data was collected. Manual SEM analysis of several hundred particles while operating the SEM in backscatter mode found no particles bearing detectable amounts of plutonium.” This unanticipated equipment failure adds uncertainty to the argument because the data to either support or disprove the conclusion were not collected.

In comparison, a February 2016 paper by Reynolds et al. hypothesizes that these particles may have been generated from PFP or unaccounted chemical mechanisms within waste tanks [56]. This paper states, “Consequently, the source of this Bi in the PFP remains unknown, along with the source of the Pu–Bi and Pu–Bi–P particles.”

While not a criticality hazard, the Board believes that thorium-bismuth and thorium-bismuth-phosphate particles discovered in tank SY-102, as described in a BNI characterization



report, can offer insight regarding the source of the Pu–Bi particles [57]. In the report, BNI does not address the source of these particles but acknowledges that thorium in Hanford tanks likely originated from the processing of irradiated thorium oxide fuel in the PUREX plant to separate  $^{233}\text{U}$  during the 1960s. Thorium was not used as a process chemical in Hanford’s PFP operations, but rather was used in a subset of PUREX operations. Therefore, it is possible that thorium-bismuth also may have formed in the tanks, potentially following a similar chemical pathway as Pu–Bi particles.

Based on the work available, there is substantial uncertainty regarding the formation and location of Pu–Bi particles. The presence of Pu–Bi particles in co-precipitated tanks would challenge a fundamental assumption in BNI’s criticality safety strategy. Methods should be developed to mitigate these uncertainties.

*Size of Plutonium-rich Particles*—The CSE-ES addresses HPP with particle sizes between 10 and 100 microns. This assumption is derived from particle size distribution (PSD) analyses in RPP-RPT-50941. PSD data in the RPP-RPT-50941 report shows evidence of plutonium oxide particles greater than 100 microns. However, the report identifies a maximum particle size of 100 microns based on “the consensus judgement of several plutonium processing subject matter experts” [35].

Following publication of RPP-RPT-50941, Los Alamos National Laboratory (LANL) released a study that contains new characterization data of  $\text{PuO}_2$  particles from Hanford waste samples. The LANL study shows that  $\text{PuO}_2$  particles between 200 and 300 microns were observed [58]. The information highlights discrepancies between the PSD analyses of particles discussed in RPP-RPT-50941 and the LANL study.

The acting EM-1’s letter to the Board [1], states, “Future testing with the proposed SHSV will assess the capability of this vessel design to mix and remove particulate material representing 100 micron diameter plutonium oxide.” However, DOE’s current full-scale SHSV test program does not address the removal of particulate material representing plutonium oxide larger than 100 micron diameter.

It is unclear how DOE’s criticality safety strategy will protect the 100 micron plutonium oxide particle size assumption. The WTP Basis of Design [59] does not yet include plutonium oxide particles greater than 10 microns. And, the WAC in ICD-19 [10] does not specifically place a limit on HPP particle size for plutonium oxide or Pu–Bi particles. If particles larger than 100 micron enter the PT facility, the SHSV design may not be capable of removing these particles from the vessel during heel cleanout operations.

*Density of Plutonium-rich Particles*—The CSE-ES assumes particle densities for plutonium metal ( $19.82 \text{ g/cm}^3$ ) and  $\text{PuO}_2$  ( $11.46 \text{ g/cm}^3$ ). A related chemistry report developed by PNNL supports this assumption [51]. The report states, “The densities of the plutonium-bismuth and plutonium-bismuth-phosphorus phases [are] unknown but likely are limited to that of the respective pure oxides or phosphates, the highest of which is  $11.46 \text{ g/cm}^3$  for  $\text{PuO}_2$ .”

The assumed particle density of 11.46 g/cm<sup>3</sup> may not be conservative. The crystal structures of plutonium-bismuth and similar actinide-bismuth compounds may have higher densities than PuO<sub>2</sub> [60]. And, a BNI memorandum states “There is no plutonium speciation information on Pu–Bi-rich particles in the Hanford tanks” [53].

In the SHSV de-inventory tests, DOE is using 150 micron bismuth oxide particles as a simulant for 100 micron plutonium oxide particles [46]. These surrogate particles have a density of 8.9 g/cm<sup>3</sup>. BNI states that basing the HPP simulant on plutonium oxide rather than plutonium metal is appropriate because plutonium metal represents a very small fraction of the total HPP [47]. DOE should protect the particle density assumption in the WAC.

*Shape of Plutonium-rich Particles*—The CSE-ES assumes that all HPP particles are spherical. The CSE-ES assumes the spherical particle shape is conservative because it maximizes plutonium separation effects through high free-settling velocities. The CSE-ES acknowledges an acicular (needle-shape) plutonium particle in a Hanford tank farm core sample was observed. The Reynolds et al. report confirms the presence of a variety of non-spherical plutonium-bismuth particles and plutonium-bismuth-phosphorous particles sampled from tanks SY-102 and TX-118 [56]. In the article, the scanning electron microscope images of plutonium-bismuth particles were identified as globular agglomerates whereas plutonium-bismuth-phosphorous particles were identified as single needle-like crystals. The spherical particle assumption may not be conservative for heel cleanout operations.

## 5. HYDROGEN IN PIPING AND ANCILLARY VESSELS

HPAV is a longstanding Board safety issue at WTP. Since 2009, the Board has performed independent oversight on DOE's initiative to remove active HPAV safety controls from the WTP design. The Board conducted a review of DOE's most recent HPAV resolution strategy and identified deficiencies with the portion of the HPAV control strategy that proposes using QRA<sup>1</sup> to design safety controls.

Specifically, the Board concludes that QRA calculations are part of the safety basis, and that DOE Standard 1628, *Development of Probabilistic Risk Assessments for Nuclear Safety Applications*, applies to any QRA models used to design safety systems (e.g., safety significant or safety class piping) [61]. Since the QRA calculations are part of the safety basis, DOE must establish a technical basis for maintenance and protection of QRA input parameters. Instead of using QRA calculations to design passive safety controls, DOE could credit HPAV preventive controls (e.g., flush, vent, or purge) on pipe routes with safety-related spray consequences. DOE could complete a revised spray leak calculation to inform its decision process. The calculation should address the reduced material-at-risk inherent in the SHSV design.

### 5.1 Issue Summary

WTP waste streams generate hydrogen and other gases, such as nitrous oxide, due to radiolysis and thermolysis. These gases can collect in process piping and non-process vessels when waste stagnates (e.g., stoppage of flow in pipes). Hydrogen accumulation in concentrations greater than the lower flammability limit has the potential to be ignited and explode within a pipe or non-process vessel. Such an explosion could rupture the pipe and initiate a vessel spill or pipe spray [14] [62]. BNI named this technical issue "HPAV" and began evaluating it following two incidents in boiling water reactors in Germany and Japan in 2001 [63]. These reactors experienced ruptured pipes due to hydrogen buildup and detonation. Since 2009, DOE and BNI have proposed various HPAV control strategies that included using QRA to evaluate event frequency and consequence.

DOE recently proposed a new strategy for resolving HPAV. In July 2016, BNI completed a deterministic calculation, *Unmitigated Consequences for Pretreatment Hydrogen in Piping and Non-Process Vessel Events*, to classify HPAV controls [64]. This calculation evaluated an HPAV event and resulting pipe spill, but did not evaluate pipe sprays or vessel spills initiated by an HPAV event. The calculation shows that the radiological consequences are low enough that safety-related controls are not required for HPAV-induced pipe ruptures and spills.

Because HPAV events are initiators for both pipe sprays and vessel spills, DOE proposed a control strategy for HPAV-initiated pipe sprays with safety-related consequences. The control strategy consists of the building structure, ventilation system, and additional controls that vary based on the pipe diameter [14] [62] [65]:

---

<sup>1</sup> DOE Standard 1628, Appendix A, provides the same definition for the terms "PRA" and "QRA."

- Pipes greater than 4 inches in diameter with safety-related spray consequences will be credited as safety class or safety significant. At least one active safety control (e.g., vent, purge, or flush) will be installed to prevent HPAV events from rupturing the pipe and causing a spray. The active safety control will have the same safety classification as the piping it is protecting. QRA is not used to model these pipes.
- Pipes less than or equal to 4 inches in diameter with safety-related spray consequences will be credited as safety class or safety significant and will be modeled using QRA. The QRA will be tailored to model each pipe route, which is typically defined as the piping and components connecting two vessels. The QRA calculates frequencies and severities of potential HPAV events (e.g., high and low speed deflagrations, or deflagration-to-detonation transitions) in each route. HPAV events with frequencies greater than  $10^{-6}$  events/year in a pipe route are used to establish design loading for that route. The pipe and components are credited as a passive barrier that withstands HPAV events predicted by the QRA.

ORP stated this control strategy meets DOE requirements and resolves the HPAV safety issue. On December 19, 2016, the ORP manager sent a memorandum to the Assistant Secretary for EM [14]. The memorandum states, “ORP considers the DNFSB concerns resolved.... ORP has determined that WTP is ready to resume PT Facility design completion in areas related to HPAV process piping.”

For an HPAV event with a resulting pipe spill, the Board concludes BNI’s safety basis calculation for HPAV, *Unmitigated Consequences for Pretreatment Hydrogen in Piping and Non-Process Vessel Events*, is conservative and consistent with DOE requirements. The Board concludes that the control strategy for pipe sizes greater than 4 inches in diameter with safety-related spray consequences also meets DOE requirements. Consistent with Chapter 1, Section 3.b(1) of DOE Order 420.1B, the control strategy provides multiple barriers of protection against safety-related consequences of spray leak accidents [39]. HPAV events in pipe sizes greater than 4 inches in diameter are prevented by at least one active safety control that protects piping integrity. These controls ensure the piping will provide a creditable physical barrier to protect against radiological releases from HPAV events. The safety class C5 ventilation system and building structure provide the second credited barrier. The Board’s safety issues would be resolved by applying this control strategy to all pipe routes with safety-related spray consequences.

The Board concludes that the proposed control strategy for pipe sizes less than or equal to 4 inches in diameter with safety-related spray consequences does not meet DOE requirements. Specific concerns are summarized below and discussed in detail in Sections 5.2 through 5.4:

*DOE Standard 1628 Applicability*—DOE has stated that the QRA is only a design tool used for piping design and DOE Standard 1628 does not apply. The Board compared the proposed usage of QRA to the applicability statement of DOE Standard 1628 and concludes the standard applies. ORP’s position is inconsistent with DOE Policy 420.1, *Department of Energy Nuclear Safety Policy* [66].

*QRA Relationship to the Safety Basis*—In the December 19, 2016, memorandum from ORP and the January 24, 2017, letter issued by the acting EM-1, DOE stated, “Specifically, the role of the QRA is restricted to piping design and is not used in nuclear safety analysis” [1] [14]. However, QRA calculations are used to demonstrate that an SSC is adequate to perform its credited safety function in the Preliminary Documented Safety Analysis (PDSA). Therefore, the Board concludes the QRA is part of the safety basis, and ORP’s position is inconsistent with Subpart B of Title 10, Code of Federal Regulations (CFR) Part 830, *Nuclear Safety Management*.

*Maintenance and Protection of QRA Input Parameters*—DOE has not established a technical basis for maintenance and protection of QRA input parameters. Given that the Board concludes QRA calculations are part of the safety basis, the Board also concludes that QRA input parameters should be maintained and protected to ensure QRA calculations remain valid over the life of the facility.

The number of pipe routes with pipe sizes less than or equal to 4 inches in diameter with safety-related spray consequences to which the Board’s conclusions apply is currently undetermined. In September 2015, a BNI calculation predicted pipe sprays would have safety-related consequences in the Feed Receipt Process, High-Level Waste Lag Storage and Feed Blending Process (HLP), and Ultrafiltration Process (UFP) systems [67]. This calculation did not consider the redesign of the HLP and UFP systems to incorporate SHSVs. The smaller volume of the SHSV will reduce the material-at-risk for potential HPAV-initiated pipe sprays. The specific number of pipe routes with safety-related spray consequences cannot be accurately determined until BNI completes the redesign of the HLP and UFP systems and updates the pipe spray calculations.

## **5.2. DOE Standard 1628 Applicability**

ORP’s proposed use of QRA and application of DOE Standard 1628 has changed over time. On July 19, 2013, DOE’s Office of Nuclear Safety sent a memorandum to EM that stated, “[I]f probabilistic calculations are utilized as a tool for better understanding accident sequences, frequencies, and uncertainties, the process for performing probabilistic risk analysis/quantitative risk analysis (PRA/QRA) identified in DOE’s Draft PRA Standard [1628], issued in December 2010 for interim use and comment, should be used until issuance of the final standard”<sup>2</sup> [68]. On August 13, 2013, ORP transmitted the memorandum to BNI and directed development of a PRA plan in accordance with the draft of DOE Standard 1628 [69].

After receiving DOE comments on a draft PRA plan, on September 29, 2014, BNI sent ORP a memorandum that stated, “In summary, BNI has no plans to apply PRA methods to determine the unmitigated or mitigated likelihood or consequences of HPAV events occurring in WTP facilities. Modification of the existing HPAV QRA process to satisfy DOE-STD-1628-2013...is not required for its current use as a tool to evaluate the adequacy of piping design in meeting ASME B31.3-1996 requirements” [70].

---

<sup>2</sup> In November 2013, DOE formally approved DOE Standard 1628.

The December 19, 2016, memorandum from the ORP Manager to the Assistant Secretary for EM endorsed BNI's position regarding the applicability of DOE Standard 1628 to the QRA model developed for HPAV. It states, "DOE developed and issued DOE-STD-1628-2013...in part to guide the use of the design methodology in the nuclear safety strategy should that approach be chosen. The project has instead elected to develop the required safety basis without reliance upon the design approach as part of the safety analysis in a role that would invoke applicability of this standard."

The QRA is being used to demonstrate that safety controls (e.g., pipes) are adequate to "perform their safety function when called upon" [39]. According to the applicability statement provided in DOE Standard 1628, "The Standard [1628] should be applied in complex analyses where the results are used as a significant input to decisions regarding the selection of or **adequacy of safety controls**, or whether to screen events and scenarios from further safety analysis [emphasis added]." Further, DOE Policy 420.1, Section 4, states that qualitative and probabilistic risk assessments should be used consistent with DOE directives. At the time DOE Policy 420.1 was written, DOE Order 251.1C, *Department Directives Program*, indicated that DOE technical standards, such as 1628, are a type of directive. Therefore, the Board concludes that DOE Standard 1628 applies.

### 5.3. Relationship of QRA to the Safety Basis

DOE contends the QRA is not part of the safety basis. As noted above, the December 19, 2016, memorandum and the January 24, 2017, letter issued by the acting EM-1 state: "Specifically, the role of the QRA is restricted to piping design and is not used in nuclear safety analysis." The Board compared this position to DOE requirements. Subpart B of 10 CFR Part 830 provides safety basis requirements for DOE nuclear facilities that include development of a PDSA, which is transitioned to a Documented Safety Analysis (DSA) during facility startup [71]. 10 CFR Part 830.204 provides requirements for a facility's DSA. It states that a DSA must "Derive the hazard controls necessary to ensure adequate protection of workers, the public, and the environment, **demonstrate the adequacy of these controls** to eliminate, limit, or mitigate identified hazards and define the process for maintaining the hazard controls current at all times and controlling their use [emphasis added]."

The QRA, using a large array of input parameters, is being used as the basis for demonstrating that an SSC (i.e., piping) is an adequate passive safety control for spray leak accidents in the PT Facility PDSA. The PDSA, Section 3.4.1.4, credits piping as a safety control for spray leaks. Section 4.4.42 defines the piping functional requirements as maintaining confinement with consideration to the stresses caused by HPAV loading. QRA calculations define the HPAV design loads and their frequencies for safety-related piping. HPAV events with frequencies greater than  $10^{-6}$  events/year are used to design pipe routes. As such, the QRA calculations demonstrate control adequacy. Therefore, the Board concludes the QRA calculations are part of the safety basis, and ORP's strategy is inconsistent with 10 CFR Part 830.

This means ORP should document the relationship between the QRA and safety basis documentation in a PRA plan prepared in accordance with DOE Standard 1628. Section 4.1.1.4 requires a PRA plan to describe "[t]he relationship between the anticipated PRA results and the

nuclear facility safety basis and safety basis documents.” The PRA plan requires DOE review and approval.

#### **5.4. Maintenance and Protection of QRA Input Parameters**

Given that the Board concludes QRA calculations are part of the safety basis, the Board also concludes that QRA input parameters should be maintained and protected to ensure QRA calculations remain valid over the life of the facility. 10 CFR Part 830.202 requires that “The contractor responsible for a hazard category 1, 2, or 3 DOE nuclear facility must establish and maintain the safety basis for the facility....Update the safety basis to keep it current and reflect changes in the facility, the work and the hazards as they are analyzed in the [DSA].” Further, 10 CFR Part 830.204 requires that the DSA “define the process for maintaining hazard controls current at all times and controlling their use.”

Maintenance and protection of QRA input parameters are critical to ensuring QRA calculations remain valid and demonstrate the piping is an adequate passive safety control for spray leak accidents. BNI’s document, *HPAV Engineering Analysis Methods and Criteria*, Section 3, states: “The QRA process evaluates nearly one hundred and twenty input elements for HPAV-affected routes in order to quantify the type, frequency, and severity of hydrogen events” [72]. The QRA input parameters include assumptions on waste temperatures, rheology, hydrogen generation rates, operating pressures, percentages of inert species in potential gas pockets, operator responses, equipment failure rates and repair times, and probability of ignition. Many of these input parameters are assumed probability distribution functions that are sampled during Monte Carlo simulation.

BNI plans to use an “HPAV multi-functional team” to establish the QRA input parameters for each QRA calculation prior to submitting these inputs to the sub-contractor responsible for running the QRA model. This team would include nuclear safety representation. There is little information available regarding the team’s review process or the extent of ORP’s oversight involvement. High-level overviews of this process are available in BNI’s documents, *Quantitative Risk Analysis of Hydrogen Events at WTP: Development of Event Frequency-Severity Analysis Model* [73], and *Quantitative Risk Analysis Data Collection Process* [74]. Moreover, there is minimal information available describing how the QRA input parameters, once established, will be maintained and protected.

In its September 3, 2010, and December 30, 2010, reports to Congress, the Board highlighted concerns with maintenance and protection of QRA input parameters [75] [76]. The Board has periodically raised this issue during staff-to-staff discussions. The Board concludes:

- DOE has not established a technical basis for maintenance and protection of QRA input parameters. Not every QRA input parameter needs protection at the technical safety requirements (TSR) level. However, DOE and BNI should evaluate each of the QRA input parameters and establish a technical basis justifying how each of them will be maintained and protected over the life of the facility. The goal of this effort should be to develop a basis for ensuring QRA calculations will remain valid. This activity could also include (1) plans to evaluate QRA data when plant-specific

operational data become available and how that data will be collected, (2) an explanation of how the QRA model will interface with the unreviewed safety question (USQ) process, (3) development of procedures to ensure thorough reviews of QRA input parameters, and (4) ORP oversight plans for the QRA process.

- ORP should document the strategy for maintaining and protecting QRA input parameters in a PRA plan prepared in accordance with DOE Standard 1628 and obtain DOE review and approval. Section 4.1.1.4 of DOE Standard 1628 states: “The PRA plan describes the process used to identify: (a) the key PRA assumptions which require protection by appropriate mechanisms; (b) the use of PRA results to inform selection of safety controls to be included in the safety basis; and (c) applicability of the USQ process relative to maintaining the PRA.”



## 6. CONCLUSIONS

The Board reviewed DOE's proposed strategies for hydrogen in vessels, criticality in vessels, and HPAV. The results of the Board's reviews identified several deficiencies. DOE must identify and implement effective safety strategies for these hazards to assure safe operation of the PT Facility.

**Hydrogen in Process Vessels Strategy.** The Board identified the following deficiencies with the control strategy for hydrogen in vessels:

- The air sparge system may not be an effective preventive control given previous test data showing the presence of a significant unmixed heel.
- DOE has not yet addressed the long-term reliability of the sparge system to ensure its operability when called upon to perform its safety function.
- The analysis supporting the control strategy for the low-solids Newtonian vessels following loss of agitation contains unverified assumptions.
- DOE has not yet specified how waste parameters important to the control strategy will be verified during operations.

**Criticality in Process Vessels Strategy.** DOE has not decided whether to direct BNI to update the WTP design basis to include treatment of HPP in the PT Facility. Making this decision early would allow DOE to integrate the HPP control strategy into the design. If DOE chooses to treat HPP in the PT Facility, the Board identified the following deficiencies with DOE's proposed strategy:

- BNI's nuclear modeling calculations, used to define mass limits, do not comply with ANSI/ANS 8 series standards.
- BNI's current mass control strategy does not meet the ANSI/ANS-8.1 double contingency principle due to reliance upon absorbers and inadequate positive controls on mass.
- BNI's mass limits depend upon faulty model calculations mentioned above and on ensuring the effectiveness of absorbers without benefit of appropriate controls as specified in ANSI/ANS-8.14.
- BNI's analysis does not include a mass balance and representative sampling approach to confirm the fissile material inventory for waste feed, transfers between process vessels, and vessel heel cleanout operations.
- DOE has not identified heel cleanout operations as a safety-related control in the test plan for full-scale testing of the SHSV design to demonstrate that heel cleanout operations are effective.

- BNI has not verified the effectiveness of selected neutron absorbers throughout the PT Facility process conditions.
- BNI has not incorporated the assumed HPP physical properties into the full-scale testing of the SHSV design and updated the WTP WAC to protect these assumptions.
- DOE has not specified the functions and requirements necessary for the TWCSF to produce feed that is compliant with the updated WAC.
- DOE has not evaluated feeding all slurry waste through TWCSF to address uncertainties in waste feed.

If DOE chooses to treat HPP in the PT Facility, BNI has the option to apply ANSI/ANS-8.10 for shielded facilities, which allows greater flexibility for mass control and waste characterization requirements.

**HPAV Strategy.** The Board identified the following deficiencies with the control strategy for HPAV:

- DOE is using QRA to determine the adequacy of a safety control. However, DOE is not applying Standard 1628 to the QRA models.
- Because the QRA calculations are part of the safety basis, DOE must establish a technical basis for maintenance and protection of QRA input parameters.

Instead of using QRA calculations to design passive safety controls, DOE could credit HPAV preventive controls (e.g., flush, vent, or purge) on pipe routes with safety-related spray consequences. DOE could complete a revised spray leak calculation to inform its decision process. The calculation should address the reduced material-at-risk inherent in the SHSV design.

## REFERENCES

- [1] Cange, S.M., Letter to J.L. Connery, *Resolution of Defense Nuclear Facilities Safety Board Technical Issues Regarding Waste Treatment and Immobilization Plant*, Department of Energy Office of Environmental Management, Washington, DC, January 24, 2017.
- [2] Schreiner, R.L., *Basis of Design*, 24590-WTP-DB-ENG-01-001, Rev 5, Bechtel National, Incorporated, May 25, 2017.
- [3] Defense Nuclear Facilities Safety Board, *27th Annual Report to Congress*, Washington, DC, April 27, 2017.
- [4] Defense Nuclear Facilities Safety Board, *Report to Congress on the Status of Significant Unresolved Issues Concerning the Design and Construction of DOE's Defense Nuclear Facilities*, Washington, DC, June 22, 2009.
- [5] Defense Nuclear Facilities Safety Board, *Report to Congress on the Status of Significant Unresolved Issues Concerning the Design and Construction of DOE's Defense Nuclear Facilities*, Washington DC, April 15, 2010.
- [6] Defense Nuclear Facilities Safety Board, *Inadequate Mixing at the Waste Treatment and Immobilization Plant*, Washington, DC, January 6, 2010.
- [7] Defense Nuclear Facilities Safety Board, *Recommendation 2010-2, Pulse Jet Mixing at the Waste Treatment and Immobilization Plant*, Washington, DC, December 17, 2010.
- [8] Defense Nuclear Facilities Safety Board, *Heat Transfer Analysis for Process Vessels in the Pretreatment Facility, Waste Treatment and Immobilization Plant*, Washington, DC, August 3, 2011.
- [9] U.S. Department of Energy, *Hanford Tank Waste Retrieval, Treatment, and Disposition Framework*, Washington, DC, September 24, 2013.
- [10] Taki, B.D., *ICD-19 – Interface Control Document for Waste Feed*, 24590-WTP-ICD-MG-01-019, Rev. 7, Bechtel National, Incorporated, Richland, WA, September 19, 2014.
- [11] Defense Nuclear Facilities Safety Board, *Board Closes Recommendation 2010-2, Pulse Jet Mixing at the Waste Treatment and Immobilization Plant*, Washington, DC, January 28, 2014.
- [12] Smith, K.W., Memorandum to M.C Regalbuto, *Resolution of Defense Nuclear Facilities Safety Board Issue on Potential for Inadvertent Criticality*, Department of Energy Office of River Protection, Richland WA, November 21, 2016.

- [13] Smith, K.W., Memorandum to M.C Regalbuto,, *Resolution of Defense Nuclear Facilities Safety Board Issue on Waste Treatment and Immobilization Plant Generation and Control of Hydrogen in Pretreatment Process Vessels*, Department of Energy Office of River Protection, Richland, WA, December 19, 2016.
- [14] Smith, K.W., Memorandum to M.C. Regalbuto, *Resolution of Defense Nuclear Facilities Safety Board Issue on Hydrogen in Piping and Ancillary Vessels*, Department of Energy Office of River Protection, Richland, WA, December 19, 2016.
- [15] Lewis, T., and K. Waltzer, *Proposed Control of Hydrogen Events in the Pretreatment Facility Pulse Jet Mixed Process Vessels*, 24590-PTF-ES-NS-15-003, Rev. 00C, Bechtel National, Incorporated, Richland, WA, November 3, 2016.
- [16] Fox, D.K., *Safety Requirements Document Volume II*, 24590-WTP-SRD-ESH-01-001-02, Rev. 8, Bechtel National, Incorporated, Richland, WA, August 2, 2016.
- [17] Eager, K., *Revised Calculation of Hydrogen Generation Rates and Time to Lower Flammability Limit for WTP*, 24590-WTP-M4C-V11T-00011, Rev. C, Bechtel National, Incorporated, Richland, WA, May 7, 2010.
- [18] Sherwood, D.J. and L.M. Stock, *Modifying the Hu Correlation to Predict Hydrogen Formation in the Hanford Waste Treatment and Immobilization Plant*, WA: 24590-WTP-RPT-RT-04-0002, Rev. 0, Bechtel National, Incorporated, Richland, WA, 2004.
- [19] Poloski, A.P., *Technical Basis for Scaling of Air Sparging Systems for Mixing in Non-Newtonian Slurries*, WTP-RPT-129, Rev. 0, Pacific Northwest National Laboratory, Richland, WA, February 2005.<sup>3</sup>
- [20] Bontha, J, et al., *Technical Basis for Predicting Mixing and Flammable Gas Behavior in the Ultrafiltration Feed Process and High-Level Waste Lag Storage Vessels with Non-Newtonian Slurries*, PNWD-3676, WTP-RPT-132, Rev. 0, Battelle–Pacific Northwest Division, Richland, WA, December 2005.<sup>4</sup>
- [21] Epstein, M., *Aerosol Production in WTP Process – A Review of Recent Aerosol Testing*, FAI/12-0598, Rev. 2, Fauske & Associates, LLC, Burr Ridge, IL, December 12, 2012.
- [22] Defense Nuclear Facilities Safety Board, *Aerosol Entrainment Coefficient Based on Testing and Data Analyses for the Waste Treatment and Immobilization Plant*, Washington, DC, March 25, 2015.

---

<sup>3</sup> Work completed by members of the Board’s technical staff prior to the staff members’ employment with the Board.

<sup>4</sup> Work completed by members of the Board’s technical staff prior to the staff members’ employment with the Board.

- [23] Diener, G.A., *Pretreatment Waste and Melter Feed Composition Variability Testing Using HLW Simulants*, VSL-09R1600-1, Rev. 0, Vitreous State Laboratory, The Catholic University of America, Washington, DC, November 20, 2009.
- [24] Poirer, M.R., et al., *SRNL Review and Assessment of WTP UFP-02 Sparger Design and Testing*, SRNL-STI-2013-00590, Rev. 1, Savannah River National Laboratory, Aiken, SC, March 2014.
- [25] Olson, J.W., *Process Inputs Basis of Design (PIBOD)*, 24590-WTP-DB-PET-09-001, Rev. I, Bechtel National, Incorporated, Richland, WA, June 2, 2011.
- [26] Poloski, A.P., et al., *Estimate of Hanford Waste Rheology and Settling Behavior*, PNNL-16857, Pacific Northwest National Laboratory, Richland, WA, October, 2007.<sup>5</sup>
- [27] Slaathaug, E., *Pretreatment Process Fluid Properties for the SHSVD in Support of Testing*, 24590-PTF-RPT-PE-15-002, Rev. 0, Bechtel National, Incorporated, Richland, WA, March 30, 2016.
- [28] Meehan, J.L., *Methods for Assessment of the Time to LFL in Select Newtonian Vessels: Post Accident Case Assuming Solids Settling*, 24590-WTP-RPT-PET-10-012, Rev. 0, Bechtel National, Incorporated, Richland, WA, May 7, 2010.
- [29] Gauglitz, P.A., et al., *Hydrogen Gas Retention and Release from WTP Vessels: Summary of Preliminary Studies*, PNNL-24255, Pacific Northwest National Laboratory, Richland, WA, July 2015.
- [30] Neeley, M., *Pretreatment Criticality Evaluation Engineering Study in Support of T2*, 24590-PTF-ES-NS-15-002, Rev 2, Bechtel National, Incorporated, April 2016.
- [31] Smith, K.W., Letter to D. Huizenga, *Request for Approval of the Justification of Mission Need for a Tank Waste Characterization and Staging Capability*, 13-ORP-0286, October 28, 2013.
- [32] American Nuclear Society, *Nuclear Criticality Safety in Operations with Fissionable Material Outside Reactors*, ANSI/ANS-8.1, 2014.
- [33] Department of Energy, Office of River Protection, *River Protection Project System Plan*, ORP-11242, Revision 7, October 2014.
- [34] American Nuclear Society/American National Standards Institute, *Criteria for Nuclear Criticality Safety Controls in Operation with Shielding and Confinement*, ANSI/ANS-8.10, September 1983.

---

<sup>5</sup> Work completed by members of the Board's technical staff prior to the staff members' employment with the Board.

- [35] Isom, W.L., et al., *Review of Plutonium Oxide Receipts into Hanford Tank Farms*, RPP-RPT-50941, Rev. 0, Washington River Protection Solutions, October 2011.
- [36] Miles, R., et al., *Preliminary Co-precipitated Plutonium Criticality Safety Evaluation Report for the WTP Project*, 24590-WTP-CSER-ENS-08-0001, Rev 1, Bechtel National, Incorporated, February 2016.
- [37] American Nuclear Society, *Validation of Neutron Transport Methods for Nuclear Criticality Safety Calculations*, ANSI/ANS-8.24, 2007.
- [38] American Nuclear Society, *Use of Soluble Neutron Absorbers in Nuclear Facilities Outside Reactors*, ANSI/ANS-8.14, 2011.
- [39] Department of Energy, *Facility Safety*, DOE Order 420.1B, Washington, DC, December 2005.
- [40] U.S. Nuclear Regulatory Commission, *Guide for Validation of Nuclear Criticality Safety Calculation Methodology*, NUREG/CR-6698, 2001.
- [41] Flora, E.M., et al., *Validation of MCNP5 for Hanford Waste Criticality Safety Calculations*, 24590-WTP-Z0C-W11T-00018, Rev. 0, Bechtel National, Incorporated, 2010.
- [42] Miles, R., *Plutonium Absorber Limits from MCNP Calculations*, 24590-WTP-Z0C-W11T-00013, Rev 2, Bechtel National, Incorporated, 2016.
- [43] Tripp, C. S., "Licensing Issues Associated with PuO<sub>2</sub> and Mixed Oxide Powder Processes," in *The Need for Integral Critical Experiments with Low-Moderated MOX Fuels*, Paris, France, 2004.
- [44] Criticality Safety Support Group, *Validation with Limited Benchmark Data*, CSSG Response to Tasking 2014-02, 2015.<sup>6</sup>
- [45] American Nuclear Society, *Administrative Practices for Nuclear Criticality Safety*, ANSI/ANS-8.19.
- [46] Peurrung, L., and P. Townson, *Test Plan for Mixing Requirements Verification Testing in the Standard High Solids Vessel Design (SHSVD-T) Vessel*, 24590-WTP-ES-ENG-15-033, Rev 0, Bechtel National, Incorporated, September 2016.
- [47] Johnson, P., *De-inventory Testing for the Standard High Solids Vessel Informal Enigneering Study*, 24590-WTP-ES-ENG-16-021, Rev 0, Bechtel National, Incorporated, September 7, 2016.

---

<sup>6</sup> Work completed by members of the Board's technical staff prior to the staff members' employment with the Board.

- [48] Neeley, M., *Heavy Plutonium Particulate Mass Limits in a Vessel and Pipe*, 24590-WTP-Z1C-W11T-00004, Rev B, Bechtel National, Incorporated, April 2016.
- [49] Trottier, R. and S. Dhodapkar, "Sampling Particulate Materials the Right Way," *Chemical Engineering*, pp. 42-49, April 2012.
- [50] Yongquan, Z. et al., "Density, Electrical Conductivity, Acidity, Viscosity, and Raman Spectroscopy of NaBO<sub>2</sub>, Na<sub>2</sub>B<sub>4</sub>O<sub>7</sub>, and NaB<sub>5</sub>O<sub>8</sub> Solutions at 298.15 and 323.15 K," *Journal of the Chemical Society - Pakistan*, vol. 35, no. 4, pp. 1066-1071, 2013.
- [51] Delegard, C.H. and S.A. Jones, *Chemical Disposition of Plutonium in Hanford Site Tank Wastes*, PNNL-23468 Rev 1. WTP-RPT-234 Rev. 1, Pacific Northwest National Laboratory, May 2015.
- [52] Reynolds, J.G., J.A. Kadinger, and T.J Venetz, *Plutonium-Bismuth Associations in Hanford Waste*, RPP-RPT-54469, Rev. 0, Washington River Protection Solutions, May 2013.
- [53] Blush, S., Memorandum to D. Busche, *Plutonium-Bismuth (Pu-Bi)-Rich Particle Issues and Questions*, CCN 252894; 24590-WTP-GPP-PADC-006, Bechtel National, Incorporated, October 2012.
- [54] Blush, S., Memorandum to D. Busche, *Plutonium-Bismuth (Pu-Bi) Rich Particles*, CCN 252893; 24590-WTP-GPP-PADC-006, Bechtel National, Incorporated, October 2012.
- [55] McCoskey, J.K. and G.A. Cooke, *Characterization of Plutonium-Bearing Waste in High-Level Waste Storage Tanks 241-SY-102, 241-TX-118, and 241-AZ-101 and the Plutonium Finishing Plant Z-9 Crib*, LAB-RPT-12-00006, Rev. 0, Washington River Protection Solutions, January 2013.
- [56] Reynolds, J.G., G. Cooke, J. McCoskey, and W. Callaway, "Discovery of Plutonium Bismuth and Plutonium-Bismuth-Phosphate Containing Phases in a Hanford Waste Tank," *Journal of Radioanalytical Nuclear Chemistry*, vol. 309, pp. 973-981., February 2016.
- [57] Callaway, W.S. and G.A. Cooke, *Distribution of Plutonium Rich Particles in Tank 241-SY-102 Sludge*, 24590-CHG-BNI-2001-00001, Rev. 00A, Bechtel National, Incorporated, May 2008.
- [58] Narlesky, J.E. et al., *Characterization of Representative Materials in Support of Safe, Long Term Storage of Surplus Plutonium in DOE-STD-3013 Containers*, LA-UR-12-23790, Los Alamos National Laboratory, February 2013.
- [59] Schreiner, R.L., *Basis of Design*, 24590-WTP-DB-ENG-01-001 Rev 4, Bechtel National, Incorporated, November 2016.

- [60] D. Hoffman, "Advancement in Plutonium Chemistry 1967-2000," *American Nuclear Society*, 2002.
- [61] Department of Energy, *Development of Probabilistic Risk Assessments for Nuclear Safety Applications*, DOE Standard 1628-2013, Washington, DC, November 2013.
- [62] Beck, J. A., *Preliminary Documented Safety Analysis to Support Construction Authorization, PT Facility Specific Information*, 24590-WTP-PSAR-ESH-01-002-02, Rev 6a, Bechtel National, Incorporated, February 2017.
- [63] Nuclear Regulatory Commission, *Hydrogen Combustion Events in Foreign BWR Piping*, Information Notice 2002-15, Washington, DC, April 12, 2002.
- [64] Frank, M.V. and R. Freer, *Unmitigated Consequences for Pretreatment Hydrogen in Piping and Non-Process Vessel Events*, 24590-PTF-Z0C-H01T-00003, Revision F, Bechtel National, Incorporated, May 24, 2016.
- [65] Department of Energy response to Defense Nuclear Facilities Safety Board's October 27, 2016, agenda, *Follow-up from October 5, 2016, Review of Waste Treatment and Immobilization Plant (WTP) Hydrogen Events in Piping and Non-Process Vessels (Technical Issue T3)*.
- [66] Department of Energy, *Department of Energy Nuclear Safety Policy*, Policy 420.1, Washington, DC, February 2011.
- [67] Van Vleet, R.J., *Spray Leak in the PT Facility*, 24590-PTF-Z0C-W14T-00022, Rev D, Bechtel National, Incorporated, September 2015.
- [68] O'Brien, J.B., Memorandum to M.B. Moury, *Use of Risk Insights to Support Design Basis Accident and Beyond Design Basis Accident Identification*, Washington, DC: CCN 261019, July 19, 2013.
- [69] Dawson, R.L., *Request for Bechtel National, Inc. (BNI) to Provide Probabilistic Risk Assessment (PRA) Plans to Address Nuclear Safety Issues in Black Cell Vessels and Piping*, 13-NSD-0027, CCN 261019, August 13, 2013.
- [70] St. Julian, J.M., Letter to W.F. Hamel, *Contract No. DE-AC27-01RV14136 – Bechtel National Inc. Use of Probabilistic Risk Assessment*, CCN 267935, Richland, Washington, September 29, 2014.
- [71] Title 10 Code of Federal Regulations, Part 830, *Nuclear Safety Management, Subpart B, Safety Basis Requirements*.
- [72] Minichiello, J., *HPAV Engineering Analysis Methods and Criteria*, 24590-WTP-RPT-ENG-07-011, Rev 7, Bechtel National, Incorporated, October 2012.



- [73] Wentink, M., *Quantitative Risk Analysis of Hydrogen Events at WTP: Development of Event Frequency-Severity Analysis Model*, 24590-WTP-RPT-10-008, Revision 4, Bechtel National, Incorporated, December 2011.
- [74] Barker, S., *Quantitative Risk Analysis Data Collection Process*, 24590-WTP-GPG-M-0065, Rev 2, Bechtel National, Incorporated, July 2012.
- [75] Defense Nuclear Facilities Safety Board, *Report to Congress on the Status of Significant Unresolved Technical Differences between the Board and the Department of Energy on Issues Concerning the Design and Construction of DOE's Defense Nuclear Facilities*, Washington DC, September 3, 2010.
- [76] Defense Nuclear Facilities Safety Board, *Report to Congress on the Status of Significant Unresolved Technical Differences between the Board and the Department of Energy on Issues Concerning the Design and Construction of DOE's Defense Nuclear Facilities*, Washington, DC, December 10, 2010.

## Appendix A - Gas Retention and Release in Low Solids Vessels

### 1. Background and Objective

The Pretreatment (PT) Facility at the Waste Treatment and Immobilization Plant (WTP) is being designed to receive Hanford tank waste for processing before the waste is sent to the Low-Activity Waste and High-Level Waste Facilities for immobilization. Hanford tank waste generates hydrogen and other flammable gases through thermolysis and radiolysis. During normal mixing operations in the PT Facility process vessels, these flammable gases are continuously released to the vessel headspace where they are removed by the forced air purge system. During a loss of agitation, the release mechanism of hydrogen from the waste to the vessel headspace depends on the waste properties. Newtonian waste without solids does not retain gas even when unmixed. Non-Newtonian waste retains the generated hydrogen until the waste is agitated or a spontaneous gas release occurs. If the concentration of hydrogen in the vessel headspace exceeds the lower flammability limit (LFL), the potential for an explosion exists.

Four PT Facility waste feed receipt vessels, FRP-VSL-00002A/B/C/D, are designed to receive low-solids Newtonian waste, which may contain up to 3.8 weight percent solids. If not agitated for a prolonged period, the waste may form a non-Newtonian solids layer that retains generated hydrogen. The WTP Safety Requirements Document (SRD) addresses the functional requirements for hydrogen control systems in process vessels to prevent an inventory of hydrogen in concentrations greater than the LFL in the vessel headspace during off-normal and post-accident conditions [1]. The SRD states that safety controls are required for process vessels with a time to reach LFL (i.e., time-to-LFL) less than or equal to 1,000 hours.

Bechtel National, Incorporated (BNI), identified a control strategy for low-solids Newtonian vessels to ensure that the hydrogen concentration in the vessel headspace remains below the LFL during 1,000 hours following loss of agitation. The control strategy relies on a forced air purge system to dilute hydrogen in the headspace and a specific administrative control to limit the waste volume [2]. This approach maintains sufficient vessel headspace volume to ensure that flammable gases retained in the waste will not result in a flammable concentration if instantaneously released and uniformly dispersed in the headspace. BNI's methodology for determining the safe operating volume is outlined in Appendix K of reference [2]. The methodology involves analyzing hydrogen gas generation and retention in a settling solids layer.

BNI's analysis relies on several modeling assumptions that may be non-conservative. In particular, the Board noted three areas where the analysis may be non-conservative: the settling rate of the solids layer after loss of mixing, the final layer thickness, and the variation of gas generation rate during settling. Uncertainties in these assumptions make it difficult to ensure that the calculation is conservative.

The objective of the Board's analysis is to evaluate these three potential non-conservatisms by using a parametric approach for evaluating spontaneous gas releases in low-solids vessels during off-normal and post-accident conditions. The approach relies on existing data and physical models where available, and minimizes the number of assumptions employed.

It also provides a foundation to identify additional data or analysis to refine the calculations or reduce uncertainty. This approach follows the method presented in a Pacific Northwest National Laboratory (PNNL) report (PNNL-24255), where the settling solids layer thickness is parameterized in terms of the fraction of solids settled [3]. This approach allows results to be obtained without making any assumptions about the thickness of the settling solids layer. The Board also used the stability criteria for spontaneous gas releases described in the PNNL report to evaluate the potential for gas releases in the settling solids layer in the FRP-VSL-00002A/B/C/D vessels.

The physical processes involved in the gas retention and release behavior of settling waste solids are complex, but the models employed are fairly simple. Further, data to support the models are limited; therefore, the results of this analysis should be considered illustrative of an approach to achieving the bounding values important to safety. More extensive work is needed to further understand the physical processes and conservatively determine safe fill levels in low-solids vessels.

## **2. Assumptions and Input Parameters**

The Board has observed that various physical mechanisms are important in determining the gas retention and release characteristics in low solids vessels during settling. The pulse jet mixing systems keep solids suspended during normal operations. In the low-solids vessels, the solids concentration (on a well-mixed volume basis) is relatively low. Consequently, the waste slurry will behave as a Newtonian fluid. Any gases generated in the slurry will form bubbles, which coalesce, rise to the surface, and release at a steady rate into the vessel headspace, where they are swept away by the ventilation system.

When mixing is lost, suspended solids begin to settle. A layer containing liquid and suspended solid particles forms as settling continues. Above this settling solids layer will be supernatant liquid. The concentration of solids within the settling solids layer increases with time. As the concentration increases, the slurry will develop a yield stress and retain the small gas bubbles that are forming due to gas generation from radiolysis and thermolysis. Further, the temperature within the settling solids layer will rise as a result of the heat load from radioactive decay. Because the hydrogen generation rate depends on the solids fraction and temperature, it will vary spatially and temporally within this settling solids layer. As gas builds up in the settling solids layer, spontaneous releases may occur.

Bubble cascade and buoyant displacement are the two principal mechanisms for spontaneous gas release from the settling solids layer. The criteria for the initiation of instabilities leading to these release events depend on the gas fraction within the settling solids layer, as well as the yield stress, bulk slurry density, and supernatant density. Hence, many time-evolving, competing processes are at play in determining if a gas release can occur, and whether it will result in a flammable headspace if released quickly.

The processes described above are modeled in the following sections of this calculation. The Board employed several simplifying assumptions to develop tractable solutions that capture the various processes involved. The simplifying assumptions are:

- The solids concentration within the settling solids layer is spatially uniform.
- The yield stress of the settling solids layer depends only on solids concentration; hence it is also spatially uniform within the settled layer.
- The settling rate of the settling solids layer is not known, and is assumed to be a constant.
- The final solids layer thickness is not known, and therefore is to be treated parametrically.
- The settling time will be taken as 1,000 hours to reach the final solids layer thickness.
- The gas generation rate in the settling solids layer is based on temperatures that are computed at 1,000 hours.
- All the gas generated within the settling solids layer is assumed to be retained prior to release. During the release, all of the gas is assumed to be released instantaneously and uniformly dispersed in the headspace.

Values for specific parameters used in developing the models in this report are discussed as they are introduced. Table A-5 in Section 4 of this appendix summarizes specific model input parameter values used to evaluate the models.

### 3. Analysis

#### 3.1 Rheology of Settling Solids Layers

The dependence of slurry yield stress on the solids fraction has been shown to be reasonably approximated by an exponential function [3] [4]:

$$\tau_y = a_1 e^{a_2 wt\%} \quad (\text{A.1})$$

Table A.1 shows fitting parameters recommended for two Hanford tank wastes [3].

*Table A-1. Curve fit parameters for slurry yield stress.*

Hanford tank waste	$a_1$	$a_2$
T-204	0.035	0.623
AZ-101	0.651	0.176

Equation (A.1) gives the slurry yield stress in terms of the weight percent<sup>1</sup> (mass fraction) of undissolved solids. The mass fraction,  $w_s$ , in a given volume of slurry is given by

---

<sup>1</sup> Weight percent is the mass fraction expressed as a percentage, i.e.,  $wt\% = 100\% \times w_s$ .

$$w_s = \frac{M_S}{M_S + M_L} \quad (\text{A.2})$$

where  $M_S$  and  $M_L$  are the masses of the solids and liquid components within the slurry volume, respectively.

An alternative and useful way of quantifying the solids concentration is the solids volume fraction  $\phi_s$  given by

$$\phi_s = \frac{V_S}{V_S + V_L} \quad (\text{A.3})$$

where  $V_S$  and  $V_L$  are the volumes of the solids and liquid components within the slurry volume, respectively.

The mass fraction and volume fraction are related through the introduction of the particle/liquid density ratio

$$s = \rho_s / \rho_L \quad (\text{A.4})$$

By manipulating Eqs. (A.2) – (A.4), it can be shown that

$$\phi_s = \frac{w_s}{s - (s - 1)w_s} \quad (\text{A.5})$$

$$w_s = \frac{s\phi_s}{(s-1)\phi_s + 1} \quad (\text{A.6})$$

During settling, the total amount of solids in the settling solids layer remains constant, but the solids concentration increases with increased settling. How much the solids settle during a mixing system outage can vary, and is not known for the WTP low solids vessels.

It is useful to characterize the settling solids layer in terms of the fraction settled,  $f$ , defined by

$$f = \frac{V_{sup}}{V_W} = \frac{V_W - V_{SL}}{V_W} = 1 - \frac{V_{SL}}{V_W} \quad (\text{A.7})$$

where  $V_W = V_{SL} + V_{sup}$  is the total waste volume and  $V_{SL}$  and  $V_{sup}$  are the volumes of the settling solids layer and supernatant, respectively. Given this definition of fraction settled, the solids volume fraction in the settling solids layer is

$$\phi_{SL} = \frac{V_S}{V_{SL}} = \frac{\phi_{s0}}{1 - f} \quad (\text{A.8})$$

Where  $V_S$  is the total volume of solids in the vessel, and  $\phi_{s0}$  is the solids volume fraction of the fully mixed (unsettled) waste:

$$\phi_{s0} = \frac{V_S}{V_W} = \frac{w_{s0}}{s - (s - 1)w_{s0}} \quad (\text{A.9})$$

The variation of the solids fraction as a function of fraction settled is illustrated in Figure A-1. The case  $f = 0$  represents the well-mixed case where the solids are fully suspended. The limit  $f = 1$  is not physically possible as the solids fraction becomes infinite as  $f \rightarrow 1$ .

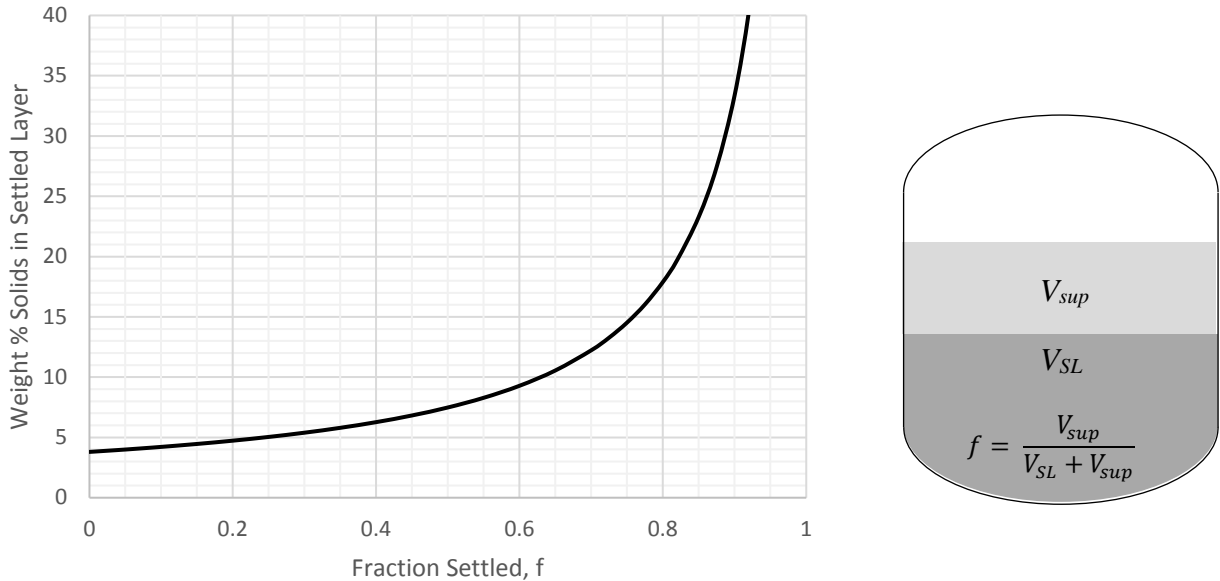


**Figure A-1.** Calculated solids loading as a function of the fraction settled. Results shown are for  $s = 1.69$  and an initial weight percent solids of 3.8% in the well-mixed waste ( $\phi_{s0} = 0.023$ ).

The variation of yield stress with the fraction settled is shown in Figure A-2 for the properties of waste in both Hanford tanks T-204 and AZ-101. This figure shows that the yield stress can vary by orders of magnitude depending on the degree of settling. The AZ-101 data fit results in higher yield stress at a low settling fraction, whereas the T-204 fit produces higher yield stress when the settling fraction is at higher values.

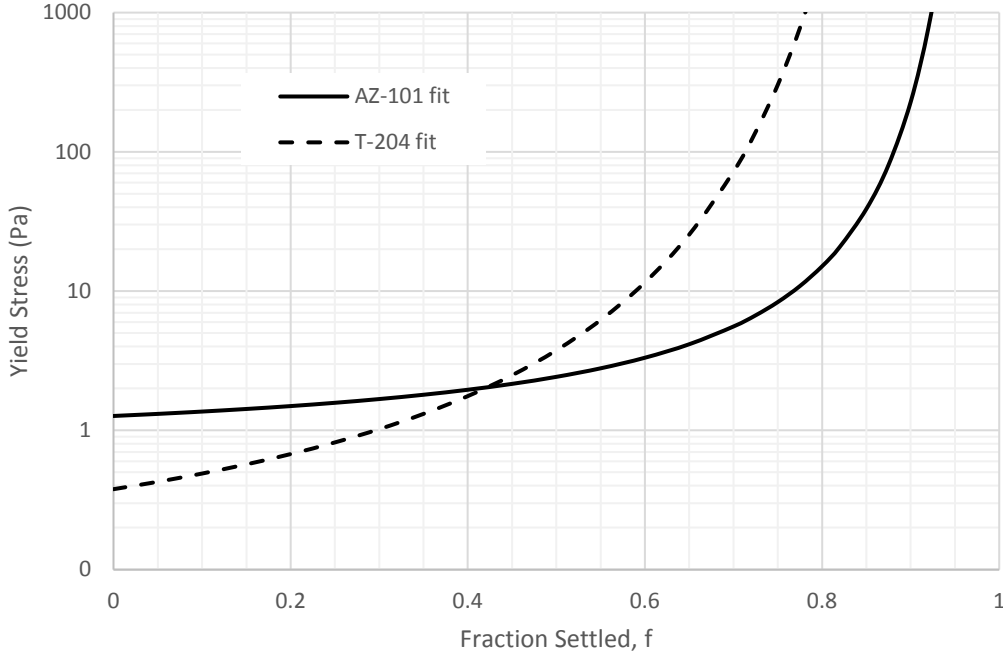


**Figure A-2.** Calculated slurry yield stress as a function of the fraction settled. Results shown are for  $s = 1.69$  and an initial weight percent solids of 3.8% ( $\phi_{s0} = 0.023$ ).

### 3.2 Sludge Sedimentation Rate

The settling characteristics of Hanford tank waste are discussed in reference [4], where it is noted that the waste has settled in the hindered settling regime. The hindered settling regime occurs when interacting particles settle as a mass, beginning with a fully suspended volume and settling to a final settled-solids volume. The report presents a model for the height of the settling solids layer, which has the following mathematical form

$$H_{SL}(t) = a + be^{-\frac{t}{\theta_s}} \quad (\text{A.10})$$

where  $H_{SL}$  is the height of the top of the settling solids layer, and  $a$ ,  $b$ , and  $\theta_s$  are constants.

The settling solids layer height can be approximately related to the volume of the settling solids layer by assuming the vessel is a right circular cylinder of diameter  $D$ :

$$V_{SL}(t) = \frac{\pi D^2}{4} H_{SL}(t) \quad (\text{A.11})$$

The initial condition at  $t = 0$  is  $V_{SL}(0) = V_w$ . The condition after a settling time  $t_f$  (1,000 hours) is  $V_{SL}(t_f) = V_w(1 - f)$ . Hence, Eq. (A.10) can be written

$$\frac{V_{SL}(t)}{V_W} = 1 - f \frac{(1 - e^{-\frac{t}{\theta_s}})}{(1 - e^{-\frac{t_f}{\theta_s}})} \quad (\text{A.12})$$

Equation (A.12) is shown in Figure A-3 for various values of the settling time constant,  $\theta_s$ . A conservative value for  $\theta_s$  is not known for the waste that will be in the low solids vessels. However, from Figure A-3, it is clear that as  $\theta_s$  approaches  $t_f$ , the sedimentation curve is approximately linear, and limits to linear as  $\theta_s > t_f$ . Mathematically this limit of Eq. (A.12) is found to be

$$\frac{V_{SL}(t)}{V_W} \cong 1 - f \frac{t}{t_f}, \quad \theta_s > t_f \quad (\text{A.13})$$

The mean time-weighted volume of the settling solids layer during settling is the integrated area under the trajectories in Figure A-3. Hence, the linear limit represents the largest volume of waste that can generate and retain gas. Therefore, it is bounding in this analysis to use the linear settling behavior given by Eq. (A.13), particularly given the fact that the settling time constant  $\theta_s$  for each batch of waste is not known.

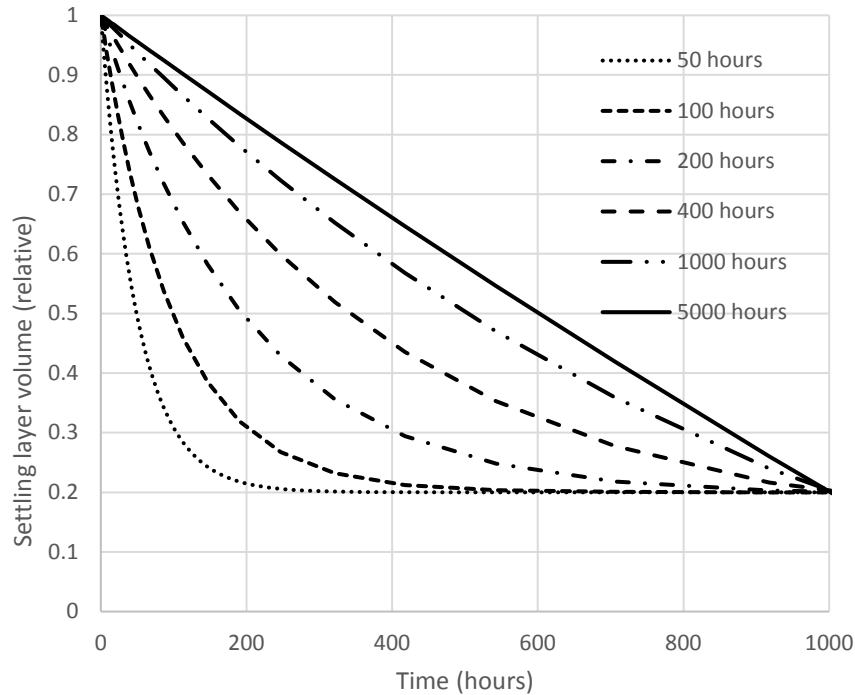


**Figure A-3.** Sedimentation curves for various values of the settling time constant,  $\theta_s$ . For this case the final settling fraction is  $f = 0.8$ . The plotted values are the ratio  $\frac{V_{SL}(t)}{V_W}$ .

### 3.3 Gas Generation During Settling

The settling solids layer will generate hydrogen and other gases due to radiolysis and thermolysis. It also will heat up due to heat generation from radioactive decay. Given the heat



generation and conduction<sup>2</sup> within the layer, the temperature will vary spatially and temporally within the settling solids layer. Because the hydrogen generation rate is a nonlinear function of temperature, the local generation rate also will vary spatially and temporally within the layer. The unit molar generation rate (moles/m<sup>3</sup>-hour) within the settling solids layer can be found by integrating over the entire volume at each moment of time according to

$$\dot{n}(t) = \frac{1}{V_{SL}(t)} \int \dot{n}(\vec{z}, t) dV_{SL} \quad (\text{A.14})$$

where  $\vec{z}$  is the position vector of the differential volume element.

The total amount of gas generated during settling is then given by

$$N_{H_2} = \int_0^{t_f} \dot{n}(t) V_{SL}(t) dt \quad (\text{A.15})$$

Determining the unit molar generation rate given by Eq. (A.14) would involve complex transient heat transfer calculations for the settling solids layer. However, there are several ways the unit molar generation rate can be approximated. For example, if  $\dot{n}$  is known as a function of the fraction settled, then Eq. (A.15) can be integrated to obtain the number of moles of hydrogen.

To this end, consider the settling fraction to be a transient variable,  $f'(t)$ , where  $f'(0) = 0$  and  $f'(t_f) = f$ .

$$f'(t) = 1 - \frac{V_{SL}(t)}{V_W} = f \frac{t}{t_f} \quad (\text{A.16})$$

Using the transformation given by Eq. (A.16), Eq. (A.15) becomes

$$N_{H_2} = \frac{V_W t_f}{f} \int_0^f \dot{n}(f')(1 - f') df' \quad (\text{A.17})$$

Two cases were used to evaluate Eq. (17). Appendix K of reference [2] assumed  $\dot{n}$  varied linearly between the design value [8] for an unsettled, well mixed vessel, and a higher value that was obtained by performing heat transfer calculations for a settling solids layer. This linear variation is expressed mathematically as

$$\dot{n}(f) = \dot{n}_0 + (\dot{n}_m - \dot{n}_0) \frac{f}{f_m} \quad (\text{A.18})$$

---

<sup>2</sup> Even a small yield stress developing in the settling solids layer will hinder or prevent natural convection from occurring, so it is conservative to assume that conduction is the only heat transfer mechanism internal to the settling layer.

In Eq. (A.18),  $\dot{n}_0$  is the value for the unsettled waste ( $f = 0$ ) and  $\dot{n}_m$  is the higher value for the waste which has settled to  $f = f_m$ . Table A shows the values used in Appendix K of [2].

**Table A-2.** Values used in reference [2] for linearly varying unit molar generation rate in a settling solids layer.

Term in Eq. (A.18)	Value	Basis
$\dot{n}_0$	3.7E-4 moles/m <sup>3</sup> -hr	Contract value for vessel FRP-02 [8]
$\dot{n}_m$	1.91E-3 moles/m <sup>3</sup> -hr	From peak temperature in stationary settled layer [2]
$f_m$	0.81	Calculated from stationary settled layer thickness of 5.7ft [2]

When Eq. (A.17) is integrated using Eq. (A.18), the result is:

$$N_{H_2} = \dot{n}_0 V_W t_f \left[ 1 + \left( \frac{\dot{n}_m}{\dot{n}_0} - 1 \right) \frac{f}{f_m} \left( \frac{1}{2} - \frac{f}{3} \right) - \frac{f}{2} \right] \quad (\text{A.19})$$

Eq. (A.19) is a quadratic function of  $f$ . The value of  $f$  that results in the largest amount of gas is obtained by setting  $\frac{dN_{H_2}}{df} = 0$  and solving for  $f$  which results in

$$f_{max} = \frac{3}{4} \left( 1 - \frac{f_m \dot{n}_0}{\dot{n}_m - \dot{n}_0} \right) \quad (\text{A.20})$$

For the conditions shown in Table A-2,  $f_{max} = 0.6$ , however, the analysis in Appendix K of [2] assumed  $f=0.81$  was a conservative case.

To obtain more detailed information on how  $\dot{n}$  varies as a function of settling, we performed heat transfer calculations to obtain the mean molar hydrogen generation rate for stationary settled solids layers (see Appendix B). The results for the generation rate at 1,000 hours are shown in Table A-3 and plotted in Figure A-4.

**Table A-3.** Unit molar hydrogen generation rates for heat transfer calculations (Appendix B).

Fraction settled, $f$	Layer height (m)	Layer volume (m <sup>3</sup> )	H <sub>2</sub> generation rate, $\dot{n}(f)$ (moles/m <sup>3</sup> -hr)
0.905	0.87	1.41E+02	1.65E-03
0.809	1.75	2.82E+02	1.07E-03
0.714	2.62	4.23E+02	8.19E-04
0.619	3.50	5.64E+02	6.86E-04
0.523	4.37	7.06E+02	6.06E-04
0.428	5.25	8.47E+02	5.55E-04
0.237	7.00	1.13E+03	4.82E-04
0.047	8.75	1.41E+03	4.33E-04

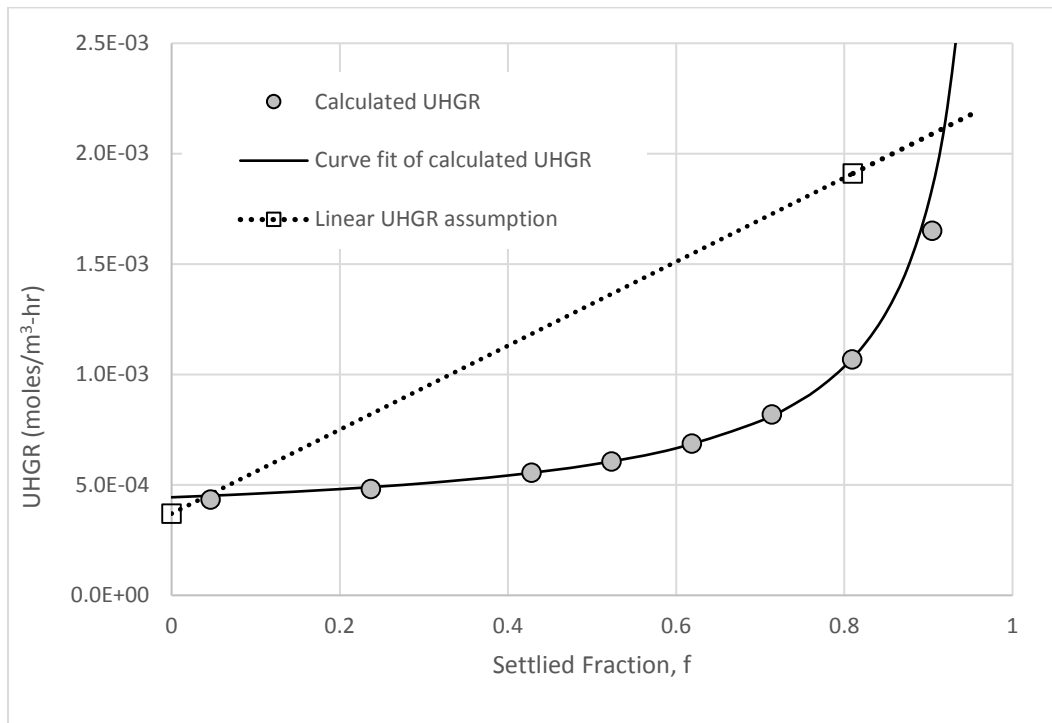


**Figure A-4.** Mean unit gas generation rate versus settling fraction from heat transfer calculations.

The curve fit of the data shown in Figure A-4 is given by

$$\dot{n}(f) = 2.96 \times 10^{-4} \left( 1 + \frac{0.5}{1-f} \right) \quad (\text{A.21})$$

Integrating Eq. (A.17) with Eq. (A.21) gives

$$N_{H_2} = 4.44 \times 10^{-4} V_w t_f \left( 1 - \frac{f}{3} \right) \quad (\text{A.22})$$

For this case, we determined that the maximum amount of hydrogen is produced for the unsettled layer ( $f = 0$ ), and it falls linearly as settling increases. Also shown for comparison in Figure A-4 is the linear varying assumption used in reference [2].

In addition to hydrogen, the settling solids layer also generates other gases. Some of these gases, such as  $\text{NO}_2$ , also contribute to flammability as either fuel or oxidizer. Independent of flammability, all generated gases contribute to the total gas buildup in the settling solids layer, leading to instability. The total gas generated is given by

$$N_g = \frac{N_{H_2}}{[H_2]} \quad (\text{A.23})$$

where  $[H_2]$  is the hydrogen fraction. Appendix H of [2] lists values of  $[H_2]$  taken from multiple samples of waste from six different waste tanks. A statistical analysis of that data indicates the mean value for the hydrogen fraction is  $[H_2] = 0.35$ , with a standard deviation of  $\pm 0.22$ .

### 3.4 Gas Retention in Settling Solids Layer

Conservatively assuming that all of the generated gas is retained, the total volume of retained gas in the settling solids layer is

$$V_{gSL} = \frac{R\bar{T}_{SL}}{\bar{p}_{SL}} N_g \quad (\text{A.24})$$

In Eq. (A.24),  $\bar{p}_{SL}$  and  $\bar{T}_{SL}$  are the average pressure and temperature in the settling solids layer, and  $R$  is the universal molar gas constant.

The average pressure can be estimated from the hydrostatic pressure based on the sludge density in the settling solids layer, which is given by

$$\bar{p}_{SL} = p_0 + \rho_L g H_L + \rho_{SL} g H_{SL} / 2 \quad (\text{A.25})$$

In Eq. (A.25),  $p_0$  is the pressure in the vessel headspace, and the liquid and settling solids layer heights are related to the fraction settled by

$$H_L = f H_W \quad H_{SL} = (1 - f) H_W \quad (\text{A.26})$$

The settling solids layer density in Eq. (A.25) is given by

$$\rho_{SL} = \phi_s \rho_s + (1 - \phi_s) \rho_L \quad (\text{A.27})$$

This gas will be in the form of distributed bubbles. The average gas volume fraction in the settling solids layer (*void fraction*) is given by

$$\alpha_{SL} = \frac{V_{gSL}}{V_{gSL} + V_{SL}} \quad (\text{A.28})$$

### 3.5 Gas Release Criteria

Two spontaneous gas release mechanisms are known to occur when gas is generated and retained in relatively low yield stress solids layers. These are the buoyant displacement gas release and bubble cascade gas release events [3].

*Buoyant displacement gas release events*—The criteria for a buoyant displacement is given in terms of a gas fraction in a solids layer [5]

$$\alpha_{BD} = \alpha_{NB} + \frac{\beta\tau_s}{\rho_{SL}gH_{SL}} \quad (\text{A.29})$$

The first term on the right-hand-side of Eq. (A.29) is the neutral buoyant void fraction,  $\alpha_{NB}$ . This is the fraction of gas required in the solids layer that will cause it to have the same density as the liquid above it. In the absence of any other restraining force, gas fractions greater than this value will cause the layer to become unstable, resulting in a spontaneous gas release.

The neutral buoyant void fraction is given by

$$\alpha_{NB} = 1 - \frac{\rho_L}{\rho_{SL}} \quad (\text{A.30})$$

For a settling solids layer, the density,  $\rho_{SL}$ , is a function of settling fraction,  $f$ . Hence, the neutral buoyant condition will be a function of settling fraction.

The second term on the right-hand-side of Eq. (A.29) accounts for the average shear strength  $\tau_s$  of the solids layer. In addition to achieving neutrally buoyant conditions, additional gas is necessary so that the upward buoyant force exceeds the resistive force of the shear strength. Generally, the contribution of this term is small unless the shear strength is large and the layer height is small. In Eq. (A.29), the parameter  $\beta$  is a constant whose value is believed to be in the range of  $1 \leq \beta \leq \sqrt{3}$ . [5] In the absence of specific knowledge of the value for shear strength, it can be estimated by relating it to the yield stress;

$$\tau_s = \gamma\tau_y \quad (\text{A.31})$$

where  $\gamma$  is on the order of 2 based on limited data for AZ-101 pretreated sludge and various non-radioactive gel materials [7].

*Bubble cascade gas release events*—The criteria for bubble cascade gas release events is based on experimental measurements [6]. In the experiments, the decomposition of hydrogen peroxide in clay simulants generated oxygen gas. The yield stress of the clay varied. The researchers used the gas fraction,  $\alpha_{BC}$ , for the onset of a bubble cascade release to determine level changes during gas generation. The experiments were repeated and the largest values of

$\alpha_{BC}$  were identified. These data<sup>3</sup>, taken from Appendix A of reference [6], are plotted in Figure A-5. Figure A-6 shows curve fits of three segments of the data. These curve fits are of the form

$$\alpha_{BC} = b_1 \ln(\tau) + b_2 \quad (\text{A.32})$$

Values for the constants  $b_1$  and  $b_2$  in Eq. (A.26) are shown in Table A-4.

**Table A-4.** Values for the curve fit constants for bubble cascade data.

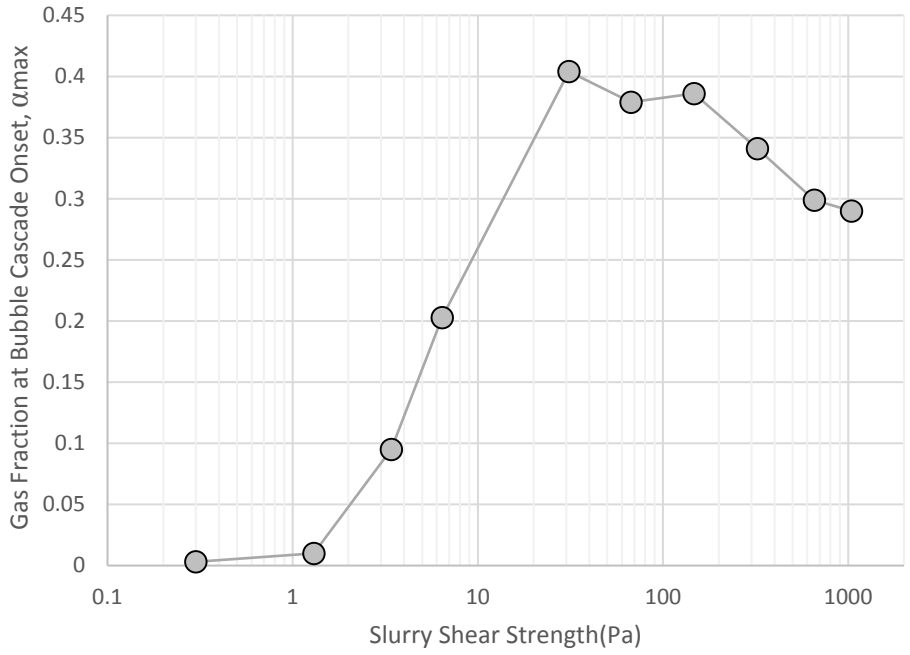
Yield stress range	$b_1$	$b_2$
$\tau < 1.3\text{Pa}$	0.0047	0.0088
$1.3\text{Pa} \leq \tau \leq 31\text{ Pa}$	0.1271	-0.0373
$\tau > 31\text{ Pa}$	-0.0337	0.5285

Figure A-7 shows the instability criteria for buoyant displacement and bubble cascade gas releases. At very low and very high  $f$  values, the bubble cascade criterion occurs at the lowest gas fraction, suggesting that the bubble cascade would occur before the buoyant displacement in this range of settling. For intermediate values of  $f$ , the buoyant displacement criterion occurs at the lowest gas fraction, suggesting the buoyant displacement would occur before the bubble cascade in this range of settling. For high values of yield stress and gas fraction, other gas release mechanisms such as percolation through connected channels occur [9]. Consequently, the regions of the buoyant displacement stability curves approaching 100 percent gas fraction should not be considered physically meaningful.

Because the buoyant displacement criterion for Hanford Tank AZ-101 results in an instability at a lower gas fraction than the curve corresponding to Hanford Tank T-102 rheology, reference [3] recommends using this curve to be conservative. As an additional measure of conservatism, the neutral buoyant condition given by Eq. (A.30) could be used as the stability criterion for buoyant displacement, particularly given the wide variability in the yield stress of settled Hanford waste.

---

<sup>3</sup> The data used for this analysis are from simulant columns approximately 32 cm tall and 2.64 cm in diameter. Tests also were performed in taller columns and larger diameter columns. Some of those tests show slightly higher gas retention values. The data set was selected because it is the largest set spanning a wide range of yield stress values.



**Figure A-5.** Maximum gas fraction for the onset of bubble cascade instability.

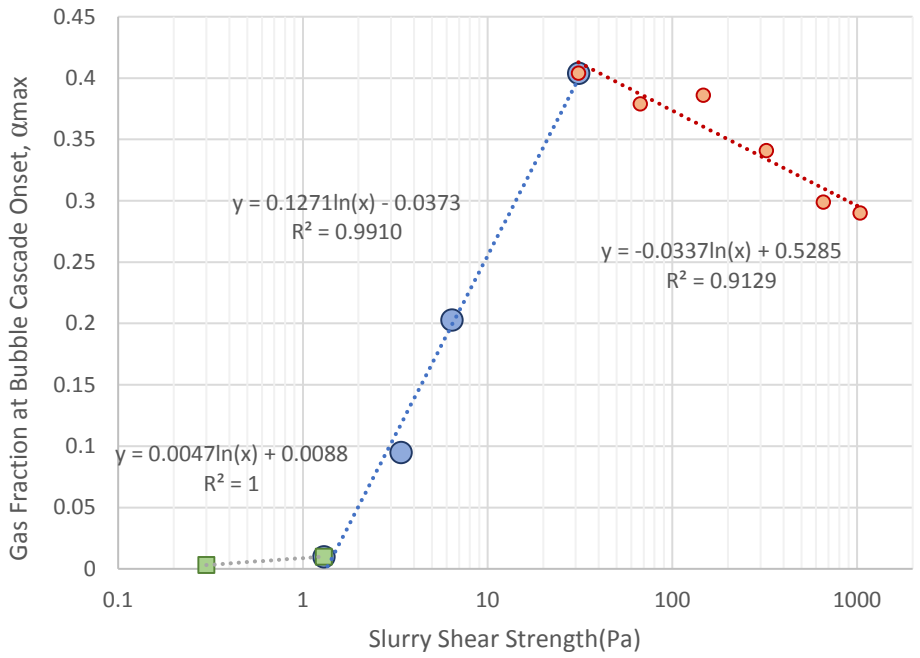


**Figure A-6.** Curve fitting the bubble cascade data in three segments using logarithmic functions.

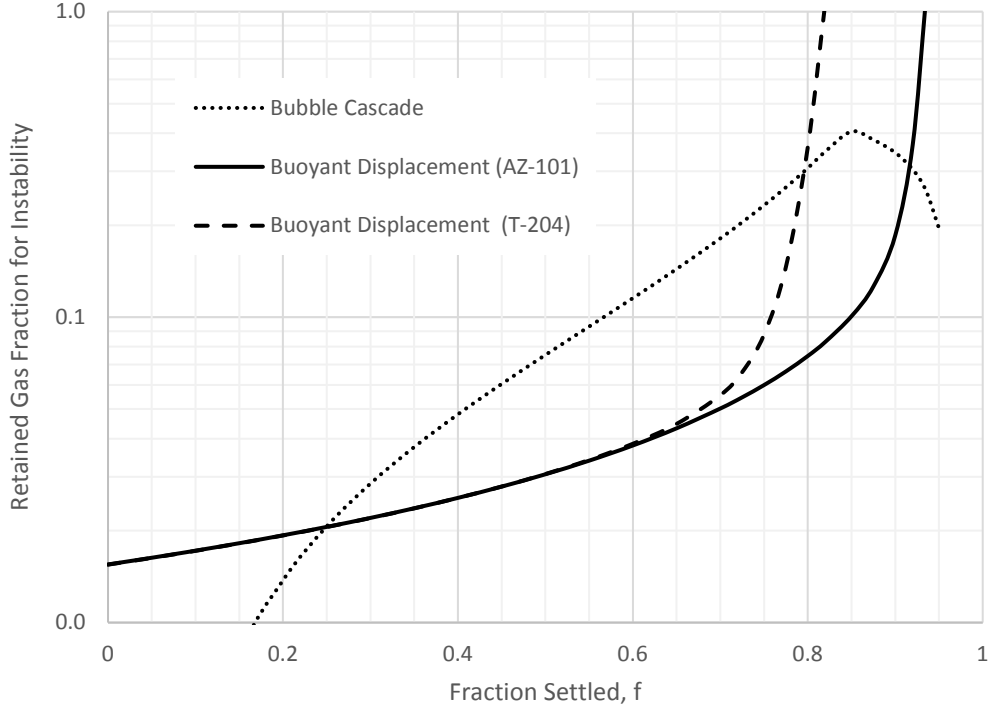


**Figure A-7.** Stability criterion for spontaneous gas release events in a settling layer. Results shown are for  $s = 1.69$ ,  $\rho_L = 1423\text{kg/m}^3$ ,  $H_W = 9.27\text{m}$ ,  $\gamma = 2$ ,  $\beta = 1$ .

### 3.6 Headspace Flammability after a Gas Release

If there is sufficient retained gas in the waste such that one of the stability criteria is met, then there will be a spontaneous gas release. It is also conservatively assumed that during a release all of the retained gas is released instantaneously into the headspace. The volume of hydrogen gas in the headspace will be

$$V_{H_2HS} = \frac{T_{HS}}{p_0} RN_{H_2} + \alpha_{HS_0} V_{HS} \quad (\text{A.33})$$

In Eq. (A.33)  $T_{HS}$  is the temperature of the headspace gas mixture, and it is assumed that the pressure in the headspace corresponds to atmospheric conditions. The term  $\alpha_{HS_0}$  is the initial hydrogen fraction in the headspace and  $V_{HS}$  is the headspace volume.

The concentration of hydrogen in the headspace after a release is given by

$$\alpha_{HS} = \frac{V_{H_2HS}}{V_{HS}} \quad (\text{A.34})$$



### 3.7 Preventing Flammable Conditions

The hydrogen control strategy for low solids Newtonian vessels in the WTP calls for controlling the vessel fill level in order to provide assurance the headspace remains below the LFL during a mixing system outage. Hence it is useful to introduce the vessel fill fraction given by

$$F_W = \frac{V_W}{V_T} \quad (\text{A.35})$$

where  $V_T = V_W + V_{HS}$

Given the headspace flammability requirement that  $\alpha_{HS} < LFL$ , Eq. (A.34) and (A.35) can be combined to give the flammability requirement in terms of vessel fill fraction

$$F_W < 1 - \frac{1}{LFL} \frac{V_{H2HS}}{V_T} \quad (\text{A.36})$$

BNI calculations correct the LFL for temperature using the following correlation

$$LFL_T = LFL_{298K} (1 - A(T - 298K)) \quad (\text{A.37})$$

In Eq. (A.37) the temperature  $T$  is in Kelvin and  $A$  is the Zabetakis attenuation factor,  $A = 0.0033 \text{ K}^{-1}$  (see Appendix M of [2]).

The analysis in Appendix K of reference [2] presents the result in terms of the time to achieve LFL. This can be obtained by rearranging Eq. (A.33) and (A.34) to determine the number of moles of hydrogen required to achieve LFL in the headspace:

$$N_{LFL} = \frac{p_0}{RT_{HS}} (LFL - \alpha_{HS_0}) \quad (\text{A.38})$$

Then Eq. (A.19) and (A.22) can be used with Eq. (A.38) to solve for the time to generate  $N_{LFL}$  moles for the two different models for generation rate distribution. When doing this,  $t_f$  in Eq. (A.19) is no longer 1,000 hours but rather is as the time to LFL,  $t_{LFL}$ . The result for the assumption of a linearly varying generation rate is

$$t_{LFL} = \frac{1}{\dot{n}_0} \frac{1 - F_W}{F_W} \frac{p_0}{RT_{HS}} (LFL - \alpha_{HS_0}) \left[ 1 + \left( \frac{\dot{n}_m}{\dot{n}_0} - 1 \right) \frac{f}{f_m} \left( \frac{1}{2} - \frac{f}{3} \right) - \frac{f}{2} \right]^{-1} \quad (\text{A.39})$$

The result for the computed generation rates as a function of settling fraction is

$$t_{LFL} = 2.25 \times 10^3 \frac{1 - F_W}{F_W} \frac{p_0}{RT_{HS}} (LFL - \alpha_{HS_0}) \left( 1 - \frac{f}{3} \right)^{-1} \quad (\text{A.40})$$

#### 4. Results

In this section, the Board applied the models previously developed to the FRP-02 vessel. The parameter values used are shown in Table A-5.

**Table A-5.** Input parameters for the gas retention and release models applied to vessel FRP-02.

Parameter	Symbol	Value	Basis
Vessel diameter	$D$	14.3m	[2]
Maximum waste volume	$V_w$	1,496m <sup>3</sup>	[2]
Minimum Headspace volume	$V_{HS}$	315m <sup>3</sup>	[2]
Maximum waste fill level	$H_w$	9.27m	Estimated assuming cylindrical vessel
Maximum vessel fill fraction	$F_w$	0.826	Calculated
Maximum solids loading (weight %)	$w_{s0}$	3.8%	[10]
Liquid density	$\rho_L$	1,423kg/m <sup>3</sup>	[2]
Solids density	$\rho_s$	2,400kg/m <sup>3</sup>	[2]
Waste temperature	$T_w$	50 °C	Assumption
Headspace temperature	$T_{HS}$	50 °C	[11]
Standard pressure	$p_0$	101,325Pa	
Standard temperature	$T_0$	0 °C	
Universal gas constant	$R$	8.314J/mole-K	
Gravitational constant	$g$	9.81m/s <sup>2</sup>	
Hydrogen fraction of generated gas	$[H_2]$	0.35	[2]
Initial headspace hydrogen concentration	$\alpha_{HS_0}$	0.01	[12]
Shear strength proportionality constant	$\gamma$	2	[7]
Time of outage	$t_f$	1,000 hours	[12]

Figure A-8 shows the retained gas fraction in the settled layer for the linearly varying generation rate case. It also shows the stability curves for buoyant displacement and bubble cascade gas releases. The three red curves in the figure correspond to different assumed values for the hydrogen fraction,  $[H_2]$ . For lower values of  $f$ , the bubble cascade stability criterion is surpassed for all three values of  $[H_2]$ . For intermediate values of  $f$  up to about 0.9, the bubble cascade stability criterion is not exceeded. However, the buoyant displacement stability criterion is exceeded in this range, except for the  $[H_2] = 0.5$  cases, where the bubble cascade criterion is not surpassed when  $f > 0.6$ . Hence from Figure A-8 it appears that the potential for a spontaneous release is high for the assumed conditions.

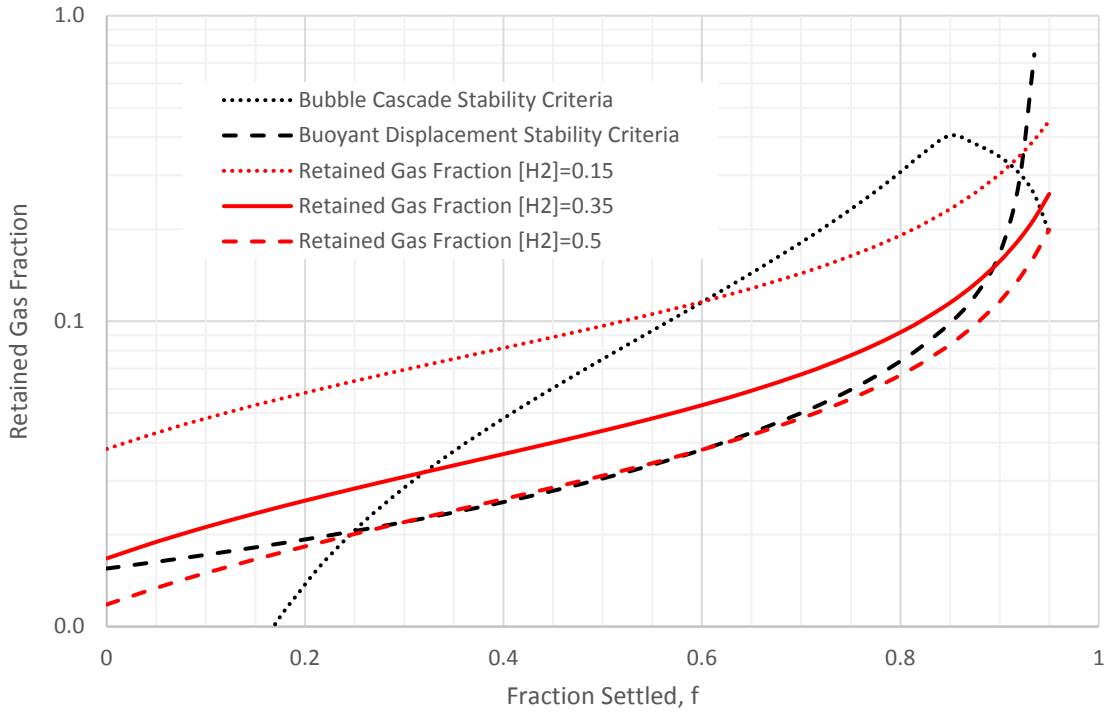
Figure A-9 shows the same plot for the computed generation rate case. The result is similar to that shown in Figure A-8, except that the retained gas fractions are lower. Here, even when assuming the mean hydrogen fraction  $[H_2] = 0.35$ , the buoyant displacement stability criterion is not exceeded for settling greater than about  $f = 0.4$ .

Both Figures A-8 and A-9 indicate that for low values of settling, the bubble cascade stability criterion is surpassed first. This suggests that bubble cascade events may be likely even while the layer is settling. This would likely reduce the total flammable gas volume; however, it is conservative to not credit bubble cascade events early in the settling process. For high values of settling, up to about  $f = 0.9$ , both curves show that neither the bubble cascade nor buoyant displacement stability criteria are exceeded. These results are highly dependent on the assumptions regarding the shear strength dependence on solids loading. They would also be affected by the solids distribution in the settled layer, a feature not considered in this model.

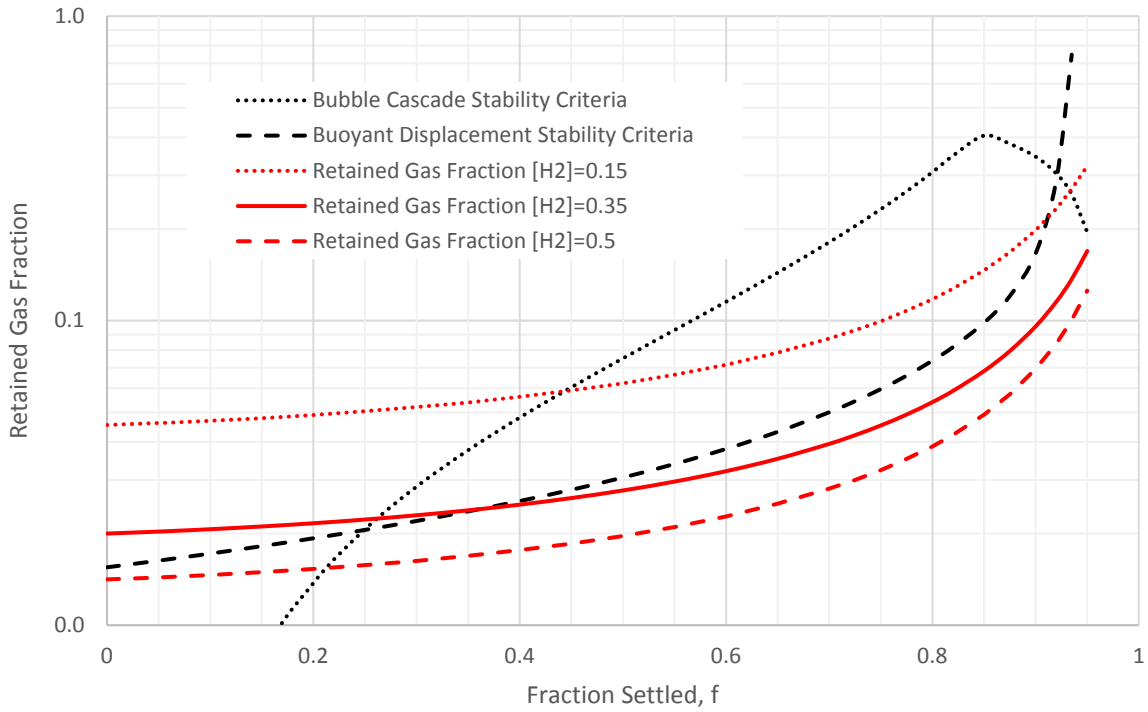
Figure A-10 shows the predicted headspace hydrogen concentrations after a spontaneous release for both gas generation variations. The LFL in the headspace is exceeded in both cases. For the linearly varying generation cases, the peak concentration occurs at an intermediate value of  $f$  consistent with Eq. (A.20). The peak concentration for the computed generation rate cases occurs at  $f = 0$ . Since this case corresponds to the improbable situation of no settling whatsoever, it follows that  $f = 0$  represents the bounding case, but not a physically meaningful case.

Figure A-11 shows a similar plot of headspace hydrogen concentration after enough waste has been removed to keep the headspace no higher than the LFL. For the linearly varying cases, this corresponds to the removal of 93kgal of waste. For the case of computed generation rates, 62kgal must be removed.

Figures A-12 and A-13 show the predicted time without agitation for a vessel to undergo a spontaneous release that would exceed the LFL in its headspace (i.e., time to LFL) for different vessel fill fractions.



**Figure A-8.** Retained gas fraction in settled layer predicted from linearly varying gas generation assumption in Appendix K of [2].



**Figure A-9.** Retained gas fraction in settled layer predicted from the curve fit of computed gas generation rates.

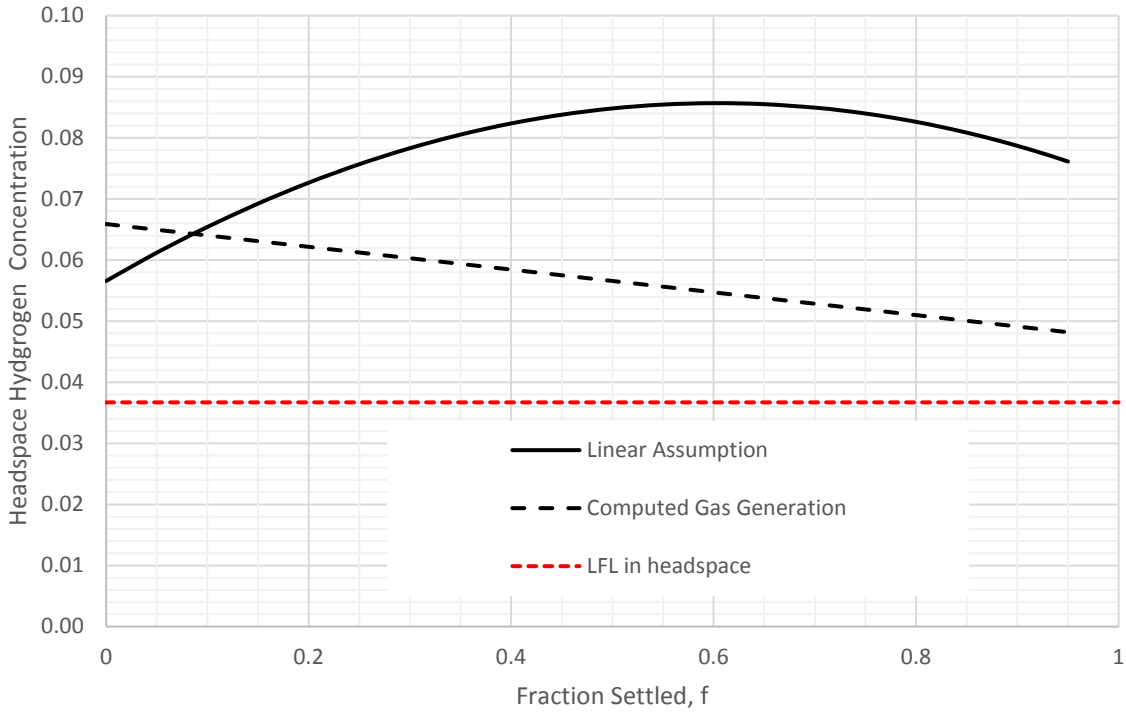


**Figure A-10.** Predicted headspace hydrogen concentration after a spontaneous release for both cases of gas generation.

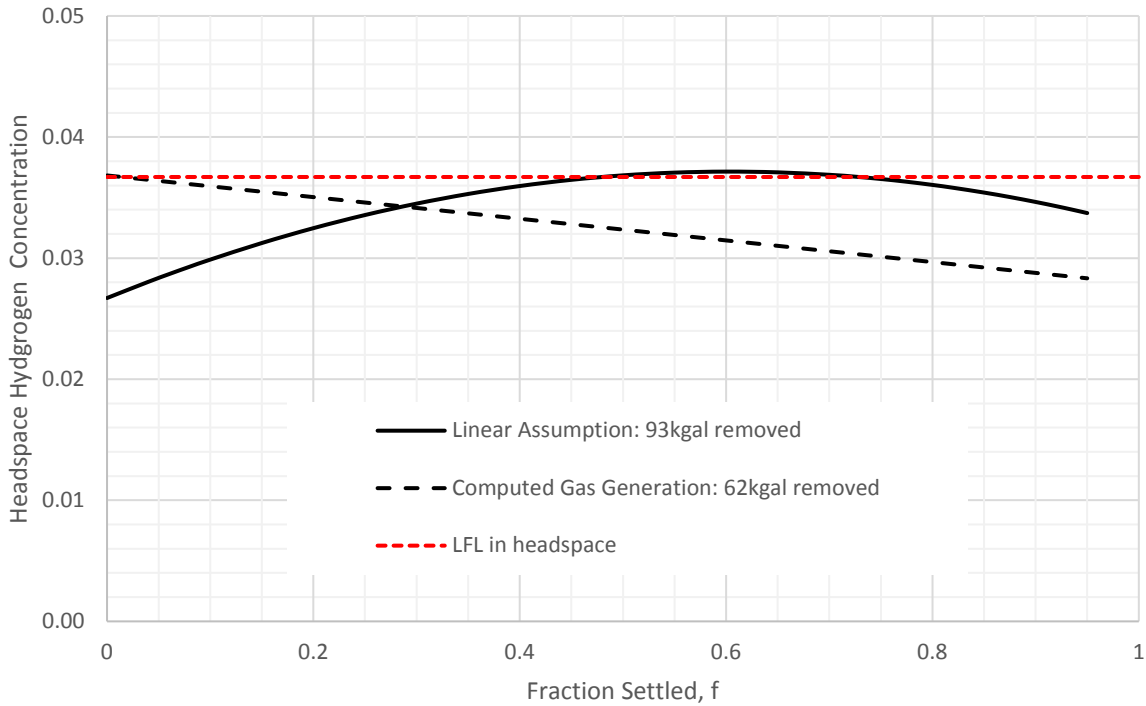


**Figure A-11.** Predicted headspace hydrogen concentration from a spontaneous release after waste reduction sufficient to prevent exceeding the lower flammability limit.

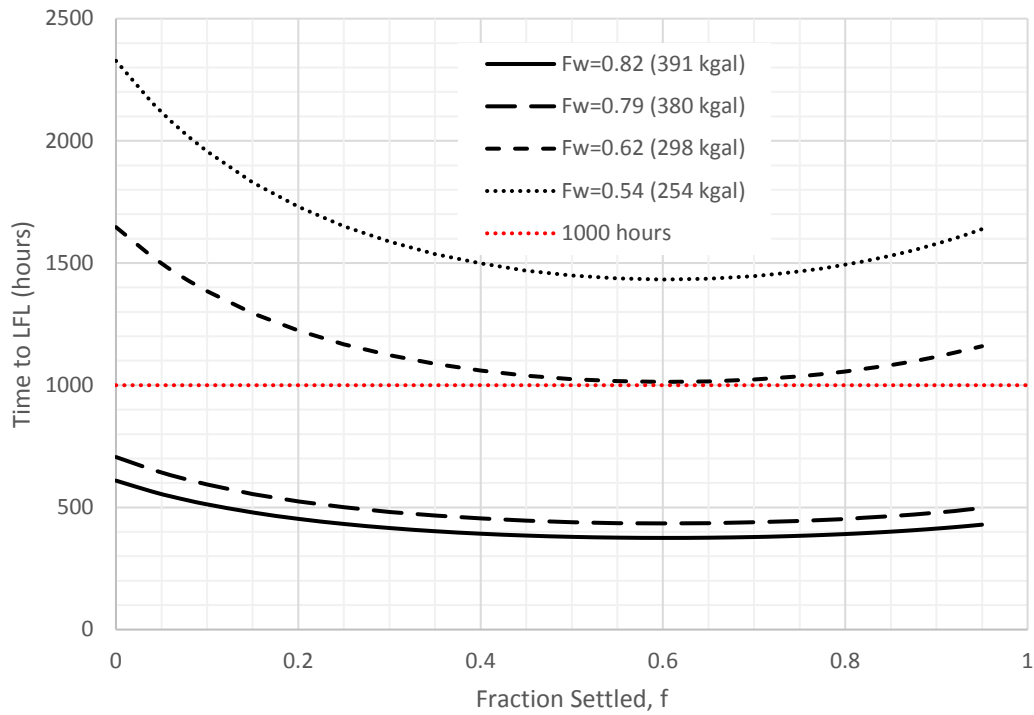


**Figure A-12.** Time to the lower flammability limit after a spontaneous release given various waste reductions for linear varying gas generation rates.

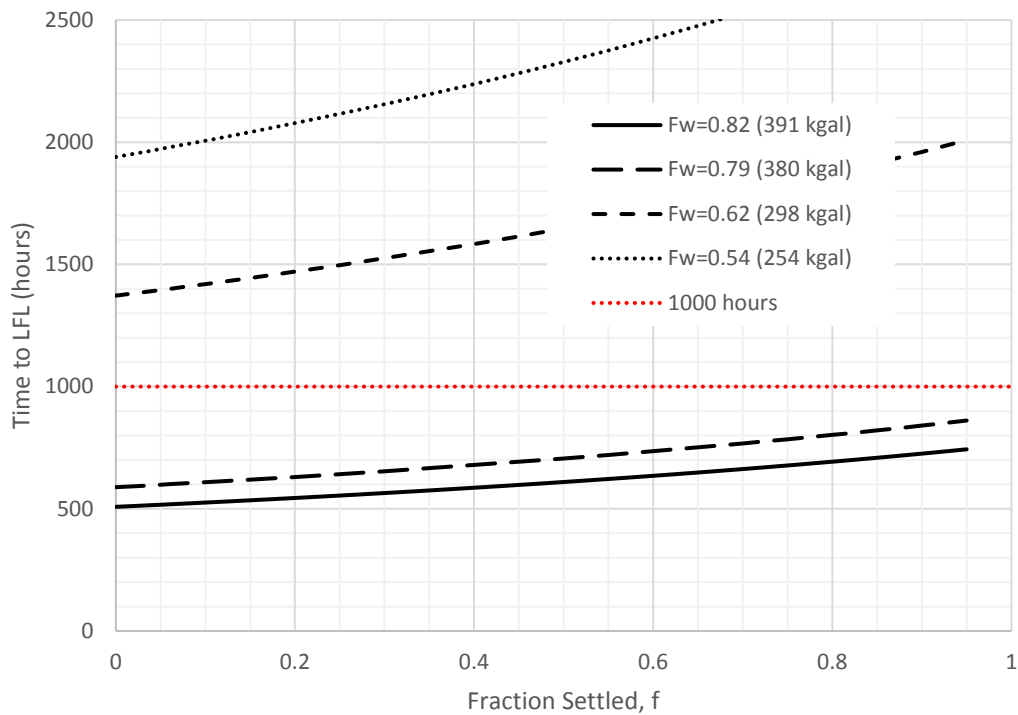


**Figure A-13.** Time to the lower flammability limit after a spontaneous release given various waste reductions for computed gas generation rates.

## 5. Conclusions

Based on the modeling and analysis conducted, the Board concludes:

- The amount of gas retained depends on the thickness of the settled layer. The specific settled layer thickness that maximizes retained gas volume depends on assumptions, including the principal assumption of how the unit hydrogen generation rate varies with settled layer depth. The BNI analysis assumed a value for the settled layer thickness. Based upon the independent calculations summarized in this appendix, the Board finds that the BNI assumed value did not correspond to the case with the highest gas retention.
- The Board's analysis indicates sufficient retained gas could be present to initiate a spontaneous release either by buoyant displacement or by bubble cascade. For lower settling fractions (less settling), the bubble cascade mechanism appears to be more likely than buoyant displacement. As settling increases, buoyant displacement appears to be the principal mechanism. At very high settling, the principal mechanism depends on waste rheology. These results hold true for both assumptions concerning the variation of the unit hydrogen generation rate within the settled layer.
- The Board's analysis shows significantly higher headspace hydrogen concentration after a gas release than the BNI analysis. The principal reason for this is that BNI assumed the solids layer settled with an exponential curve that mostly settled within 400 hours (see Appendix K of [2]), whereas the Board assumed linear settling behavior over 1000 hours, which bounds all potential trajectories. BNI has not shown that its assumed settling curve is conservative.
- BNI assumed that the gas generation rate varied linearly between the design value for the well-mixed vessel and a higher value determined from a heat transfer calculation in a stationary solids layer. The Board computed the unit gas generation rate for various stationary solids layer thicknesses (see Appendix B). The Board concludes that BNI's linear generation rate assumption results in a larger volume of retained hydrogen.
- Based on the models and assumptions in this analysis, the Board concludes that the principal hydrogen control strategy of limiting waste volume in the low-solids vessels is viable. However, the Board also concludes that additional work is required to determine a technically defensible safe operating level with sufficient margin to ensure a flammable headspace is not credible.

## 6. References

- [1] Fox, D.K., *Safety Requirements Document Volume II, 24590-WTP-SRD-ESH-01-001-02, Rev. 8*, Bechtel National, Incorporated, Richland, WA, 2016.
- [2] Lewis, T., and K. Waltzer, *Proposed Control of Hydrogen Events in the Pretreatment Facility Pulse Jet Mixed Process Vessels*, 24590-PTF-ES-NS-15-003 Rev 00C, Bechtel National, Incorporated, November 3, 2016.
- [3] Gauglitz, P.A., et al., *Hydrogen Gas Retention and Release from WTP Vessels: Summary of Preliminary Studies*, PNNL-24255, Pacific Northwest National Laboratory, Richland, Washington, 2015.
- [4] Poloski, A.P., et al., *Estimate of Hanford Waste Rheology and Settling Behavior*, PNNL-16857, Pacific Northwest National Laboratory, Richland, Washington, 2007.<sup>4</sup>
- [5] Meyer, P.A., et al., *Gas Retention and Release Behavior in Hanford Double-Shell Waste Tanks*, PNNL-11536 Rev.1, Pacific Northwest National Laboratory, Richland, Washington, 1997.<sup>5</sup>
- [6] Gauglitz, P.A., et al., *Mechanics of Gas Bubble Retention and Release: Results for Hanford Waste Tanks 241-S-102 and 241-SY-103 and Single-Shell tank Simulants*, PNNL-11298, Pacific Northwest National Laboratory, Richland, Washington, 1996.
- [7] Poloski, A.P., et al., *Rheological and Physical Properties of AZ-101 HLW Pretreated Sludge and Melter Feed*, WTP-RPT-096 Rev. 0, Battelle – Pacific Northwest Division, Richland, Washington, 2003.<sup>6</sup>
- [8] Taki, B.D., *Interface Control Document (ICD) - 19 for Waste Feed*, 24590-WTP-ICD-MG-01-019, Rev 7, Bechtel National, Incorporated, September 19, 2014.
- [9] Gauglitz, P.A., et al., *Strong-Sludge Gas Retention and Release Mechanisms in Clay Simulants*, PNNL-21167, Pacific Northwest National Laboratory, Richland, Washington, 2012.
- [10] Olson, J.W., *Process Inputs Basis of Design (PIBOD)*, 24590-WTP-DB-PET-09-001, Rev. 1, Bechtel National, Incorporated, June 2, 2011.

---

<sup>4</sup> Work completed by members of the Board's technical staff prior to the staff members' employment with the Board.

<sup>5</sup> Work completed by members of the Board's technical staff prior to the staff members' employment with the Board.

<sup>6</sup> Work completed by members of the Board's technical staff prior to the staff members' employment with the Board.



- [11] Eager, K., *Revised Calculation of Hydrogen Generation Rates and Times to Lower Flammability Limit for WTP*, 24590-WTP-M4C-V11T-00011, Rev C, Bechtel National, Incorporated, May 2010.
- [12] Beck, J. A., *Preliminary Documented Safety Analysis to Support Construction Authorization; PT Facility Specific Information*, 24590-WTP-PSAR-ESH-01-002-02, Rev. 6a, Bechtel National, Incorporated, February 2017.

## **Appendix B - Dependence of Hydrogen Generation Rate and Time-to-Lower Flammability Limit on Settled Fraction in Low-Solids Vessels**

### **1. Background and Objective**

The Pretreatment (PT) Facility at the Waste Treatment and Immobilization Plant (WTP) is intended to receive Hanford tank waste for processing before the waste is sent to the Low-Activity Waste and High-Level Waste Facilities for immobilization. Hanford tank waste generates hydrogen and other flammable gases through thermolysis and radiolysis. In the PT Facility process vessels, the release mechanism of hydrogen from the waste to the vessel headspace depends on the waste properties. In no-solids Newtonian waste, the hydrogen continuously releases into the headspace. High-solids Newtonian and non-Newtonian wastes retain the generated hydrogen until the waste is agitated or a spontaneous release occurs. If the concentration of hydrogen in the vessel headspace exceeds the lower flammability limit (LFL), the potential for an explosion exists.

Four PT Facility waste feed receipt vessels, FRP-VSL-00002A/B/C/D, are designed to receive Newtonian waste from the tank farms [1]. These vessels may contain up to 3.8 weight percent solids [2]. If not agitated for a prolonged period, the waste may form a settling solids layer (i.e., sludge layer) that retains generated hydrogen. The WTP Safety Requirements Document (SRD) defines the functional requirements for hydrogen control systems in process vessels to prevent an inventory of hydrogen in concentrations greater than the LFL in the vessel headspace during off-normal and post-accident conditions [3]. The SRD defines the LFL as 4 percent of hydrogen by volume. The SRD states that safety controls are required for process vessels with a time to reach LFL (i.e., time-to-LFL) less than or equal to 1,000 hours. The WTP project relies on providing sufficient agitation of the waste on a periodic basis to prevent hydrogen accumulation, as well as using a forced air purge system to dilute the hydrogen concentration in the vessel headspace to levels below the LFL.

Bechtel National, Incorporated (BNI), analysts developed heat transfer analyses for the PT Facility process vessels to calculate time-dependent waste temperatures during off-normal conditions, assuming loss of agitation [2] [4]. The analysts used those waste temperatures to calculate the hydrogen generation rate (HGR) and the time-to-LFL to determine whether safety controls are required to prevent flammable conditions in the vessel headspace. For these heat transfer analyses, BNI analysts assume that the waste instantaneously settles on loss of agitation and develops two distinct stationary layers—a sludge layer and supernatant layer (i.e., liquid layer). The time-to-LFL calculations only use the hydrogen generated in the sludge layer, as it retains generated gases. The hydrogen generated in the supernatant layer is not a significant contributor to the hydrogen concentration in the headspace during a spontaneous release.

The Board determined that it is not evident that BNI's assumption of instantaneous waste settling is conservative. Instantaneous waste settling would result in higher sludge layer temperatures, which in turn would result in higher HGRs. In addition, instantaneous settling of the sludge layer would result in lower concentrations of organic compounds and water in the sludge layer, which would decrease HGR compared with waste that settled more slowly. If the amount of organic compounds and water present in the sludge layer, rather than the temperature

changes, govern hydrogen production, then the assumption of instantaneous waste settling may lead to lower estimates of generated hydrogen.

A member of the Board completed the following analyses to determine how the settled fraction<sup>1</sup> affects the amount of hydrogen generated in the sludge layer and the time-to-LFL:

- Finite element model using ANSYS<sup>®</sup> software to evaluate the spatial and temporal distribution of the sludge layer temperature;
- MATLAB<sup>®</sup> code to calculate the HGR and the time-to-LFL using the temperature distributions derived in the finite element analyses; and
- Parametric study for varying settled fraction.

## 2. Assumptions and Input Parameters

The FRP-VSL-00002A/B/C/D process vessel has an inside diameter of 564 inches (14.33 m), a wall thickness of 1 inch (0.0254 m), and a total volume of 472,859 gallons (1,789.97 m<sup>3</sup>) [4] [5]. Located in the middle of the black cell, it is spaced 2.6 feet (0.79 m) from the cell walls, 3 feet (0.91 m) from the cell floor, and 12.4 feet (3.78 m) from the cell ceiling [6] [7]. The finite element model represents the process vessel as a right cylinder. The Board derived the vessel height based on the total vessel volume. This approach is consistent with the modeling assumption in [4] [5] [6].

The initial temperature of the black cell and its environment is 113 °F (45 °C), and the initial temperature of the process vessel is 120 °F (49 °C), i.e., the maximum allowable operating temperature established by the safety requirements [1] [8]. Table B.1 presents material properties of the black cell and the process vessel.

*Table B.1. Material properties for black cell and process vessel [9].*

<b>Component</b>	<b>Material of Construction</b>	<b>Density</b> $\frac{\text{kg}}{\text{m}^3} \left( \frac{\text{lb}}{\text{in}^3} \right)$	<b>Thermal Conductivity</b> $\frac{\text{W}}{\text{m} \cdot ^\circ\text{C}} \left( \frac{\text{BTU}}{\text{s} \cdot \text{in} \cdot ^\circ\text{F}} \right)$	<b>Specific Heat</b> $\frac{\text{J}}{\text{kg} \cdot ^\circ\text{C}} \left( \frac{\text{BTU}}{\text{lb} \cdot ^\circ\text{F}} \right)$	<b>Emissivity</b>
Black Cell	Concrete	2,200 (0.0795)	1.5 ( $2.01 \times 10^{-5}$ )	880 (0.2102)	0.90
Process Vessel	Stainless Steel	8,000 (0.2890)	16 ( $2.14 \times 10^{-4}$ )	500 (0.1194)	0.50 [10]

The waste in the process vessel fully settles to a 37,271-gallon (141.09 m<sup>3</sup>) sludge layer and a 353,636-gallon (1,338.66 m<sup>3</sup>) liquid layer [8]. This results in the settled fraction of 0.905

<sup>1</sup> The settled fraction is a ratio of the liquid layer to the total waste volume in the process vessel. The settled fraction has a higher value for a thinner sludge layer.

and an 81,952-gallon (310.22 m<sup>3</sup>) vessel headspace. The initial temperature of the sludge and liquid layers is 120 °F (49 °C), i.e., initial temperature of the process vessel [1] [8].

Tables B.2 and B.3 present material properties of the sludge and liquid layers. The BNI analysts assumed that the liquid layer has the same properties as water [4] [5] [6]. While the thermal conductivity of water is about 0.6  $\frac{W}{m \cdot ^\circ C}$  ( $8.03 \times 10^{-6} \frac{BTU}{s \cdot in \cdot ^\circ F}$ ), the specific heat is much higher than the value for the sludge layer. Higher values of specific heat result in lower sludge layer temperatures. Therefore, the Board assumed that the thermal conductivity and specific heat of the liquid layer are the same as those for the sludge layer.

Heat generation per unit volume for the sludge and liquid layers is derived based on the heat loads of the sludge and liquid layers provided in 24590-WTP-M4C-V11T-00011, Rev. C [8]. The heat transfer coefficient for natural convection in air is assumed to be 5.0  $\frac{W}{m^2 \cdot ^\circ C}$  ( $1.699 \frac{BTU}{s \cdot in^2 \cdot ^\circ F}$ ), which is an average value for the natural convection range [10].

**Table B.2.** Material properties for sludge and liquid layers [8].

Constituent	Density $\frac{kg}{m^3} \left( \frac{lb}{in^3} \right)$	Thermal Conductivity $\frac{W}{m \cdot ^\circ C} \left( \frac{BTU}{s \cdot in \cdot ^\circ F} \right)$	Specific Heat $\frac{J}{kg \cdot ^\circ C} \left( \frac{BTU}{lb \cdot ^\circ F} \right)$	Heat Load $W \left( \frac{BTU}{s} \right)$
Sludge Layer	1,660 (0.0600)	0.6 ( $8.03 \times 10^{-6}$ )	2,400 (0.5732)	4,171 (3.953)
Liquid Layer	1,450 <sup>2</sup> (0.0524)	0.6 ( $8.03 \times 10^{-6}$ )	2,400 (0.5732)	1,242 (1.177)

### 3. Analytical Methods and Computations

#### 3.1 Heat Transfer Analyses

The Board developed a three-dimensional finite element model using ANSYS® software to evaluate the spatial and temporal distribution of the sludge layer temperature in FRP-VSL-00002A/B/C/D vessels (i.e., a transient thermal analysis). Figure B.1 presents the finite element model discretization employed in the Board analyses. The black cell and the process vessel are constructed using 10-node thermal solid elements, and the sludge and liquid layers are constructed using 20-node thermal solid elements. The model analyzes conduction, natural convection, and radiative heat transfer processes within the black cell and the process vessel. The entire outside surface area of the process vessel undergoes radiative cooling to the surrounding black cell walls, whereas only the top and cylindrical surfaces of the process vessel undergo convective cooling. The liquid layer also undergoes convective cooling to the vessel

<sup>2</sup> The density value is for caustic diluted waste feed.

headspace. The finite element analysis estimates the sludge layer temperature for a duration of 2,000 hours using constant input parameters (see Section 2). A typical element size for the sludge layer is 12 inches (0.30 m).

**Table B.3.** *Properties for constituents in the sludge and liquid layers [8]<sup>3</sup>*

<b>Property</b>	<b>Value</b>
Solids Density in Sludge Layer	2,400 $\frac{\text{kg}}{\text{m}^3}$ (0.0867 $\frac{\text{lb}}{\text{in}^3}$ )
Total Mass of Solids in Sludge Layer	81,265 kg (179,158.7 lb)
Alpha Decay Heat Load of Liquid Phase	$3.96 \times 10^{-6} \frac{\text{W}}{\text{L}}$ ( $8.52 \times 10^{-7} \frac{\text{BTU}}{\text{s} \cdot \text{gal}}$ )
Alpha Decay Heat Load of Solids	$3.77 \times 10^{-4} \frac{\text{W}}{\text{kg}}$ ( $9.72 \times 10^{-6} \frac{\text{BTU}}{\text{s} \cdot \text{lb}}$ )
Reactivity Coefficient for Organic Species In Double-Shell Tank Waste	0.7 [11]
Concentration of Total Organic Carbon in Liquid Phase	0.52
Total Concentration of Aluminum Species in Liquid Phase	1.74
Nitrate Concentrations in Liquid Phase	3.09
Nitrite Concentrations in Liquid Phase	2.01

<sup>3</sup> These input parameters are documented in Appendix G of [8] in electronic format as an MS Excel file.

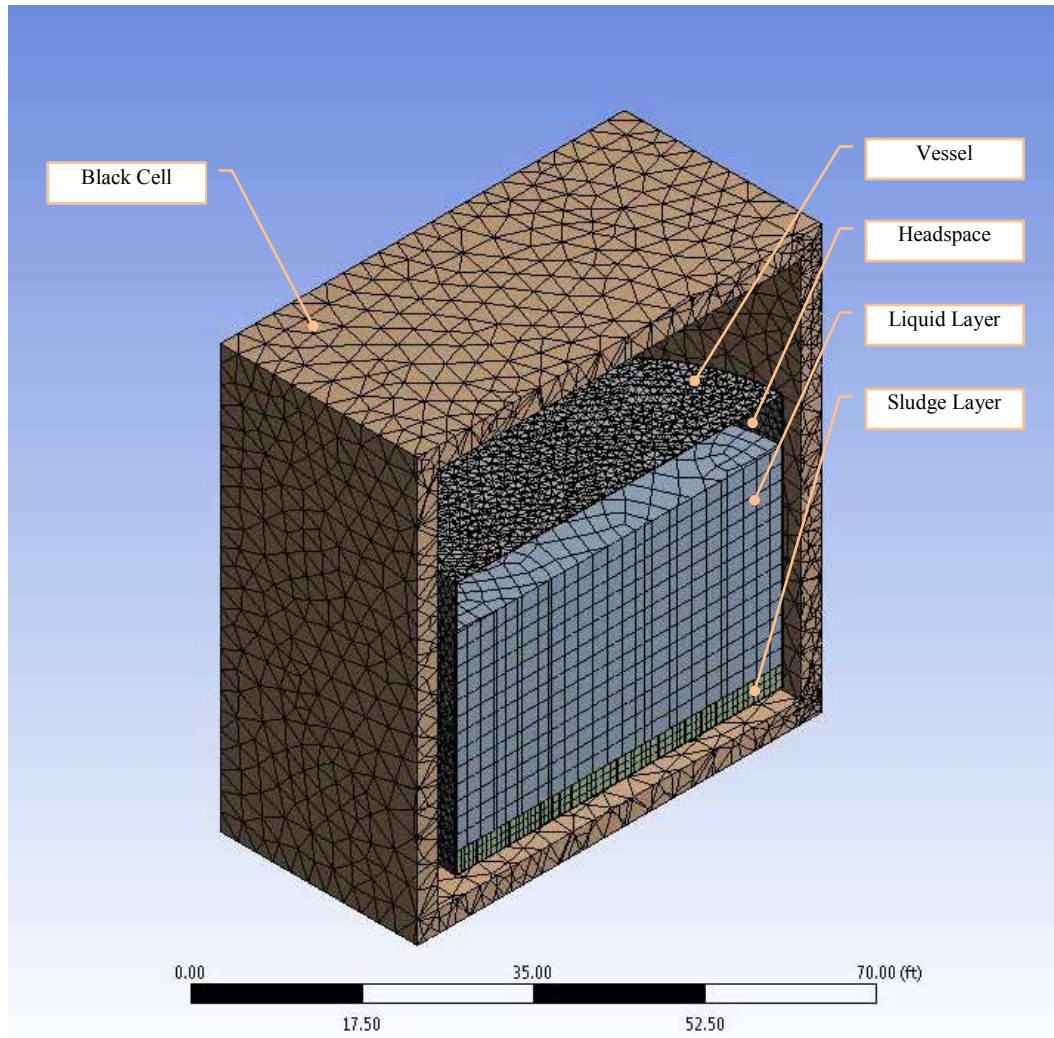


**Figure B.1.** Discretization of the finite element model.

### 3.2 Hydrogen Generation Analyses

The Board assembled a MATLAB<sup>®</sup> code to calculate the HGR and the time-to-LFL in FRP-VSL-00002A/B/C/D vessels. This code uses the time-varying temperature distribution derived in the heat transfer analyses (refer to Section 3.1) to calculate the HGR and the time-to-LFL using equations B.1 through B.11 and associated constants obtained from the modified Hu correlation [11].

The total HGR is a sum of HGR terms for thermolysis ( $HGR_{therm}$ ) and radiolysis ( $HGR_{rad}$ ):

$$HGR = HGR_{therm} + HGR_{rad} \quad (B.1)$$

The thermolysis term is

$$HGR_{therm} = a_T \cdot f \cdot [TOC] \cdot [AL]^{0.4} \cdot f_L \cdot e^{-Q_t/RT} \quad (B.2)$$

where  $a_T$  is the thermolysis correlation coefficient of  $2.76 \times 10^9 \frac{\text{mol}}{\text{kg} \cdot \text{day}}$ ;  $f$  is the reactivity coefficient for organic species;  $[TOC]$  is the concentration of total organic carbon in the liquid phase;  $[AL]$  is the total concentration of aluminum species in the liquid phase;  $f_L$  is the fraction of liquid in the waste (i.e., liquid weight fraction);  $Q_t$  is the thermolysis activation energy of 89,300 J/mol (84.64 BTU/mol);  $R$  is the ideal gas constant; and  $T$  is the waste temperature.

The radiolysis term is

$$HGR_{rad} = f_L \cdot C \cdot [H^\alpha \cdot G(H_2)^\alpha + H^{\beta/\gamma} \cdot G(H_2)^{\beta/\gamma}] \quad (B.3)$$

where  $C$  is a conversion factor of  $0.00895 \frac{100 \text{ eV} \cdot \text{mol}}{\text{W} \cdot \text{day}}$ ;  $H^\alpha$  and  $H^{\beta/\gamma}$  are the respective decay heat loads for  $\alpha$  and  $\beta/\gamma$  sources; and  $G(H_2)^\alpha$  and  $G(H_2)^{\beta/\gamma}$  are the total G-values for  $\alpha$  and  $\beta/\gamma$  sources.

The total G-values for  $\alpha$  and  $\beta/\gamma$  sources are the respective sums of the G-values for radiolysis of water,  $G_0(H_2)^\alpha$  and  $G_0(H_2)^{\beta/\gamma}$ , and interactions of radiolysis products with organic compounds,  $G_{TOC}(H_2)^\alpha$  and  $G_{TOC}(H_2)^{\beta/\gamma}$ :

$$G(H_2)^\alpha = G_0(H_2)^\alpha + G_{TOC}(H_2)^\alpha \quad (B.4)$$

$$G(H_2)^{\beta/\gamma} = G_0(H_2)^{\beta/\gamma} + G_{TOC}(H_2)^{\beta/\gamma} \quad (B.5)$$

The G-values for radiolysis of water are

$$G_0(H_2)^\alpha = \frac{1.05}{1 + 2.4[NO_3] + 0.62[NO_2]} + \frac{0.35}{1 + 3,900[NO_3] + 1,400[NO_2]} \quad (B.6)$$

$$G_0(H_2)^{\beta/\gamma} = \frac{0.34}{1 + 2.4[NO_3] + 0.62[NO_2]} + \frac{0.11}{1 + 120[NO_3] + 43[NO_2]} \quad (B.7)$$

where  $[NO_3]$  and  $[NO_2]$  are the nitrate and nitrite concentration in the liquid phase respectively.

The G-values for interactions of radiolysis products with organic compounds are

$$G_{TOC}(H_2)^\alpha = 0.5a_0 \cdot f \cdot [TOC] \cdot e^{-Q_{rad}/RT} \quad (B.8)$$

$$G_{TOC}(H_2)^{\beta/\gamma} = a_0 \cdot f \cdot [TOC] \cdot e^{-Q_{rad}/RT} \quad (B.9)$$

where  $a_0$  is the radiolysis correlation coefficient of  $2.49 \times 10^6 \frac{1}{100 \text{ eV}}$ ; and  $Q_{rad}$  is the radiolysis activation energy of 44,300 J/mol (41.99 BTU/mol).

The Board calculated the decay heat loads for  $\alpha$  and  $\beta/\gamma$  sources,  $H^\alpha$  and  $H^{\beta/\gamma}$ , following the methodology outlined in Appendix G of [8], as follows:

$$H^\alpha = \frac{H_L^\alpha \cdot V_{LS} + H_S^\alpha \cdot m_S}{V_{LS} \cdot \rho_{SL}} \quad (\text{B.10})$$

$$H^{\beta/\gamma} = \frac{H_{SL} \cdot V_{SL}}{m_{LS}} \quad (\text{B.11})$$

where  $H_L^\alpha$  is the alpha decay heat load of liquid phase;  $H_S^\alpha$  is the alpha decay heat load of solids;  $V_{LS}$  is the volume of liquid in the sludge layer;  $m_S$  is the mass of solids in the sludge layer;  $\rho_{SL}$  is the sludge layer density;  $H_{SL}$  the heat generation of the sludge layer;  $V_{SL}$  is the volume of the sludge layer; and  $m_{LS}$  is the mass of liquid in the sludge layer.

### 3.3 Element Formulation and Incremental Volume

The output of the finite element model includes the temperature data at individual nodes of each element at a given time and the spatial coordinates of each node. The MATLAB<sup>®</sup> code uses the spatial coordinates to calculate the volume of each element. The code uses these volumes as the incremental volumes for calculating the HGR and the amount of generated hydrogen.

Using a formula for the volume of a general hexahedral cell, Equation B.12 [12], the code calculates the incremental volume,  $V$ , for each individual element using the vertex node data as follows:

$$V = \frac{1}{6} [ |(\vec{x}_7 - \vec{x}_0), (\vec{x}_1 - \vec{x}_0), (\vec{x}_3 - \vec{x}_5)| + |(\vec{x}_7 - \vec{x}_0), (\vec{x}_4 - \vec{x}_0), (\vec{x}_5 - \vec{x}_6)| + |(\vec{x}_7 - \vec{x}_0), (\vec{x}_2 - \vec{x}_0), (\vec{x}_6 - \vec{x}_3)| ] \quad (\text{B.12})$$

where  $\vec{x}_0, \vec{x}_1, \vec{x}_2, \vec{x}_3, \vec{x}_4, \vec{x}_5, \vec{x}_6, \vec{x}_7$  are the coordinate vectors of vertex nodes.

The code calculates the effective temperature of an element at a given time as an average of the temperature of all of the nodes comprising that element.

### 3.4 Hydrogen Generation and Time-to-LFL

The code calculates the HGR at a given time using the modified Hu correlation, Equations B.1–B.9, for each incremental volume based on its average temperature and the sludge layer properties. The output gives the amount of generated hydrogen in moles per kilogram of waste per day. The code calculates the hydrogen generated within the incremental volume using



numerical integration of the HGR as a function of time and multiplying the result by the waste density, incremental volume, and appropriate conversion factors. The code repeats this calculation for all incremental volumes over time and determines the total hydrogen generated in the waste (in moles) by summing the results over all incremental volumes.

The results of the finite element modeling indicated that the liquid layer tends to cool down to the black cell environment temperature. Generated hydrogen in the sludge layer would pass through the liquid layer before reaching the headspace. Therefore, the code uses the black cell environment temperature to convert from moles to volume of generated hydrogen, using the ideal gas law. One mole of an ideal gas at standard temperature and pressure occupies approximately 22.4 L. The code uses this relationship to calculate the volume occupied by a gas at higher temperatures.

The amount of hydrogen present in the headspace at time zero is assumed to be 1 percent by volume, which is the maximum concentration allowed during normal operations [1]. The code approximated the time-to-LFL by interpolating between the two consecutive time steps before and after the LFL is exceeded.

### **3.5 Parametric Study for Varying Settled Fraction**

The Board performed a parametric study for the settled fraction varying from 0.905 to 0.047. For the study, the Board developed eight finite element models by varying the sludge layer volume from the baseline of 37,271 gallons (141.09 m<sup>3</sup>) to 372,710 gallons (1,410.86 m<sup>3</sup>), 10 times the baseline value. The amount of solids in the sludge layer, and, therefore, the total decay heat load from solids are assumed to remain constant in all models. The sludge layer volume increases due a larger amount of liquid phase added. Tables B.4 and B.5 present additional input parameters for the parametric study. For the baseline model (Model 1), the Board derived the heat generation per unit volume for the sludge and liquid layers based on the heat loads of the sludge and liquid layers provided in 24590-WTP-M4C-V11T-00011 [8]. The heat generation of the liquid layer stays constant at  $0.93 \frac{W}{m^3}$  ( $1.4445 \times 10^{-8} \frac{BTU}{s \cdot in^3}$ ) in all models. For additional models, the Board calculated the sludge layer density and the heat generation of the sludge layer using a volumetric average approach.

**Table B.4.** Input parameters for the parametric study (Models 1 – 4).

<b>Parameter</b>	<b>Model 1</b>	<b>Model 2</b>	<b>Model 3</b>	<b>Model 4</b>
Settled Fraction	0.905	0.809	0.714	0.619
Sludge Layer Volume gallons (m <sup>3</sup> )	37,271 (141.09)	74,542 (282.17)	111,813 (423.26)	149,084 (564.34)
Liquid Layer Volume gallons (m <sup>3</sup> )	353,636 (1,338.66)	316,365 (1,197.57)	279,094 (1,056.49)	241,823 (915.40)
Sludge Layer Density $\frac{\text{kg}}{\text{m}^3} \left( \frac{\text{lb}}{\text{in}^3} \right)$	1,660.00 (0.0600)	1,555.00 (0.0561)	1,520.00 (0.0549)	1,502.50 (0.0543)
Sludge Layer Heat Generation $\frac{\text{W}}{\text{m}^3} \left( \frac{\text{BTU}}{\text{s} \cdot \text{in}^3} \right)$	29.56 (4.5912×10 <sup>-7</sup> )	15.25 (2.3686×10 <sup>-7</sup> )	10.47 (1.6262×10 <sup>-7</sup> )	8.09 (1.2565×10 <sup>-7</sup> )
Liquid Weight Fraction	0.66	0.82	0.87	0.90
Sludge Layer Decay Heat Load for $\alpha$ Sources $\frac{\text{W}}{\text{kg}} \left( \frac{\text{BTU}}{\text{s} \cdot \text{lb}} \right)$	1.68×10 <sup>-4</sup> (7.22×10 <sup>-8</sup> )	7.87×10 <sup>-5</sup> (3.38×10 <sup>-8</sup> )	5.16×10 <sup>-5</sup> (2.22×10 <sup>-8</sup> )	3.85×10 <sup>-5</sup> (1.66×10 <sup>-8</sup> )
Sludge Layer Decay Heat Loads for $\beta/\gamma$ sources $\frac{\text{W}}{\text{kg}} \left( \frac{\text{BTU}}{\text{s} \cdot \text{lb}} \right)$	2.62×10 <sup>-2</sup> (1.13×10 <sup>-5</sup> )	1.18×10 <sup>-2</sup> (5.07×10 <sup>-6</sup> )	7.80×10 <sup>-3</sup> (3.53×10 <sup>-6</sup> )	5.90×10 <sup>-3</sup> (2.54×10 <sup>-6</sup> )

**Table B.5.** Input parameters for the parametric study (Models 5 – 8).

<b>Parameter</b>	<b>Model 5</b>	<b>Model 6</b>	<b>Model 7</b>	<b>Model 8</b>
Settled Fraction	0.523	0.428	0.237	0.047
Sludge Layer Volume gallons (m <sup>3</sup> )	186,355 (705.43)	223,626 (846.52)	298,168 (1,128.69)	372,710 (1,410.86)
Liquid Layer Volume gallons (m <sup>3</sup> )	204,552 (774.31)	167,281 (633.23)	92,739 (351.06)	18,197 (68.88)
Sludge Layer Density $\frac{\text{kg}}{\text{m}^3} \left( \frac{\text{lb}}{\text{in}^3} \right)$	1,492.00 (0.0542)	1,485.00 (0.0536)	1,476.25 (0.0533)	1,471.00 (0.0531)
Sludge Layer Heat Generation $\frac{\text{W}}{\text{m}^3} \left( \frac{\text{BTU}}{\text{s} \cdot \text{in}^3} \right)$	6.65 (1.0329×10 <sup>-7</sup> )	5.70 (8.8532×10 <sup>-8</sup> )	4.51 (7.0049×10 <sup>-8</sup> )	3.79 (5.8866×10 <sup>-8</sup> )
Liquid Weight Fraction	0.92	0.94	0.95	0.96
Sludge Layer Decay Heat Load for $\alpha$ Sources $\frac{\text{W}}{\text{kg}} \left( \frac{\text{BTU}}{\text{s} \cdot \text{lb}} \right)$	3.07×10 <sup>-5</sup> (1.32×10 <sup>-8</sup> )	2.55×10 <sup>-5</sup> (1.10×10 <sup>-8</sup> )	1.92×10 <sup>-5</sup> (8.26×10 <sup>-9</sup> )	1.53×10 <sup>-5</sup> (6.58×10 <sup>-9</sup> )
Sludge Layer Decay Heat Loads for $\beta/\gamma$ sources $\frac{\text{W}}{\text{kg}} \left( \frac{\text{BTU}}{\text{s} \cdot \text{lb}} \right)$	4.80×10 <sup>-3</sup> (2.06×10 <sup>-6</sup> )	4.08×10 <sup>-3</sup> (1.75×10 <sup>-6</sup> )	3.20×10 <sup>-3</sup> (1.38×10 <sup>-6</sup> )	2.67×10 <sup>-3</sup> (1.15×10 <sup>-6</sup> )

## 4. Results

Figure B.2 presents a typical temperature distribution for FRP-VSL-00002A/B/C/D vessels at 2,000 hours following loss of agitation calculated by the baseline model (Model 1). Significant cooling occurs on the outside of the vessel and the waste due to convective and radiative losses. Heating occurs in the middle of the sludge layer due to internal heat generation. The calculated temperature at the center of the sludge increases above its initial temperature of 120 °F (49 °C).

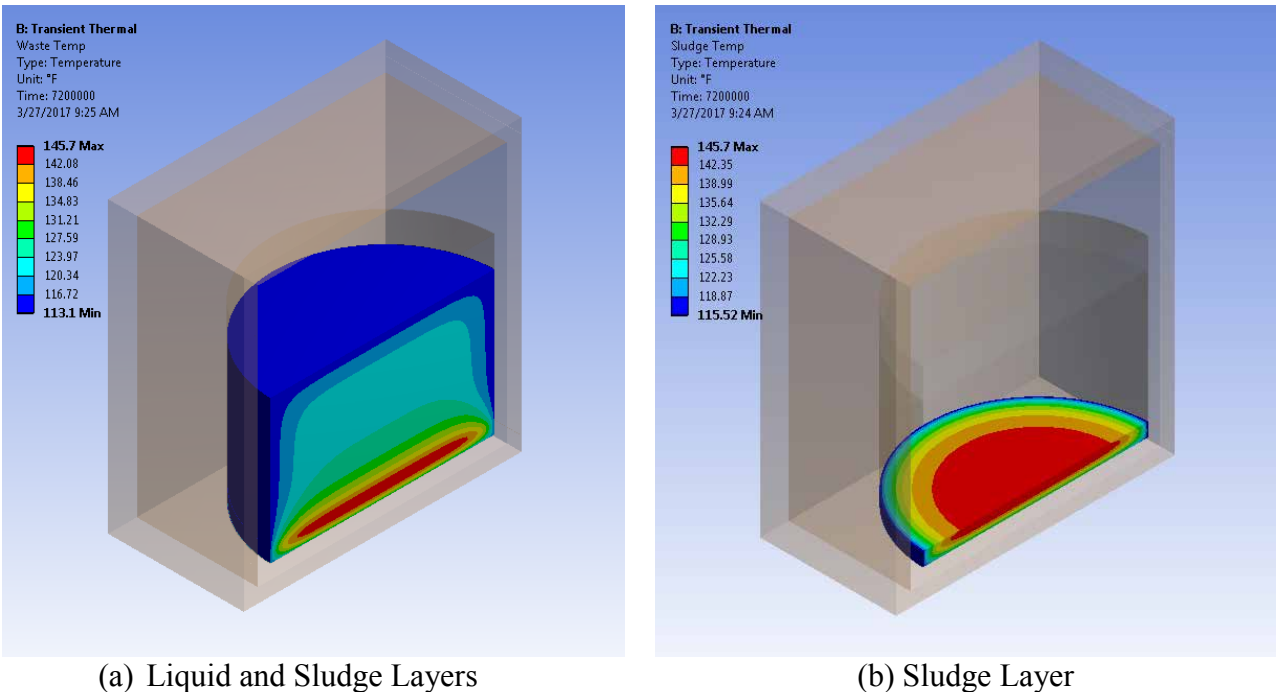


**Figure B.2.** Typical temperature distribution.

Figure B.3 presents typical temperature results for the sludge layer up to 2,000 hours following loss of agitation calculated by the baseline model (Model 1). After initial cooling, the minimum, volumetric average, and maximum temperature values in the sludge increase over time. The volumetric average temperature indicates that most of the sludge layer is above the initial temperature. In other words, the sludge layer undergoes heating.

Figure B.4 confirms the same trend for all cases showing that the volumetric average temperature in the sludge layer increases over time. Table B.6 presents the maximum temperature after 2,000 hours for all eight models. Data presented in Figure B.4 and Table B.6 indicate that, in general, the sludge layer experiences higher temperatures for higher values of the settled fraction. This trend is reversed for a more compacted sludge layer with the settled fraction of 0.9, which undergoes more cooling than a sludge layer with the settled fraction of 0.8. This is likely caused by the reduced thickness of the sludge layer, which allows for an increase in heat transfer from the sludge layer into the liquid layer.

Figure B.5 presents the average unit HGR (UHGR) for the sludge layer for all eight models. The Board calculated the UHGR using a volumetric average approach based on the UHGR values of all elements in the finite element model at a given time step, as follows:

$$\text{UHGR} = \frac{\sum_{i=1}^n \text{HGR}_i \cdot V_i}{\sum_{i=1}^n V_i}, \quad (\text{B.13})$$

where  $\text{HGR}_i$  is hydrogen generation rate of the  $i$ -th element, and  $V_i$  is the volume of the  $i$ -th element. These calculations indicate that the UHGR increases over time, which is due to the temperature increase. The figure also indicates that the UHGR decreases as the settled fraction decreases.

**Table B.6.** Maximum temperature after 2,000 hours (Models 1 – 8).

	<b>Model 1</b>	<b>Model 2</b>	<b>Model 3</b>	<b>Model 4</b>	<b>Model 5</b>	<b>Model 6</b>	<b>Model 7</b>	<b>Model 8</b>
<b>Settled Fraction</b>	0.905	0.809	0.714	0.619	0.523	0.428	0.237	0.047
<b>Maximum Temperature, °F (°C)</b>	145 (63)	147 (64)	146 (64)	144 (62)	142 (61)	140 (60)	136 (58)	133 (57)

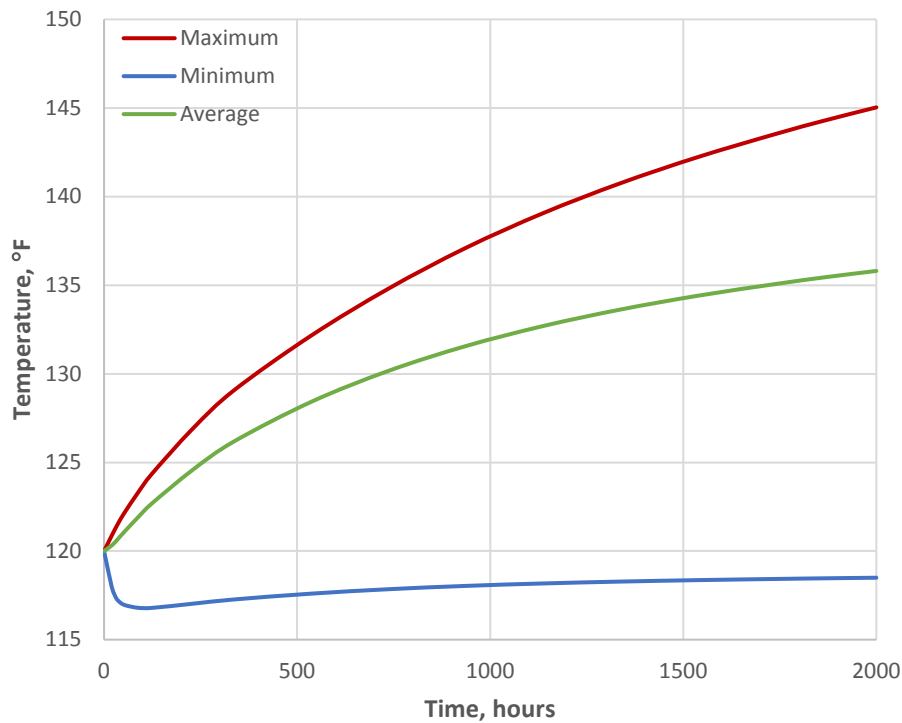


**Figure B.3.** Typical temperature vs. time in the sludge layer.

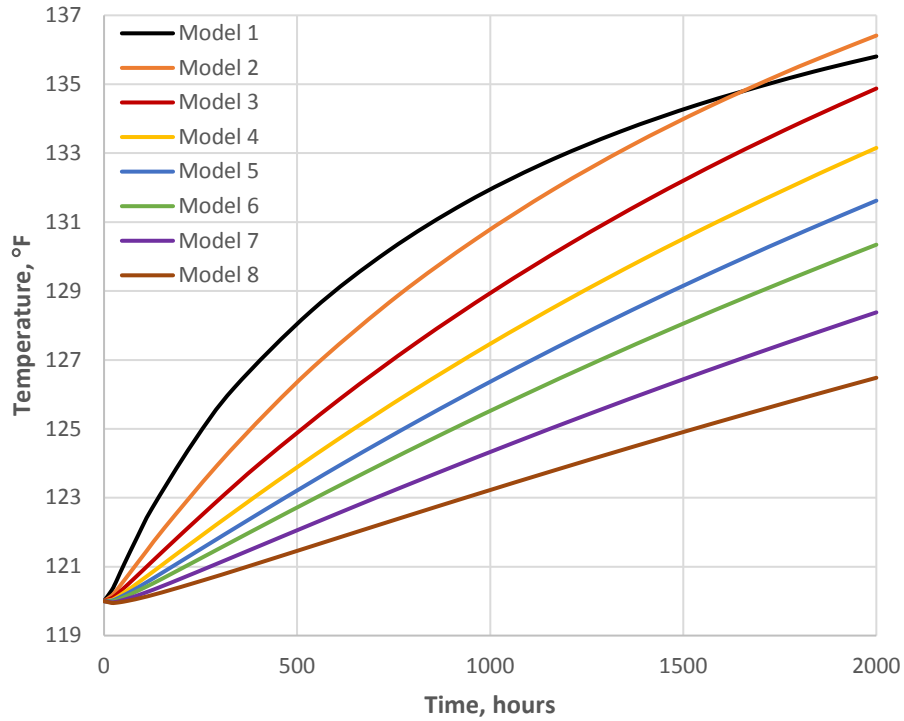


**Figure B.4.** Average temperature vs. time in the sludge layer.

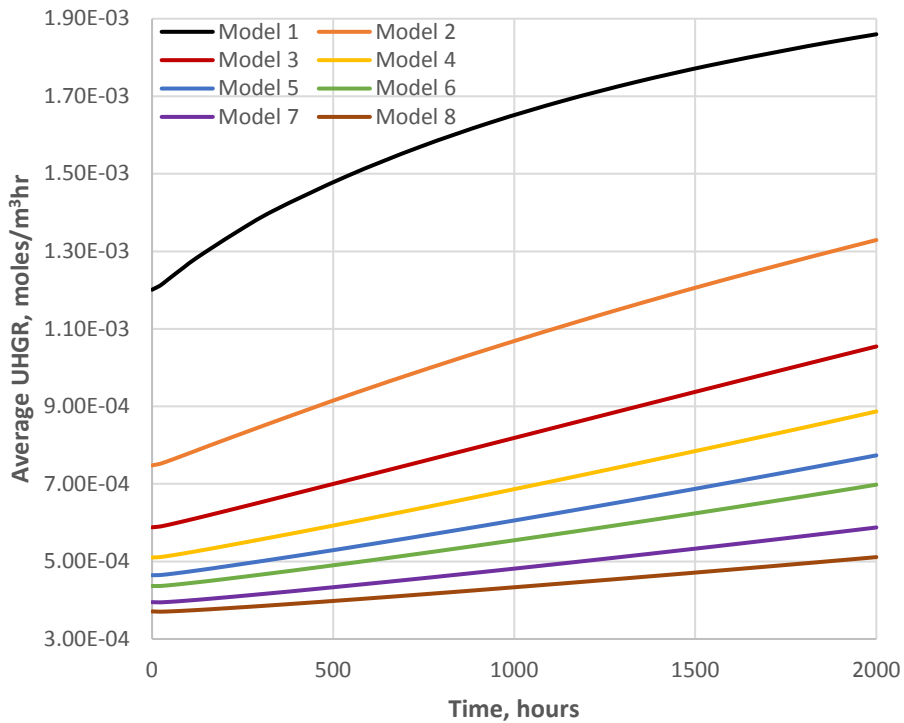


**Figure B.5.** Average UHGR vs. time in the sludge layer.

Table B.7 presents the time-to-LFL for all eight models. Results presented in the table show that the time-to-LFL decreases as the settled fraction decreases. This indicates that the amount of hydrogen generated in the sludge layer is higher for models with a lower UHGR. One possible explanation of this result is that the volume of hydrogen-generating media rather than the temperature changes govern hydrogen production in FRP-VSL-00002A/B/C/D vessels.

The Board performed a mesh sensitivity study by reducing the typical element size for the sludge layer from 12 inches (0.30 m) to 6 inches (0.15 m). The results of the sensitivity study showed negligible differences in the peak temperatures (less than 0.2 percent) and in the time-to-LFL (less than 0.75 percent).

**Table B.7.** Time to reach LFL (Models 1 – 8).

	<b>Model 1</b>	<b>Model 2</b>	<b>Model 3</b>	<b>Model 4</b>	<b>Model 5</b>	<b>Model 6</b>	<b>Model 7</b>	<b>Model 8</b>
<b>Settled Fraction</b>	0.905	0.809	0.714	0.619	0.523	0.428	0.237	0.047
<b>Time-to-LFL, hours</b>	1,618	1,316	1,169	1,054	958	872	747	652

## 5. Conclusions

The Board evaluated the time-varying temperature distribution and calculated the HGR and the time-to-LFL for FRP-VSL-00002A/B/C/D vessels to determine how the settled fraction affects the amount of generated hydrogen in the sludge layer. The results show that, while the UHGR is higher for a more compacted sludge layer, the total amount of generated hydrogen is smaller. Therefore, assuming an instantaneously settled sludge layer is not conservative because it results in lower estimates of generated hydrogen during off-normal conditions.

## 6. References

- [1] Beck, J.A., *Preliminary Documented Safety Analysis to Support Construction Authorization; PT Facility Specific Information*, 24590-WTP-PSAR-ESH-01-002-02, Rev. 6a, Bechtel National, Incorporated, Richland, WA, 2017.
- [2] Lewis, T., and K. Waltzer, *Proposed Control of Hydrogen Events in the Pretreatment Facility Pulse Jet Mixed Process Vessels*, 24590-PTF-ES-NS-15-003, Rev. 00C, Bechtel National, Incorporated, Richland, WA, 2016.
- [3] Fox, D.K., *Safety Requirements Document Volume II*, 24590-WTP-SRD-ESH-01-001-02, Rev. 8, Bechtel National, Incorporated, Richland, WA, 2016.
- [4] Summers, M., *Vessel Sizing Calculation - FRP-VSL-00002A/B/C/D*, 24590-PTF-MTC-FRP-00001, Rev. E, Bechtel National, Incorporated, Richland, WA, 2007.

- [5] Lanning, R., and M. Gebhardt, *Vessel Temperature Calculations During a Post-Design Basis Event Using the FATE Model*, 24590-WTP-M4C-M12T-00001, Rev. A, Bechtel National, Incorporated, Richland, WA, May 31, 2012.
- [6] Whitish, J., *Pretreatment Facility Structural Concrete Wall Forming Partial Plan El 0'-0" SH5*, 24590-PTF-DB-S13T-00019, Rev. 6, Bechtel National, Incorporated, Richland, WA, 2002.
- [7] Almeida, F., *Pretreatment Facility General Arrangement Plan at El. 0'-0"*, 24590-PTF-P1-P01T-00001, Rev. 8, Bechtel National, Incorporated, Richland, WA, November 10, 2011.
- [8] Eager, K., *Revised Calculation of Hydrogen Generation Rates and Time to Lower Flammability Limit for WTP*, 24590-WTP-M4C-V11T-00011, Rev. C, Bechtel National, Incorporated, Richland, WA, 2010.
- [9] Lanning, R.D., *Vessel Temperature Calculations Using HADCRT Computer Code*, 24590-WTP-U0C-50-00002, Rev. D, Bechtel National, Incorporated, Richland, WA, 2008.
- [10] Holman, J.P., *Heat Transfer*, 5th ed., McGraw-Hill, Inc., New York, NY, 1981.
- [11] Sherwood, D.J., and L.M. Stock, *Modifying the Hu Correlation to Predict Hydrogen Formation in the Hanford Waste Treatment and Immobilization Plant*, 24590-WTP-RPT-RT-04-0002, Rev. 0, Bechtel National, Incorporated, Richland, WA, 2004.
- [12] Grandy, J., *Efficient Computation of Volume of Hexahedral Cell*, UCRL-ID-128886, Lawrence Livermore National Laboratory, Livermore, CA, 1997.



## Appendix C - Hydrogen Generation in Standard High-Solids Vessel Following Loss of Agitation

### 1. Background and Objective

The Pretreatment (PT) Facility at the Waste Treatment and Immobilization Plant (WTP) is designed to receive and process waste from the Hanford Tank Farms before it is sent to the Low-Activity Waste and High-Level Waste (HLW) Facilities for immobilization. This radioactive waste continuously generates hydrogen and other flammable gases due to thermolysis and radiolysis. Hydrogen gas generated in the waste can accumulate in process vessel headspaces. If the concentration of hydrogen in the vessel headspace exceeds the lower flammability limit (LFL), it may result in an explosion.

To address open technical and safety issues related to mixing in process vessels, the Department of Energy (DOE) plans to redesign the PT Facility to incorporate a new standard high-solids vessel (SHSV) design. The SHSV design would replace existing process vessel designs for treatment of waste containing high-solids concentrations (i.e., HLW). When not agitated, the solids in this waste type settle, creating a liquid (i.e., supernatant) layer at the top of the waste and a settling solids layer (i.e., sludge layer). Hydrogen generated in the supernatant region continuously releases into the vessel headspace. The sludge layer retains hydrogen until the waste is agitated or enough gas is accumulated to release spontaneously.

DOE relies on providing sufficient agitation of the waste on a periodic basis to prevent hydrogen accumulation, as well as using a forced air purge system to dilute the hydrogen concentration in the vessel headspace to levels below the LFL. To establish mixing frequency, Bechtel National, Incorporated (BNI), plans to use a time-independent unit hydrogen generation rate (UHGR) for a constant temperature. For example, the waste acceptance criteria (WAC) in *Interface Control Document 19* (ICD-19) defines a UHGR of  $2.1 \times 10^{-6}$  gmol/L-hr ( $5.83 \times 10^{-7}$  gmol/m<sup>3</sup>-s) for the maximum allowed waste feed temperature of 150 °F (338.7 K) for the HLW feed receipt vessels, HLP-VSL-00022A/B/C [1].

A small change in temperature (10 °F) can result in a major change in hydrogen generation rate (40 to 70 percent) making it vital to have a conservative calculation of maximum temperatures expected in the waste. The waste temperature in SHSVs may increase above the maximum allowed waste feed temperature following loss of agitation. Therefore, using the UHGR corresponding to the maximum allowed waste feed temperature may not be conservative for establishing the mixing frequency.

The Board performed a computational study to assess whether the UHGR exceeds the value reported in the WAC. For this study, the Board:

- Developed a computational fluid dynamics (CFD) model for the HLW feed receipt vessels HLP-VSL-00022A/B/C using ANSYS® FLUENT software;
- Evaluated the spatial and temporal distribution of the sludge layer temperature during the first 1,000 hours following loss of agitation; and

- Calculated the volumetric average UHGR and the amount of hydrogen accumulated in the sludge layer using the temperature distributions derived in the CFD analyses.

## 2. Assumptions and Input Parameters

The Board developed a CFD model with a simplified axisymmetric geometry of the SHSV vessel in ANSYS® FLUENT software. This simplification is appropriate because the heat transfer is dominated by the heat diffusion in the sludge layer. The Board also simplified the locations and geometry of the inlet and the outlet of the forced air purge system in the vessel headspace. The inlet is represented by an annulus toward the edge of the vessel head. The location of the outlet is at the center of the vessel head. These geometric representations of the inlet and outlet do not have appreciable effect on the heat transfer in the sludge layer.

### 2.1 Geometry

Figure C-1 shows the model geometry. The SHSV vessel rests on a cylindrical structure forming a skirt. This skirt has an opening that allows air to move freely below the vessel. The model does not include the pulse jet mixers inside the vessel. The modeled waste configuration assumes that the waste settled on loss of agitation and developed two distinct layers—a sludge layer and supernatant layer. The content of the vessel comprises three zones: the sludge layer, supernatant layer, and the vessel headspace. The model also includes a fourth zone to represent the air inside the skirt. The headspace and skirt regions have gas properties, the supernatant layer has liquid properties, and the sludge region has properties of a solid.

The SHSV vessel has a total volume of 39,600 gallons (149.9 m<sup>3</sup>). The vessel is 29 feet (8.84-m) tall and has a diameter of 16 feet (4.88 m). The vessel is elevated 4.5 feet (1.37 m) above the black cell floor. The total waste volume is assumed to be the maximum operating volume (up to the overflow line). Table C-1 and C-2 summarize various volumes and levels used in the model. These parameters are consistent with the assumptions BNI used to calculate UHGR in the SHSV vessels (HLP-VSL-00022A/B/C) [2].

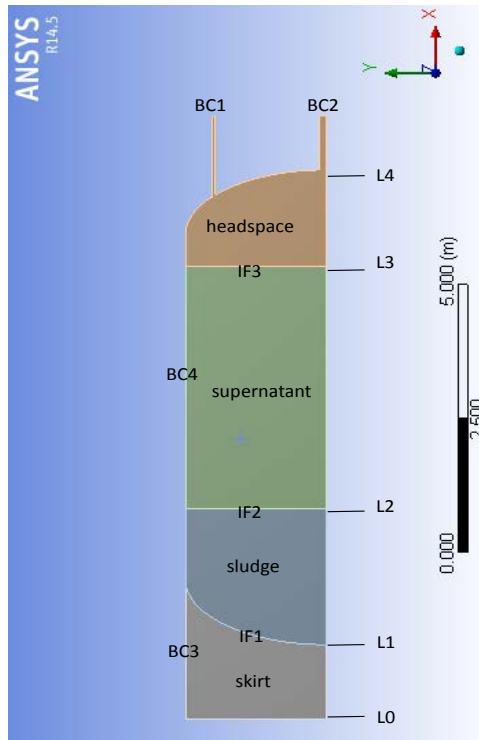


**Figure C-1.** Simplified geometry of the SHSV vessel in the CFD model.

**Table C-1.** Computational regions.

Region	Volume, gallons (m <sup>3</sup> )	Height, feet (m)
Sludge Layer	10,483 (39.68)	8.3 (2.53)
Supernatant Layer	22,225 (84.13)	14.7 (4.48)
Headspace	6,892 (26.09)	6 (1.83)
Total	39,600 (149.9)	29 (8.84)

**Table C-2.** Vessel elevations.

Levels in Figure C-1	Description	Vessel Elevation, feet (m)
L0	Black Cell Floor Level	0.0 (0.0)
L1	Bottom of the Vessel Level	4.5 (1.37)
L2	Sludge Level	12.8 (3.9)
L3	Supernatant Level	27.5 (8.38)
L4	Top of the Vessel Level	33.5 (10.21)

## 2.2 Initial Conditions

The model simulated the first 1,000 hours after a loss of mixing [3]. The following are the initial conditions:

- The initial temperature of the three regions inside the vessel and the air inside the skirt space is 150 °F (338.7 K) [1].
- The initial velocities in the x and y-directions inside the domain are zero.
- The operating pressure is one atmosphere (101,325 Pa).

### 2.3 Boundary Conditions

There are four computational boundaries in the model: the inlet at the vessel head (BC1), the outlet at the vessel head (BC2), the skirt opening (BC3), and the vessel surface (BC4). Figure C-1 shows these boundaries. The model assumes an adiabatic condition at the black cell floor.

The volumetric flow rate of the inlet air is 5 scfm (0.00236 m<sup>3</sup>/s) [4]. The radial location of the inlet to the annulus is the same as the radial location of nozzle N71, as identified in the equipment assembly drawing [5]. The inlet temperature of the forced air purge is 95 °F (308.15 K) [4]. The diameter of the headspace outlet is the same as the pipe identified as nozzle N25 in the equipment assembly drawing [5]. The outlet is located at the center of the axisymmetric domain with a radius of 22 inches (0.61 m). The pressure at this boundary is one atmosphere (101,325 Pa). The skirt below the vessel has two openings, each with a diameter of approximately 19.69 in (0.5 m). Due to the axisymmetric modeling assumption, the opening in the skirt below the vessel is represented as a single circumferential opening, which is 19.69 in (0.5 m) wide [6]. The pressure at this boundary is one atmosphere (101,325 Pa).

The model does not include the black cell where the SHSV vessel is located. Therefore, the heat transfer induced by the airflow inside the black cell is defined by convective heat transfer and a thermal radiation boundary condition at the surface of the vessel. The model calculates the convective heat transfer on the exterior of the vessel using the black cell temperature and a pre-calculated heat transfer coefficient. The black cell air temperature is 100.4 °F (311.15 K) for the base case, which represents the maximum allowable supply air temperature for the C5 ventilation (C5V) [7].

The heat transfer coefficient (HTC) is based on a 55 percent reduction of C5V volumetric flow rate of 2,200 scfm (3,737.8 m<sup>3</sup>/h). BNI assumes that this flow reduction would occur under loss of site power or during post-design basis accident conditions [4]. The vessel is located in black cell P-102A, which has a volume of approximately 201,187 ft<sup>3</sup> (5,697 m<sup>3</sup>) [8]. The Board calculated the air change per hour (ACH) of 0.65 by dividing the volumetric flow by the volume of the cell. The Board used Equation C-1 to calculate HTC for a ceiling inlet configuration [9], which yields a HTC value of 0.135 W/m<sup>2</sup>-K.

$$HTC = 0.19 \cdot ACH^{0.8} \quad (C.1)$$

The emissivity of steel ranges between 0.2 for a polished surface to 0.8 for an oxidized surface [10]. The model calculates thermal radiation at the vessel surface using the average emissivity of 0.5 for the base case. The analysis assumes the black cell wall temperature is

113 °F (318.15 K) for the base case, which is the maximum indoor design temperature of the C5 zone [7].

## 2.4 Interface Conditions

The model represents the interface between the sludge layer and the skirt as a 1-in (0.0254 m) thick steel surface [4], which is coupled to allow heat transfer between the two regions. The model represents the interface between the supernatant and sludge layer as a coupled wall with zero thickness and non-slip condition. This allows heat transfer between the sludge and the supernatant layers. The model represents the interface between the headspace and supernatant layer as a coupled wall with zero thickness and slip condition. This allows heat transfer between the headspace and the supernatant layer. Also, the slip condition allows balancing the momentum equation between the two regions.

## 2.5 Input parameters

Table C-3 summarizes the thermal properties of the materials used in the model for the base case. The thermal properties are consistent with the previous BNI analysis [2].

*Table C-3. Material thermal properties.*

Property	Air	Sludge	Supernatant	Steel
Density, kg/m <sup>3</sup> (lb/in <sup>3</sup> )	1.225 (4.42×10 <sup>-5</sup> )	1,680 (0.060)	1,450 (0.0524)	8,030 (0.29)
Thermal Conductivity, W/m-K (BTU/s-in-°F)	0.0242 (3.25×10 <sup>-7</sup> )	0.2 – 0.6 (2.68×10 <sup>-6</sup> – 8.03×10 <sup>-6</sup> )	0.6 (8.03×10 <sup>-6</sup> )	16.27 (2.18×10 <sup>-4</sup> )
Heat Capacity, J/kg-K (BTU/lb-°F)	1,006.43 (0.2403)	2,400 (0.5732)	2,400 (0.5732)	502.48 (0.12)
Viscosity, kg/m-s (lb/ft-s)	1.789×10 <sup>-5</sup> (1.202×10 <sup>-5</sup> )	–	1.0×10 <sup>-3</sup> [10] (6.921×10 <sup>-4</sup> )	–
Heat Source <sup>a</sup> , W/m <sup>3</sup> (BTU/s-in <sup>3</sup> )	–	29.65 (4.5×10 <sup>-7</sup> )	0.98 (1.52×10 <sup>-8</sup> )	–

<sup>a</sup> These input parameters are documented in Appendix G of [12] in electronic format as an MS Excel file.

## 2.6 Cases Description

In addition to the base case, the Board performed a parametric study. Table C-4 summarizes the six cases evaluated in this study. The Board selected these cases to study the impact of five different thermal parameters. The first parameter evaluated is the thermal conductivity of the sludge layer. The Board selected the value of 0.6 W/m-K for the base case (Case 1), which is the thermal conductivity of water. This is consistent with the BNI analysis [2]. Hydrogen gas generated and trapped in the sludge layer could reduce the thermal conductivity of the mixture. The thermal conductivity of hydrogen is 0.2 W/m-K [10]. For that

reason, the Board selected the thermal conductivity of hydrogen as the lower bounding thermal conductivity for Case 2.

The Board used the HTC value of 0.135 W/m<sup>2</sup>-K (see Section 2.3) for the base case. The HTC value could fluctuate between 1.8 and 8 for laminar and turbulent flow, respectively. The Board used an average HTC value of 5 W/m<sup>2</sup>-K for Case 3 to evaluate the sensitivity of convection at the surface of the vessel [11]. The black cell air temperature to calculate the heat transfer at the exterior surface of the vessel is 100.4 °F (311.15 K) for the base case. The Board increased this temperature to 113 °F (318.15 K) for Case 4, which is the maximum indoor design temperature of the C5 zone [7].

**Table C-4. Cases simulated.**

<b>Variable</b>	<b>Case 1 (base case)</b>	<b>Case 2</b>	<b>Case 3</b>	<b>Case 4</b>	<b>Case 5</b>	<b>Case 6</b>
Sludge Thermal Conductivity, W/m-K (BTU/s-in-°F)	0.6 (8.03×10 <sup>-6</sup> )	0.2 (2.68×10 <sup>-6</sup> )	0.6 (8.03×10 <sup>-6</sup> )	0.6 (8.03×10 <sup>-6</sup> )	0.6 (8.03×10 <sup>-6</sup> )	0.6 (8.03×10 <sup>-6</sup> )
Vessel Surface HTC, W/m <sup>2</sup> -K (BTU/s-in <sup>2</sup> -°F)	0.135 (0.0286)	0.135 (0.0286)	5 (1.699)	0.135 (0.0286)	0.135 (0.0286)	0.135 (0.0286)
Free Stream Temperature, °F (K)	100.4 (311.15)	100.4 (311.15)	100.4 (311.15)	113 (318.15)	100.4 (311.15)	100.4 (311.15)
Vessel Surface Emissivity	0.5	0.5	0.5	0.5	0.8	0.5
Black Cell Wall Temperature, °F (K)	113 (318.15)	113 (318.15)	113 (318.15)	113 (318.15)	113 (318.15)	131 (328.15)

The Board selected the vessel surface emissivity of 0.5 for the base case and a value of 0.8 for Case 5 to evaluate the effect of emissivity on thermal radiation at the surface of the vessel. A value of 0.8 represents an upper bounding value for an oxidized surface [10]. For the thermal radiation model, the Board used the black cell wall temperature of 113 °F (318.15 K) for the base case [4]. The adjacent vessel is assumed to be at the maximum allowable waste feed

temperature of 150 °F (338.7 K) [1]. The average between the black cell wall temperature and an adjacent vessel temperature is 131 °F (328.15 K). The Board used this average temperature of 131 °F (328.15 K) for Case 6 to evaluate the thermal radiation effect of other vessels present in the same black cell.

### 3. Analytical Methods and Computations

The turbulent flow in the gas and liquid regions was modeled using the Reynolds-Averaged Navier-Stokes (RANS) k-epsilon (k-e) approach, which correlates the dissipation and generation of turbulent kinetic energy. The RANS k-e approach was used with an enhanced treatment near the wall [13]. The model solves the momentum and energy balance equations using a second order numerical scheme. The convergence criteria were  $1.0 \times 10^{-6}$  for the energy equation and  $1.0 \times 10^{-3}$  for turbulent kinetic energy, momentum and mass conservation.

The Board performed the grid sensitivity study using four grids with different mesh sizes: 0.035 m (base case), the coarse mesh with a size of 0.05 m, and the two fine meshes with sizes of 0.025 m and 0.017 m. The Board used the temperature at the center of the sludge layer, supernatant layer, and headspace to evaluate the mesh refinement effect in the results. The results of the grid sensitivity study showed negligible differences in the temperatures.

The Board used the methodology outlined in the BNI analysis [12]<sup>1</sup> to calculate the hydrogen generation rate in the sludge layer and hydrogen concentration in the headspace. The Board performed these calculations through the custom field functions entered in the CFD model. The model calculates the amount of generated hydrogen in each discrete grid element in the sludge layer.

### 4. Results

Figure C-2 illustrates the base case results for sludge temperature changes during 1,000 hours following loss of agitation. The figure shows that the average temperature increases by 18 °F (10 K), the maximum temperature increases by 44.4 °F (24.7 K), and the minimum temperature decreases by 23.99 °F (13.3 K) from the initial temperature after 1,000 hours. Figure C-3 illustrates the results for the average sludge temperature for all cases. The figure shows that the average temperature increases by 27.1 °F (15.1 K) in Case 2, 13.1 °F (7.3 K) in Case 3, 18.2 °F (10.1 K) in Case 4, 16.5 °F (9.2 K) in Case 5, 22.9 °F (12.7 K) in Case 6. Figure C-4 illustrates how the temperature gradients in the sludge layer change with time. These temperature gradients demonstrate that heat diffuses in two directions (radial and axial). For this reason a two-dimensional model is appropriate to capture the heat transfer in SHSVs.

Figure C-5 shows the calculated area-weighted average UHGR in the sludge layer during 1,000 hours following loss of agitation. The figure also includes the value from ICD-19 for comparison [1]. These results show that the average UHGR increases non-linearly with time.

The model calculates the UHGR for each discrete grid element in hourly increments. Using these UHGRs, the model calculates the amount of hydrogen in moles for each discrete

---

<sup>1</sup> These input parameters are documented in Appendix G of [12] in electronic format as an MS Excel file.

grid element within the sludge layer. The total hydrogen generated for each hourly increment is the sum of the hydrogen generated in each grid element. The hydrogen generated for each hourly increment is totaled at 1,000 hours. The Board used the ideal gas equation to convert moles of hydrogen to volume to estimate the concentration in the headspace. In doing this, the Board used the sludge temperature and the headspace temperature to bound anticipated conditions. Table C-5 summarizes the concentration of hydrogen in the headspace after 1,000 hours for the lower and upper bounds.

*Table C-5. Hydrogen concentration in vessel headspace after 1,000 hours.*

Modeling Cases	Case 1	Case 2	Case 3	Case 4	Case 5	Case 6
Lower Bound, Percent	33.65	40.31	31.08	33.72	32.81	36.73
Upper Bound, Percent	37.90	45.83	34.88	37.97	36.91	41.51

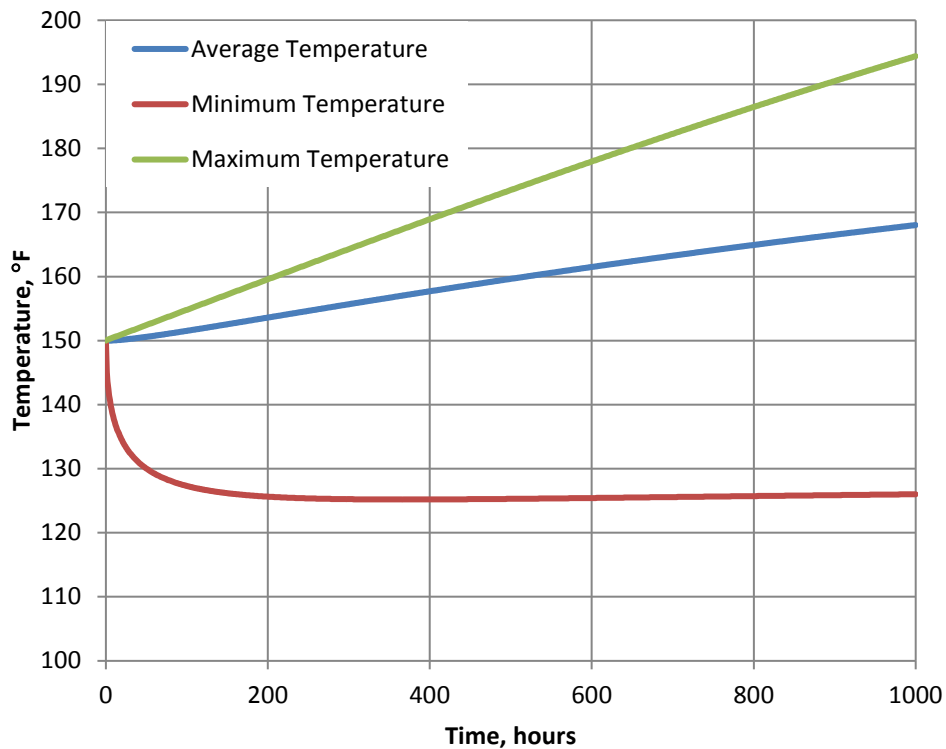


*Figure C-2. Sludge temperature for base case.*



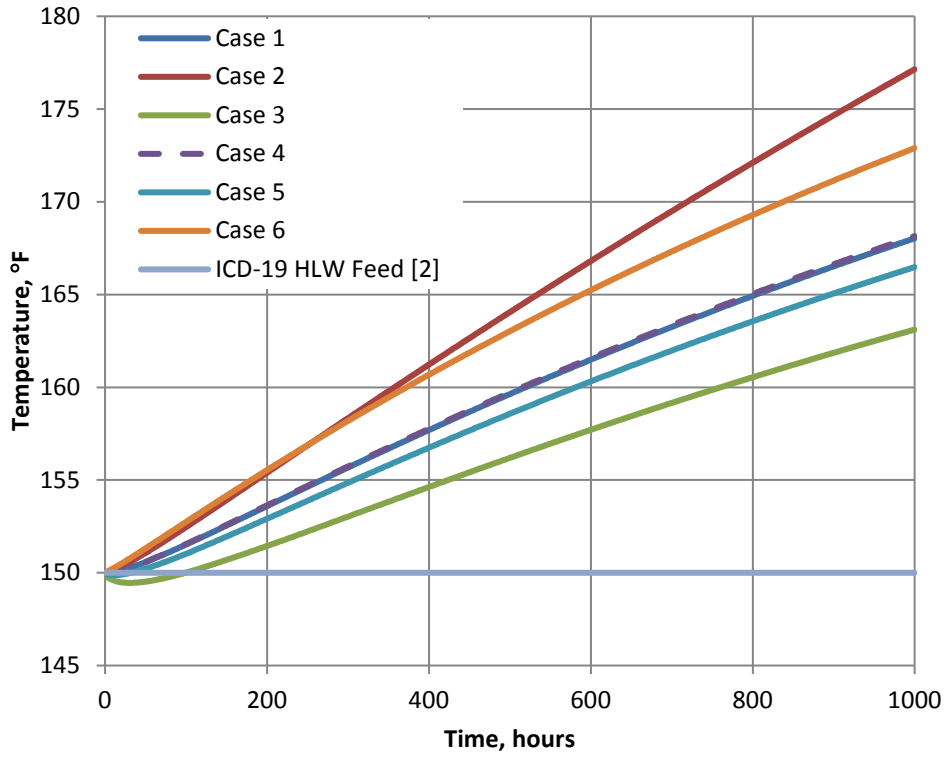


*Figure C-3. Average temperature of the sludge layer for all cases.*

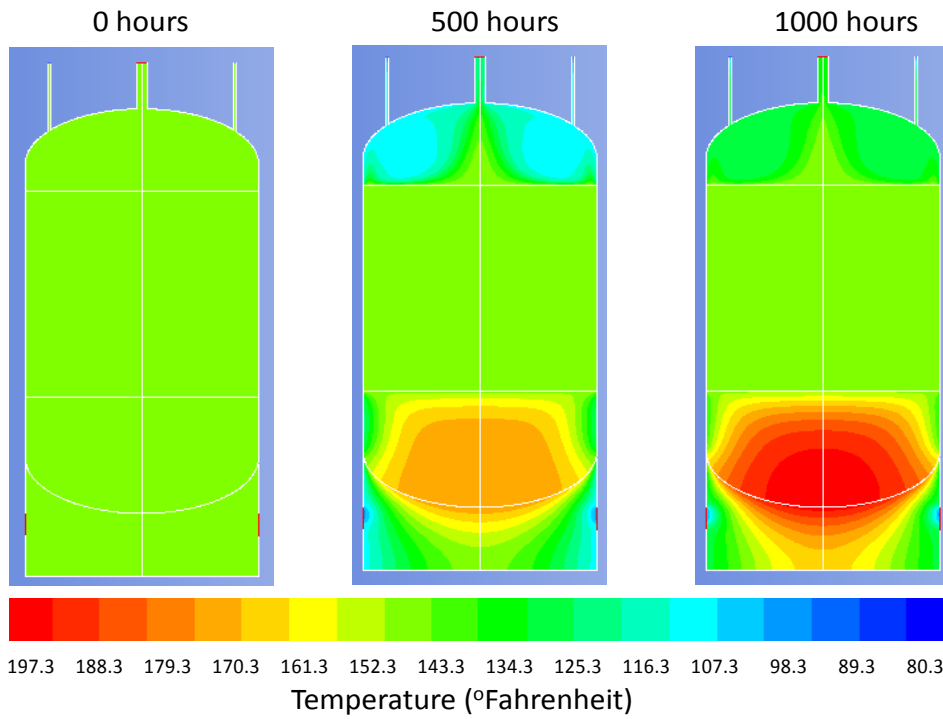


*Figure C-4. Two-dimensional temperature profile at 0, 500, and 1,000 hours.*

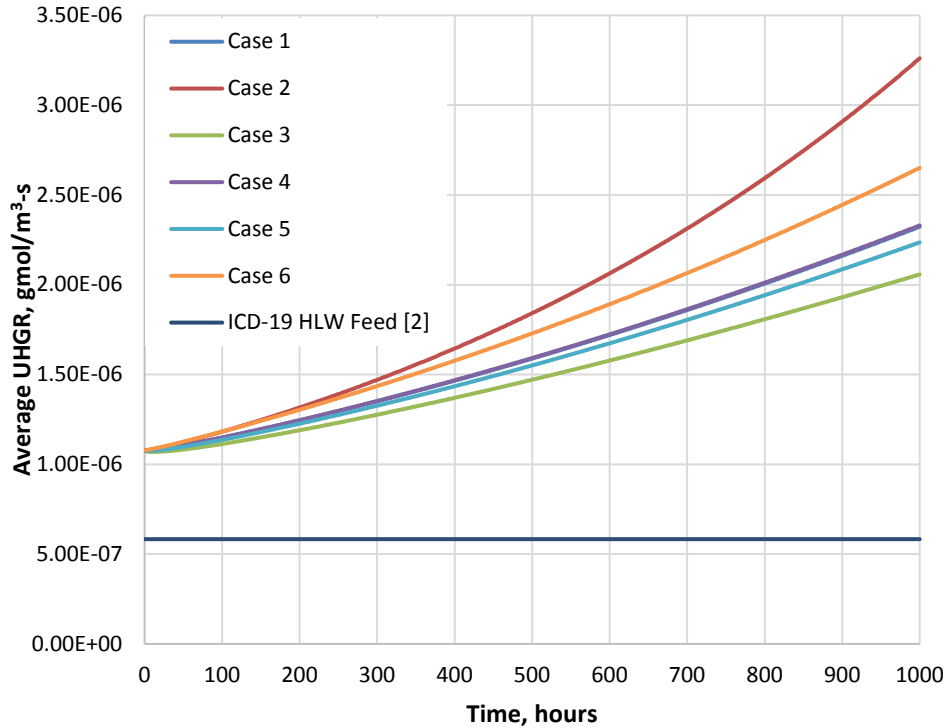


**Figure C-5.** Average UHGR calculated in CFD model.

## 5. Conclusions

The results of this study show that the temperature of the sludge layer increases following a loss of agitation. This leads to an increase in the volumetric average UHGR. Therefore, the Board concludes that using the bulk time-independent temperature and UHGR reported in the WAC may not be conservative for establishing the mixing frequency/schedule.

Based on the sensitivity analyses, the Board finds that the thermal conductivity of the sludge was the most important parameter affecting the heat transfer and subsequent sludge temperature in the SHSV. Additionally, the Board finds that radiative heat transfer to the surrounding black cell is significant. Therefore, the Board finds that additional analysis is necessary to determine technically defensible UHGR for the SHSV. These analyses should incorporate a bounding value of the thermal conductivity of the sludge and a more detailed radiative heat transfer model at the surface of the vessel.

## References

- [1] Taki, B.D., *ICD 19 - Interface Control Document for Waste Feed*, 24590-WTP-ICD-MG-01-019, Rev. 7, Bechtel National, Incorporated, September 19, 2014.
- [2] Lewis, T., and K. Waltzer, *Proposed Control of Hydrogen Events in the Pretreatment Facility Pulse Jet Mixed Process Vessels*, 24590-PTF-ES-NS-15-003, Rev. 00C, Bechtel National, Incorporated, November 3, 2016.

- [3] Beck, J.A., *Preliminary Documented Safety Analysis to Support Construction Authorization; PT Facility Specific Information*, 24590-WTP-PSAR-ESH-01-002-02, Rev. 6a, Bechtel National, Incorporated, February 2017.
- [4] Mauss, J., *Pretreatment Facility Standard High Solid Vessel Design (SHSVD) Concept Study for Black Cell (BC) Planning Areas 02, 03 and 04*, 24590-PTF-ES-ENG-15-010, Rev. D, Bechtel National, Incorporated, February 29, 2016.
- [5] Arulampalam, M., *Equipment Assembly SHS-VSL-00001T Test Vessel Plan*, 24590-WTP-MV-M59T-00035001, Rev. 7, Bechtel National, Incorporated, November 6, 2014.
- [6] Arulampalam, M., *Equipment Assembly SHS-VSL-00001T Test Vessel Elevation and Sections*, 24590-WTP-MV-M59T-00035002, Rev. 7, Bechtel National, Incorporated, November 6, 2014.
- [7] Reed, R.J., *Pretreatment Facility C1, C2, C3, C5, and Atmospheric Reference Ventilation Systems Design Description*, 24590-PTF-3ZD-10-00001, Rev. A, Bechtel National, Incorporated, July 2, 2015.
- [8] Lanning, R. and M. Gebhardt, *Vessel Temperature Calculations During a Post-Design Basis Event Using the FATE Model*, 24590-WTP-M4C-M12T-00001, Rev. A, Bechtel National, Incorporated, May 31, 2012.
- [9] Pedersen, C.O., and D.E. Fisher, *Convective Heat Transfer in Building Energy and Thermal Load Calculation*, American Society of Heating, Refrigerating and Air-Conditioning Engineers (ASHRAE) Transactions 1997, Vol 103, Part 2, 1997.
- [10] Incropera, F.P., and D. P. DeWitt, *Fundamentals of Heat and Mass Transfer, 3<sup>rd</sup> Edition*, John Wiley & Sons, New York, 1990.
- [11] Holman, J.P., *Heat Transfer, 5<sup>th</sup> Edition*, McGraw-Hill, Inc., New York, 1981.
- [12] Eager, K., *Revised Calculation of Hydrogen Generation Rates and Times to Lower Flammability Limit for WTP*, 24590-WTP-M4C-V11T-00011, Rev. C, Bechtel National, Incorporated, May 7, 2010.
- [13] Ferziger, J.H. and M. Perić, *Computational Methods for Fluid Dynamics, 3<sup>rd</sup> Edition*, Springer, New York, 2002.